The Applied Phycology and Biochemistry of Managed Reservoirs in the East of England

Amie L Parris

A Thesis Submitted for the Degree of Doctor of Philosophy
In Environmental Sciences

School of Life Sciences
University of Essex
October 2020

“If creatures of so low an Order in the great Scale of Nature are endued with Faculties to enable them to fill up their Sphere of Action with such Propriety, we likewise, who are advanced so many Gradations above them, owe to ourselves, and to Him who made us and all things, a constant Application to acquire that degree of Rectitude and Perfection to which we also are endued with Faculties of attaining”

These inspiring and thought provoking words went on a long journey to find me and so it is my duty to oblige their efforts and pass them on to you. This quote was originally written by John Ellis in *An Essay Towards a Natural History of the Corallines (1755).* They later appeared as the opening quote of *Ponds & Rock Pools (1894)* by Henry Scherren*.* I came to my 1st Edition (1st Printing) copy of *Ponds and Rock Pools* at GFB Rare Bookshop in the historic Colchester Essex during the second year of my PhD. I suspect my book has seen many shelves since print but one of note is that of a Mr. Samuel Brown. According to a glued insert on the cover, Mr. Brown won our copy of *Ponds & Rock Pools* as a prize in Reading from Church Schools in Melton Mowbray (Leicestershire, England) in 1895. 125 years later, it now sits on my bookshelf while I present to you my application to acquire that degree of Rectitude and Perfection to which I am also endued with Faculties of attaining”

ABSTRACT

Climate Change is one of the greatest threats to drinking water supplies around the world. Managing these vulnerable systems is complex, requiring mitigation and adaptation strategies that can combat multiple stressors (i.e. drought and eutrophication). This is especially true for reservoirs in the East of England, which are facing climate extremes such as heat and drought to a greater extent than other parts of the UK. To understand how these and other climate stressors are currently affecting drinking water reservoirs and their vulnerability under future climate change, this thesis performs whole-system ecological studies that investigate biodiversity, eutrophication, and internal sediment dynamics driving the succession of harmful algal blooms. These studies were designed to provide a baseline assessment of climate stressors in the East of England, identify potential risk, and address management strategies and challenges faced by the UK water industry. The outcome of these investigations identified toxin-producing cyanobacteria dominated throughout the year resulting in lower biodiversity and increased risk to recreational users and treatment practices. Furthermore, it was found internal loading is feeding these blooms providing a steady supply of the limiting nutrient, phosphorus. While a management bund wall is currently in place to trap phosphorus in the reservoir inlet, it was found to be inefficient, in turn allowing nutrients to flow down the reservoir gradient. In order to address these management concerns and prepare UK reservoirs for the threats of climate change, a multi-disciplinary approach that address multiple stressors will be necessary to allow drinking water reservoirs to remain thriving ecosystems under a changing climate.

ACKNOWLEDGEMENTS

First, thank you to my primary supervisor Dr. Tom Cameron for supporting my vision for an applied PhD and ensuring I graduated with the skills, connections, professional training, and confidence to advance my career. Secondly, I must thank Anglian Water and Stuart Knott for believing in my work, supporting my research and goals, being a mentor in the water industry and for the financial assistance that made this degree possible. A special thank you also to CEFAS and Andrew Turner for the training and partnership that saved my toxins chapter. I would next like to thank Dr. Rupert Perkins for his guidance and support in the field of sediment ecology and the opportunities I gained from working with him and his team at Cardiff University. Another big thank you to John Green for spending hundreds of hours with me sampling, for his training and support in the lab and above all for his friendship. A special thank you to my friend and fellow toxin enthusiast, Dr. Brisneve Edullantes, who joined me in many wonderful adventures exploring the UK and offered his patience, support, and guidance teaching me R. Next, I must thank Dr. Danielle Harris and Dr. Fionnuala McKenna for keeping me focused and motivated during my write up and being my most cherished friends. To my family who supported me through the passing of my mother so I remained on course to finish my degree. To my aunt for never forgetting to send me a card, care packages, and a set of open arms whenever I came home. Finally, thank you to my dad who is my biggest advocate and who supports me in everything I do without question.

Thank you to everyone else who was a part of this amazing journey.

DECLARATION

I declare the work contained within this thesis is the result of my own work under the supervision of Dr. Tom Cameron, Dr. Rupert Perkins, and Dr. Andrew Turner.

Nutrient Analysis: All biogeochemical water and sediment analysis performed at the University of Essex was done so under the direct supervision and training of Senior Technician, John Green. When applicable, Mr. Green performed all auto-analyzer system calibrations, maintenance, and setup as the trained instrument technician.

Sample Collection: Samples collected in chapters 2, 3, 4, and 5 (2017-2019) were done so with the assistance of Dr. Tom Cameron, Mr. Russel Smart, and Mr. John Green.

Chapter 2 & 3: Phytoplankton cell and colony counts and species identification were analysed by algal taxonomists at the Anglian Water Central Laboratory (Osprey House, Kingfisher Way, Huntingdon PE29 6FN). Microcystin variant quantification and analysis was performed with the assistance of Dr. Andrew Turner, Principal Chemist of Food Safety at the Centre for Environment Fisheries & Aquaculture Science (CEFAS) (Barrack Road, Weymouth, Dorset, DT4 8UB). Dr. Turner also oversaw all UPLC/MS/MS system calibrations, maintenance, and performance. His team at CEFAS also assisted with quality control measures by reviewing all datasets before release.

Data Analysis: Mining and preparation of phytoplankton community composition data was performed with the assistance and training of Dr. Brisneve Edullantes using the statistical software package R.

Amie Parris

University of Essex

October 2020

Table of Contents

List of Figures

List of Tables

INTRODUCTION

Climate change is the greatest environmental challenge facing our planet and future generations (European Environment Agency, 2020; Wright and Nyberg, 2017). In addition to global security, human health, sea level rise, carbon emissions, natural disasters, extreme weather events, and extinction, water safety and security is a significant threat from climate change and impacting some 27% of the world's population (United Nations et al., 2020). According to the 2020 United in Science Report by the United Nations and the World Meteorological Organization, 12% of the world population consumes unsafe drinking water, 2 billion people live in high water-stress countries, and a projected 3.2 billion people will live in water scarcity by 2050 (United Nations et al., 2020). Furthermore, as the demand for water increases with an increase in the world population, these situations are expected to worsen (United Nations, 2018).

In the United Kingdom, the 2019 (UK-Convection-Permitting) Model Projections Report confirms the UK remains on course for warmer (+1.8 - 3.3 ºC) wetter (+16 - 42%) winters, and hotter (+3.6 - 5.0 ºC) drier (+16 - 46%) summers (Kendon et al., 2019; Lowe et al., 2018). From this, the greatest increase in hot spells (30 °C or higher for two or more consecutive days) and the number of hot days overall will occur in the southern UK. Precipitation is also expected to increase throughout the UK, except in the southeast where hourly precipitation will decrease but the intensity of that precipitation will increase (Kendon et al., 2019).

Drinking water reservoirs are at an increased risk from climate change due to drought, heat, and demand (i.e. increasing populations in high stress regions). In the East of England, climate change stressors are even more prominent as this region is projected to see more extremes (i.e. drier and hotter summers) compared to other parts of the UK. Nevertheless, the preservation of drinking water reservoirs is of paramount importance. In addition to drinking water, they provide ecosystem services such as fishing, swimming, bird watching, and boating. Managing multi-use systems is complex and requires a multi-disciplinary approach where climate change research is focused on understanding the interactions of multiple stressors in each reservoir.

1.1 Climate Stress on Drinking Water Reservoirs

1.1.1 Storm Intensity and Eutrophication

One such stressor is storm intensity. Less precipitation but larger, more intense storm events from changing climate patterns promotes eutrophication (excessive nutrients) in freshwater lakes (Morabito et al., 2018). Heavy rainfall over a short time period flushes nutrients from agricultural land and over fertilized lawns into source waters to create nutrient rich waters that support phytoplankton growth (Bol et al., 2018; Daniel et al., 1998). Phytoplankton respond quite rapidly to eutrophication (Navarrete et al., 2019) leading initiatives such as the Water Framework Directive to use phytoplankton as predictive indicators of ecosystem health (Jakhar, 2013; Perkins et al., 2010a). While increased storm events promote phytoplankton biomass through nutrient input, flushing events from intense storms can de-stratify the water column, which conversely, may reduce the formation of cyanobacteria

blooms (Reichwaldt and Ghadouani, 2011). In shallow, polymictic lakes (well-mixed with no thermal stratification), predictive models identified variability among climate variables driving thermal stratification, where these lakes experienced less sensitivity to temperature or stratification (Taranu et al., 2012).

1.1.2 Biodiversity, Acidification, and Invasive Species

Among phytoplankton, biodiversity and community composition are strongly effected by eutrophication and warmer waters. Freshwater biodiversity has decreased by 76% since the 1970s, almost faster than both terrestrial (39%) and marine (39%) diversity combined (World Wildlife Fund International et al., 2014). This is caused by a multitude of stressors acting both directly and indirectly including: acidification from more sulphur and nitrogen in the atmosphere (Jesus et al., 2018; Leduc et al., 2013), fluctuations in water temperature and nutrients (Elliott et al., 2006), and non-native species that are better able to adapt and exhibit higher thermal tolerance in warmer waters (Kernan, 2015).

1.1.3 Temperature

Air temperature is linked to water temperature and hotter days under a changing climate have the potential to increase water temperatures more quickly (Clarke, 2009). In freshwater systems, hot spells also known as heat waves are shown to have damaging impacts on ecosystem functioning including thermal and physiological stress and altered succession in fish (Badr, 2019), invertebrates (Paraskevopoulou et al., 2018), and primary

producers (Hansson et al., 2020). In addition, hot spells alter the hydrological cycle by increasing evaporation (Kundzewicz, 2008) while concurrently increasing inter and extra-cellular reactive oxygen species in phytoplankton from UV light penetrating the water column (Paerl and Otten, 2013).

1.1.4 Reactive Oxygen Species and Cyanotoxins

Reactive Oxygen Species (ROS) are produced as intercellular by-products during metabolic activity (Sharma et al., 2012). Under normal physiological conditions, excess ROS is scavenged by the cell. However, when faced with climate stressors such as changes in light intensity, the cell may not effectively or efficiently process ROS, resulting in a rise of intercellular ROS and potentially killing the cell (Apel and Hirt, 2004). Extracellular oxidative stress is also a result of climate change and has been studied extensively in cyanobacteria (Ding and Ong, 2003; Qiao et al., 2020; Zilliges et al., 2011). Extracellular oxidative stress against cyanobacteria begins with excess reactive nitrogen species and other stable chemicals (i.e. chlorofluorocarbons) in the atmosphere. These anthropogenic pollutants break down the earth's ozone layer resulting in intensified ultraviolet radiation (UVR) (Singh et al., 2010). Environmental ROS are created by UVR where the UVR produce superoxide (O_2^-) and hydrogen peroxide (H_2O_2) from dissolved organic carbon. Excessive H_2O_2 from this process imposes oxidative stress on cyanobacteria by diffusing into the cell (Paerl and Otten, 2013). Cyanobacteria work to mitigate stress from H_2O_2 by implementing antioxidant defence mechanisms (Latifi et al., 2009). One such mechanism is through toxin production. Under oxidative stress, the cyanotoxin microcystin

covalently binds to cellular proteins whereby defending the proteins from proteolytic degradation (Paerl and Otten 2013). This binding is then strengthened during oxidative stress and increased light intensity (Zilliges et al., 2011). This method of defence allows for continued growth and even competitive growth despite external cellular stress. Increased growth under oxidative stress from climate change is further supported by experimentation on the cyanobacterium *Dolichospermum sp*. where a significant correlation was found between growth rates and intercellular toxins with both increasing significantly as temperature increased (Brutemark et al., 2015). Given this, water managers need to consider more than algal biomass as a predictor of risk but look towards monitoring algal toxins as the threat from climate change lies in their composition and proliferation.

1.1.5 Harmful Algal Blooms and Recreational Exposure

In freshwater reservoirs, toxins are inferred visually from surface scums known as harmful algal blooms or HABs. HABs are an accumulation of algal (photosynthetic eukaryotic organisms) and phytoplankton (autotrophic plankton) overgrowth. HABs are the result of many climate stressors working together to create a “perfect storm” which perpetuates their threat. Toxins from these blooms then enter the food chain and become more concentrated via bioaccumulation from smaller to larger fish (Berry and Lind, 2010; Xie et al., 2005). Populations who then rely on fish as a protein source and even those who fish recreationally are at an increased risk from consumption. This effect is similar to that of mercury bioaccumulation in many fresh and marine fish species (Allen-Gil et al., 1995).

1.1.6 Combined Effects

On their own, climate change stressors (i.e. heat and precipitation) have negative consequences on biodiversity (Mantyka-Pringle et al., 2014), ecosystem functioning (Malmqvist and Rundle, 2002; Perkins et al., 2010b), and ecosystem services (Jordaz-Capdevila et al., 2019; Postel and Carpenter, 1997) in fresh waters. However, combined, their interactions are known to cause further complications both directly and indirectly, some of which are not completely understood (Hering et al., 2010). An example of combined effects of climate stressors is the spring phytoplankton bloom. In shallow temperate lakes, the spring phytoplankton bloom is largely initiated by increased light and UV rays from longer days and ice melt, which increases light to the water column (Arvola, 1986; Bleiker and Schanz, 1997). Under normal climate conditions, predation would cause the spring bloom to collapse and the onset of a clear water phase (Scheffer et al., 1997). However, climate change stressors affect this process where warmer waters result in earlier ice melt thereby altering the timing of zooplankton succession (Huber et al., 2008; Korhonen, 2006). In addition, in eutrophic waters, spring blooms may be dominated by grazer-resistant phytoplankton, eliminating the clear water phase completely (Klausmeier and Litchman, 2012). This leads to altered zooplankton succession from changes in feeding patters and in turn impacts the zooplankton to fish energy transfer (Sommer and Lengfellner, 2008).

1.2 Climate Adaptation and Mitigation in the UK

While many water management companies are still working to understand how future climate scenarios will affect their systems, some have proactively taken action to adapt and mitigate these stressors.

An example of this is Abberton Reservoir, managed by Essex and Suffolk Water, located in Essex, UK. Abberton underwent a climate resilience expansion increasing their capacity by 58% to mitigate drought and population increases as well as creating wetlands for wildlife and carbon reduction. To address drought and population increases, five pump stations were installed to carry more source water from local rivers to the reservoir. Additionally, the reservoir dam was raised from 19.8m to 22.7m to accommodate the increase in water level (Wilson, 2012). Examples such as Abberton show by identifying global climate threats, local projections, and site-specific characteristics and functioning of each system, managers can mitigate these threats and implement adaptation strategies to prepare for vulnerability and extreme stressors in a future climate.

Climate mitigation and adaptation efforts are also being undertaken by government groups such as the UK Centre for Ecology and Hydrology, Lancaster. Their work involves lake ecosystem modelling which combines laboratory experiments, field observations, environmental variables and mathematics to create predictive models of algal blooms, for example and drivers of eutrophication. One such model is PROTECH. PROTECH (**P**hytoplankton Resp**O**nses **T**o **E**nvironmental **CH**ange) works to understand

and model the development of phytoplankton in freshwater lakes and has been in use for over a decade (Elliott, 2020).

1.3 Current Management Practices

Guiding adaptation and mitigation efforts at the local level are national and international organisations such as the World Health Organisation (WHO), which sets the safe standards for cyanobacteria toxins. However, the standards currently in place were last updated in 1999 and may not be the most protective of public health given the immense research on the topic over the past few decades. Additionally, WHO guidance only covers one (Microcystin-LR) of the approximately 240 known toxin variants (Johansson et al., 2019). This presents an even greater risk to public health and justification for local water authorities to set standards specific for their waterbodies.

1.4 Thesis Rationale

To highlight the effects of multi-stressor interactions and management challenges facing drinking water supplies, this PhD performs whole-reservoir assessments to understand how climate change is effecting the ecology of drinking water reservoirs in the East of England. To achieve this, I repeat ecological assessments from the 1980s and 1990s that examined spatial gradients of nutrients, biodiversity, and sediment dynamics. In doing so, I examined the spatial and temporal ecology of summer and autumn phytoplankton blooms, cyanotoxins, environmental stressors, nutrient limitation and sediment dynamics to see if current reservoir ecology is similar

to what it was 30 years ago. This information will provide vital insight into how drinking water reservoirs are adapting and responding to climate change and what can be expected in the coming years. This work also brings attention to the importance of site-specific, whole-system studies across multiple themes as an effective management strategy to avoid over estimating problematic species that could prove costly to water treatment (i.e. clogged filtration) while not underestimating potentially dangerous conditions and toxins.

1.5 Thesis Structure

- In Chapter 2, I assess phytoplankton community composition and abundance between shallow and deep-water habitats across a spatial and temporal scale to identify if a single, pelagic sample is representative of the reservoir and thus an appropriate management strategy for whole-system management.

- In Chapter 3, I characterise the group of phytoplankton most associated with climate change stressors and at the forefront of reservoir management, Cyanobacteria: by quantifying bloom composition and toxicity, strain dominance, and the biogeochemical parameters that may be driving these communities.

- In Chapter 4, I assess a key nutrient in eutrophication and a focus of drinking water managers, phosphorus: by quantifying concentrations from the sediment to the surface, calculating sediment's ability to act

as a source or sink for phosphorus, and identify the potential for internal loading to support phytoplankton growth in a changing climate.

- In Chapter 5, I assess the effectiveness of a management bund wall to trap nutrient inputs from source waters, document the status of nutrient limitation along a reservoir gradient (reservoir inlet/bund-wall to the main basin), and investigate phytoplankton's ability to support growth across that gradient under nutrient limitation.

CHAPTER 2

PHYTOPLANKTON DIVERSITY AND ABUNDANCE ARE HOMOGENEOUS BETWEEN HABITATS IN TWO SHALLOW, MIXED RESERVOIRS

2.0 INTRODUCTION

As a key primary producer, phytoplankton community dynamics play a vital role in freshwater biodiversity, energy flow, and nutrient cycling (Belokda et al., 2019; Jindal et al., 2014). Nutrients (i.e. nitrogen and phosphorus) are essential to phytoplankton growth (Redfield, 1958) but excessive nutrient inputs can increase phytoplankton biomass (Smith, 2003), alter community composition (Chellappa et al., 2008), trophic status (i.e. eutrophic) (Carpenter et al., 1985), and even cause system-wide regime shifts (Iacarella et al., 2018), (Navarrete et al., 2019; Pasztaleniec, 2016; Reynolds, 1984; Xu et al., 2010).

Regime shifts from eutrophication are known to reduce phytoplankton biodiversity (Hilt et al., 2017). However, freshwater biodiversity studies have focused primarily on pelagic communities with little attention on shoreline (littoral) habitats (Cattaneo et al., 2011; Schweizer, 1997) despite evidence of littoral habitats being more diverse than the pelagic (Zohary and Ostrovsky, 2011). Littoral habitats are also an important part of a reservoir's total primary

production and may present a different community structure than the pelagic due to unique, habitat-specific influences (Mukhortova et al., 2015). For example, the shallow littoral edges of reservoirs experience increased disturbance to the sediment from fish spawning (Winfield, 2004) and water-level fluctuations (Logez et al., 2016). These activities re-suspend nutrients to the water column resulting in increased biomass. The littoral habitat is also home to filamentous plankton such as metaphyton, which provide strata for fish eggs and protection from predation (i.e. zooplankton) (Tessier et al., 2008).

Despite these unique differences, reservoirs are connected systems where benthic and pelagic communities interact (Lodge et al., 1988). In Paradox of the Plankton, Hutchinson noted littoral phytoplankton communities may migrate to the pelagic due to competition for resources (Hutchinson, 1961). Whereas, Cattaneo et al. found the littoral may serve as refuge for pelagic species (Cardoso et al., 2019; Cattaneo et al., 2011).

In many drinking water reservoirs throughout the UK, water samples used to quantify community composition and abundance are collected from a single location in the pelagic (the draw-off tower) (Turner et al., 2018). This is despite evidence from the previously mentioned studies showing potential for reservoir-wide diversity, bringing into question if a pelagic sample is representative of the reservoir and thus appropriate practice for making management decisions. If a reservoir is found to be more diverse in the littoral, a pelagic sample may not capture important species that increase recreational

risk and clog expensive treatment filters. Additionally, if a single pelagic sample is more diverse than the littoral, the sample may be overestimating certain communities resulting in potentially unnecessary reservoir closures.

In the 1980s, In the East of England (Ardleigh reservoir), Abdul-Hussein and Mason (1988) documented 58 phytoplankton species over a two-year study with cyanobacteria dominating the summer bloom. While this study did not distinguish littoral communities from pelagic, it did show higher horizontal unevenness during the spring and summer (Abdul-Hussein and Mason, 1988). During this time, Ardleigh was recognized as eutrophic, resulting in multiple closures to the drinking water treatment works (Hayes and Greene, 1984 as cited in Abdul-Hussein and Mason, 1988). Similarly, a second reservoir in the East of England (Alton Water), was also investigated where summer phytoplankton blooms were documented in the main basin from 1981 until 1993 when the reservoir entered a four-year (1993-1997) clear-water, partial recovery phase. In this time, macrophytes dominated and the reservoir was reclassified as mesotrophic (Perkins and Underwood, 2002). Perkins and Underwood analysed phytoplankton community data taken over both phases (1981 -1997) and found the shallow, top end of the reservoir dominated by the diatom *Stephanodiscus* from 1983-1997 where it was the most numerically abundant taxa. In the pelagic main basin, the cyanobacteria *Aphanizomenon* and *Woronichinia* dominated causing severe blooms in 1990 and 1992. It was also concluded both biomass and species richness were lower in the main basin than the shallow reservoir inlet.

To assess the validity of pelagic sampling for management decisions, the present study evaluated spatial and temporal variability in diversity and abundance of phytoplankton communities between shallow, shoreline (littoral) habitats and deeper, open-water (pelagic) habitats in the East of England. Specifically, the following research questions were studied. (1) What is the community composition of Alton and Ardleigh and how does it compare to the 1980s and 1990s? (2) Is there a relationship between biomass, abundance, and functional diversity within habitats? (3) Community composition is currently assessed from one sample in the pelagic habitat (draw-off tower), is this sample representative of the reservoir as a whole? (4) In this study, both microscopy and *in situ* spectrofluorometery were used to assess community composition, how do these methods compare at the phylum level?

2.1 METHODS

2.1.1 Study Sites

Alton Water is a 1.642 km^2 manufactured drinking water supply in the southeast United Kingdom. Alton's northern most point is a pumped input flowing southeast to an open main basin where it is pumped out through a draw off tower. The reservoir's inlet is shallow (< 2 m), capturing nutrients and algal biomass behind a 400 m bund wall (Perkins and Underwood, 2000). From the inlet, depth gradually increases down the length of the reservoir until it reaches a maximum of 18 m in the main basin (Fig. 2.1).

Ardleigh reservoir is an artificial drinking water supply in Colchester, UK. It has a surface area of 0.507 km^2 and a mean depth of 4.15 m (Environment

Agency, 2017). The River Colne supplies Ardleigh through two pumped inputs on the northern and western banks. In the main basin and next to the draw-off tower are two artificial mixers or bubble curtains (Abdul-Hussein and Mason, 1988) (Fig. 2.2).

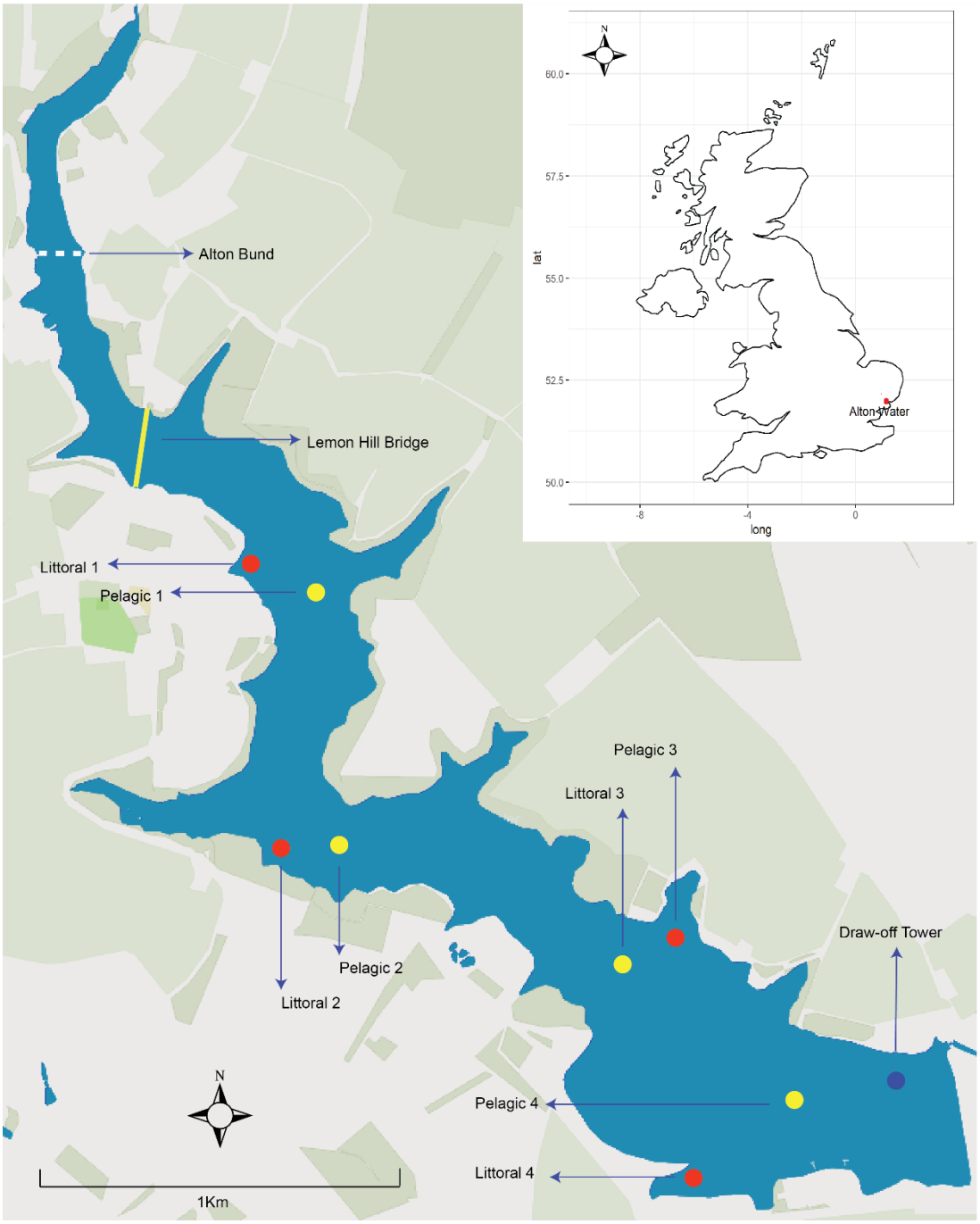

Figure 2.1 Alton Water in the East of England (top right) and nine sample locations within the reservoir. All littoral habitat sites are marked by a red dot and pelagic sites marked by a yellow dot. Sample points begin towards the top of the reservoir and follow the depth gradient to the main basin. The reservoir's drawoff tower is also located in the main basin and marked with a blue dot. Figure Credit: Amie L. Parris.

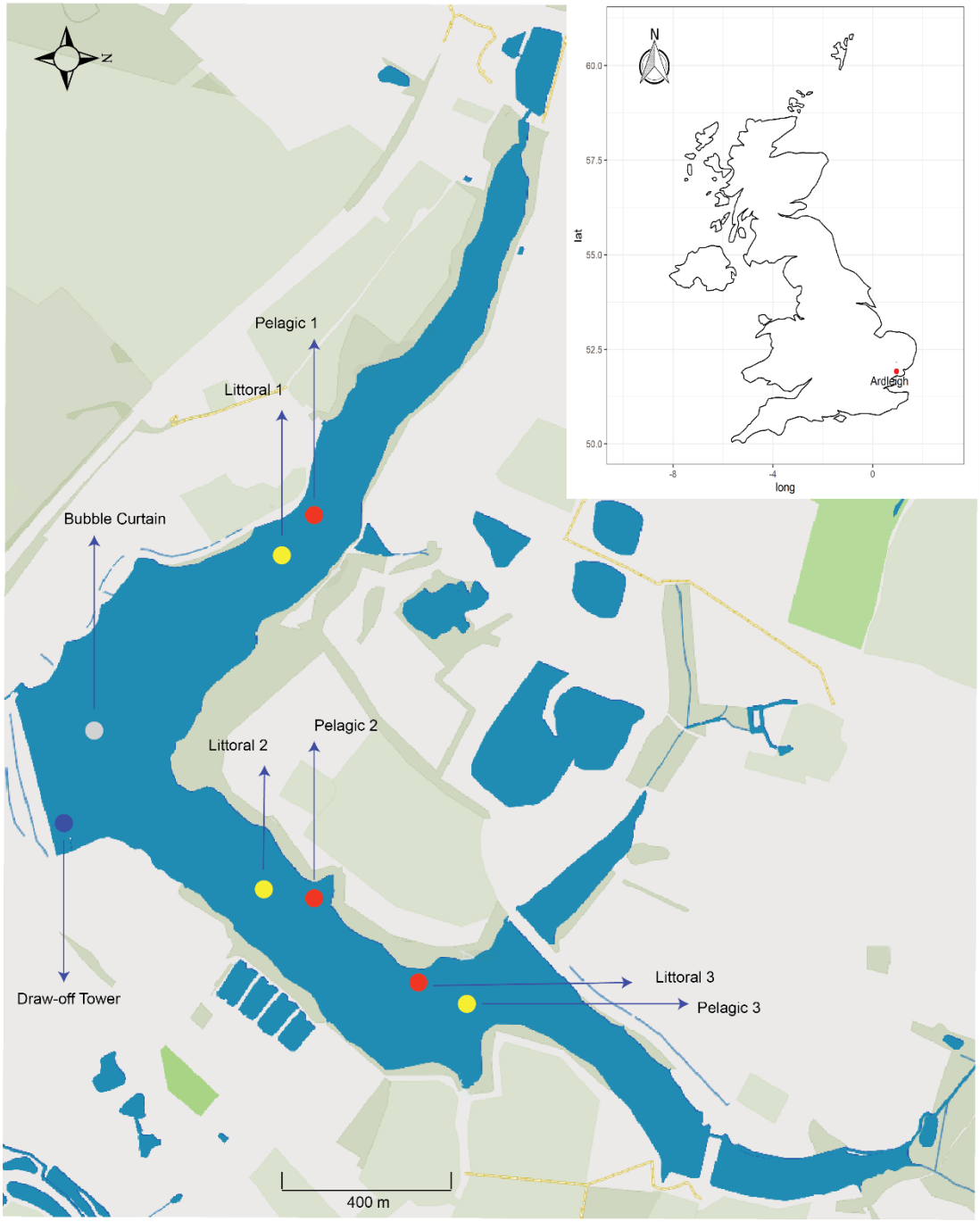

Figure 2.2 Ardleigh Reservoir located in the East of England (top right) and eight sample locations within the reservoir. All littoral habitat sites are marked by a red dot and pelagic sites marked by a yellow dot. Sample points extend up each arm of the reservoir with two points in the main basin, the drawoff tower maked by a blue dot and the bubble curtain marked by a white dot. Figure Credit: Amie L. Parris

2.1.2 Sample Collection

Alton and Ardleigh were monitored twice monthly from May through September (2017) and once monthly from October through April (2017/2018). Within each reservoir, surface water samples (<2 m) and vertical water column profiles were captured in the littoral and pelagic habitats. For Ardleigh, triplicate samples of each habitat were sampled with two additional monitoring stations at the draw-off tower and bubble curtain. In Alton, four replicates of each habitat were sampled with one additional monitoring station at the draw-off tower in the main basin. Littoral monitoring stations feature direct public access to the waterfront and a shallow depth of less than 3 m. Pelagic stations run along the reservoir's middle corridor with a summer depth between 5 m and 12 m.

2.1.3 Chlorophyll-*a*

As a proxy for phytoplankton biomass, chlorophyll-*a* (µg/L) was captured by filtering a fresh, unpreserved sample through a 47 mm binder-free glass microfiber GF/F filter (GE Healthcare Whatman 1825-047). Filtration was performed using a vacuum pump with an attached filtration funnel. Sample filtration volume varied as follows to account for seasonal changes in biomass: May 2017 (2000 mL), first sampling event of June 2017 (2000 mL), remainder of June 2017 (1000 mL), July – November 2017 (500 mL), and December 2017 through April 2018 (1000 mL). Filters were stored in the dark in 90% (v/v) acetone for 18 hours at 0°C. Prior to analysis, filters were removed and the remaining sample was centrifuged for five-minutes at 3000 RPM (Sartory, 1982). Wavelengths were recorded on a Shimadzu UV-1800

spectrophotometer at 630nm, 674nm, 664nm, and 691nm following the protocol of Ritchie (2008). An additional reading was recorded at 750nm to account for turbidity.

2.1.4 Community Composition

2.1.4.1 In situ Fluoroprobe

To capture phytoplankton community composition a BBE-Moldaenke fluoroprobe (item number: BG0035.0000) was used *in situ* to record cell counts of four planktonic classes (green algae, cyanobacteria, diatoms, and cryptophytes). The fluoroprobe used six light-emitting diodes (LED) where each LED is calibrated to the planktons unique fluorescence excitation spectrum. The following absorbances were used based on the manufacturer's specifications, 470 nm (green algae), 610 nm (cyanobacteria), 525 nm (diatoms), and 571 nm (cryptophyta).

To begin, the fluoroprobe was lowered into the water until fully submerged. It was then slowly lowered to the benthos and finally raised back to the surface. Careful attention was taken to prevent the fluoroprobe from touching the bottom and re-suspending the sediment. Class data was captured in the fluoroprobe unit and later exported using bbe++ version 2.6.5.407 software.

2.1.4.2 Microscopy

To measure phytoplankton community composition to the species level, taxonomic microscopy was performed on preserved samples. At each littoral and pelagic site, a 20 µm phytoplankton net was lowered 2 m into the water

column. For littoral sites where the maximum depth did not reach 2 m, the net was lowered to the maximum allowable depth without disturbing the benthos. Net contents were poured into a 50 mL falcon tube, preserved with acidic Lugols solution and placed in the dark for analysis.

Quantitative analysis was performed on the preserved sample by first inverting the sample by hand to re-suspend the settled pellet. A 1 mL aliquot of the mixed sample was then added to 9 mL of sterile, distilled water. From the 10 mL diluted sample, 2.5 mL was transferred to a 2.5 mL settlement chamber and allowed to settle for 1 hour prior to analysis. Samples were read from three random fields of view using an inverted microscope or until at least 100 cells of the dominant species were identified. Microscopic counts were multiplied up to reach a value in cells/mL.

2.1.5 Statistical Analysis

2.1.5.1 Difference between Habitats

To test for statistical differences in biomass, total abundance, species richness, Shannon and Simpson diversity indices, and relative abundance, one-way analysis of variance (ANOVA) models were performed to test whether these variables were significantly different in the littoral and pelagic habitats. Two-way ANOVA models were also performed with habitat, month, and their interaction as explanatory variables. Post hoc Tukey tests then examined which combinations, if any, were significant and driving the model output.

2.1.5.2 Relationship between Variables

To evaluate the relationships among richness, abundance, biomass, and Shannon and Simpson diversity indices, Spearman rho rank-based correlation coefficient tests were applied to each pair of variables. Individual tests were run for each habitat within the two reservoirs. From the rho values, statistical significance testing was performed to determine if the correlation could be accepted.

2.1.5.3 Community composition

To assess community composition in both spectrofluorometery and microscopy datasets, a distance matrix was created from rarefied cell counts and visualized using nonmetric multidimensional scaling (NMDS). The Manhatten Index was used to create the matrix as it was the highest ranked method for the data. To test the differences in community composition between habitats and months, Adonis permutational multivariate analysis of variance (PERMANOVA) was carried out on the distance matrix using 999 permutations.

Analysis for this chapter was conducted using R Statistical Software (R Core Team, 2020) with figures produced using the package ‘ggplot2’ version 3.3.1 (Wickham, 2009). Analysis packages include: ‘vegan’ (Oksanen et al., 2019), ‘tidyverse’ (Wickham et al., 2019), and ‘ggeffects’ (Lüdecke, 2018).

2.1.6 Figures

Figures 2.1 and 2.2 were made using Mapbox© Studio, Adobe Illustrator software (version 23.1), and Adobe Lightroom software (version 3.4) from Adobe Inc. under personal Creative Cloud license ADB001443181EDU.

2.2 RESULTS

2.2.1 Chlorophyll-*a*

In Ardleigh Reservoir, a concentration of 1479 µg/L was observed in the littoral habitat however, this has been attributed to either an error or aggregation of phytoplankton giving bias, and therefore the value was removed from the dataset prior to analysis.

Surface water samples were collected by hand in the top 2 m of the water column from May 2017 through April 2018 and processed for chlorophyll-*a*. In Alton Water, concentrations ranged from 0.22 µg/L (May) to 265.14 µg/L (Aug) in the littoral habitat. In the pelagic, concentrations ranged from 0.24 µg/L (May) to 178.65 µg/L (Aug). May also had the lowest mean concentration of the year in both the littoral (0.43 µg/L) and pelagic (0.56 µg/L). Similarly, August had the highest monthly mean of the year in both the littoral (107.82 µg/L) and pelagic (95.84 µg/L) (Fig. 2.3). Chlorophyll-*a* concentrations varied significantly between months (pseudo-$F_{11, 118}$ = 56.131, P < 0.000) but not between habitats in any month (pseudo-$F_{11, 118}$ = 1.126, P = 0.347).

In Ardleigh Reservoir, concentrations ranged from 0.13 µg/L (Jun) to 582.02 µg/L (Aug) in the littoral habitat. In the pelagic, chlorophyll-*a* concentrations

ranged from 0.20 µg/L (Jun) to 253.83 µg/L (Aug). Nov had the lowest mean concentration of the year in the pelagic habitat (3.84 µg/L) whereas Aug had the highest yearly mean in the littoral (244.00 µg/L) (Fig. 2.4). Chlorophyll-*a* concentrations varied significantly between months (pseudo-$F_{9, 84}$ = 28.890, P < 0.000) but not between habitats in any month (pseudo-$F_{9, 84}$ = 0.763, P = 0.650).

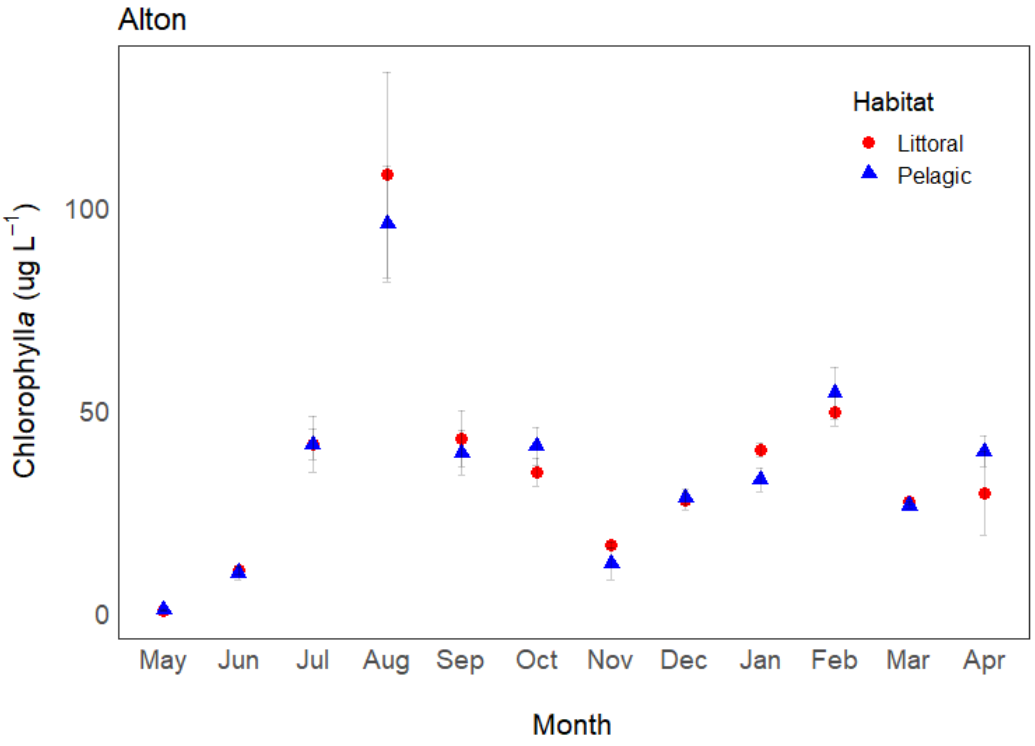

Figure 2.3 Mean inter-annual chlorophyll-*a* (µg/L^{-1}) concentrations in the littoral (red dots) and pelagic habitats (blue triangles) of Alton Water. Error bars indicate standard error between replicates. May 2017: littoral (n=8) pelagic (n=10), Jun 2017: littoral (n=4) pelagic (n=5), Jul-Sep 2017: littoral (n=10) pelagic (n=10), Oct 2017: littoral (n=9) pelagic (n=10), Nov 2017: littoral (n=3) pelagic (n=3), Dec 2017-Apr 2018: littoral (n=4) pelagic (n=5).

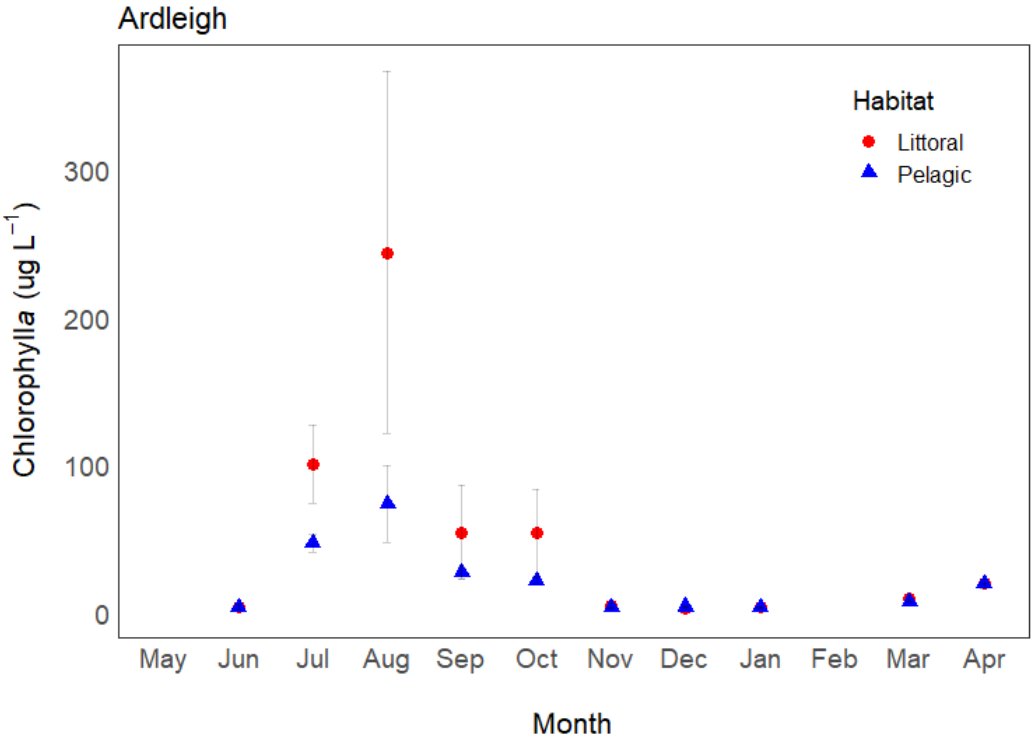

Figure 2.4 Mean inter-annual chlorophyll *a* (µg/L^{-1}) in the littoral (red dots) and pelagic habitats (blue triangles) of Ardleigh Reservoir. Error bars indicate standard error between replicates. Jun-Jul 2017: littoral (n=6) pelagic (n=8), Aug 2017: littoral (n=5) pelagic (n=8), Sep-Oct 2017: littoral (n=6) pelagic (n=8), Nov 2017-Apr 2018: littoral (n=3) pelagic (n=4).

2.2.2 Abundance and Alpha Diversity

2.2.2.1 Total Abundance

Mean total abundance in the littoral habitat ranged from 19,716 cells/mL (Ardleigh; Nov) and 26,026 cells/mL (Alton; Nov) to 4.9 million (Ardleigh; Sep) and 10.1 million (Alton; Apr). In the pelagic, mean total abundance ranged from 17,463 cells/mL (Ardleigh; Jun) and 24,223 cells/mL (Alton; Aug) to 3.1 million (Ardleigh; Sep) and 14.8 million (Alton; Feb) (Fig. 2.5). Analysis of

Variance tests determined abundance did not vary significantly between habitats (Alton; pseudo-$F_{1, 129}$ = 0.105, P = 0.746, Ardleigh; pseudo-$F_{1, 87}$ = 0.17, P = 0.681) or between habitats in any month (Alton; pseudo-$F_{11, 107}$ = 1.152, P = 0.329, Ardleigh; pseudo-$F_{10, 67}$ = 0.570, P = 0.833). However, as with biomass, abundance varied significantly between months within each habitat (Alton; pseudo-$F_{11, 107}$ = 25.650, P < 0.000, Ardleigh; pseudo-$F_{10, 67}$ = 7.821, P < 0.000).

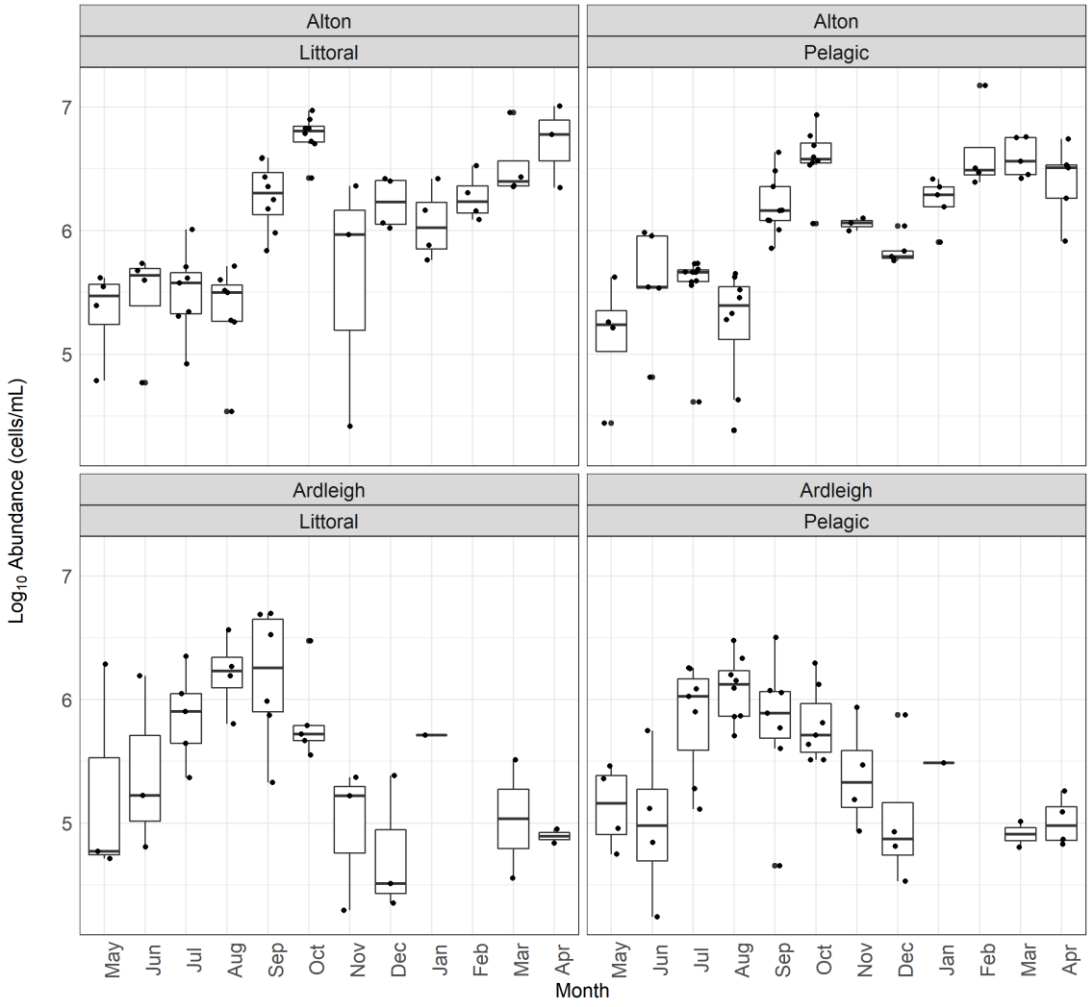

Figure 2.5 Mean total abundance in Alton Water (top) and Ardleigh Reservoir (bottom) between two habitats (littoral and pelagic) and over a temporal scale of 12 months (May 2017 – April 2018). For each boxplot, the boundary of the box closest to zero indicates the 25th percentile, the black line within the box indicates the median, and the boundary of the box farthest from zero indicates the 75th percentile. Whiskers above and below the box mark the 10th and 90th percentiles while the points above and below the whiskers indicate outliers outside the 10th and 90th percentiles.

2.2.2.2 Species Richness

In Alton Water, microscopy recorded a range in species richness from three (Apr, Dec, Nov, Oct, May) to 10 species (Sep, Jan, Jul, Aug) in the littoral habitat and a range of two (Sep and Nov) to 13 species (Aug) in the pelagic. Similarly, Ardleigh species richness ranged from two (Jun and Sep) to nine unique species (Apr, Aug) in the littoral habitat while in the pelagic, only one species was recorded as the lowest (Sep and Dec) and 11 species as the highest (Jul) (Fig. 2.6). Analysis of Variance tests determined species richness did not vary significantly between habitats (Alton; pseudo-$F_{1, 129}$ = 0.101, P = 0.751, Ardleigh; pseudo-$F_{1, 87}$ = 0.309, P = 0.58) or between habitats in any month (Alton; pseudo-$F_{11, 107}$ = 1.531, P = 0.131, Ardleigh; pseudo-$F_{10, 67}$ = 0.148, P = 0.998). However, as with biomass and total abundance, species richness varied significantly between months within each habitat (Alton; pseudo-$F_{11, 107}$ = 5.548, P < 0.000, Ardleigh; pseudo-$F_{10, 67}$ = 4.199, P < 0.000).

A Spearman's correlation coefficient test was used to determine the relationship between species richness and total abundance in each habitat. Analysis revealed a weak, negative monotonic correlation between species richness and total abundance in both Alton and Ardleigh littoral habitats and Alton pelagic. In Ardleigh pelagic, no correlation was identified between the values however; their relationship was found to be linear. Significance tests confirmed correlation outputs in both Alton habitats but not in Ardleigh (Table 2.1).

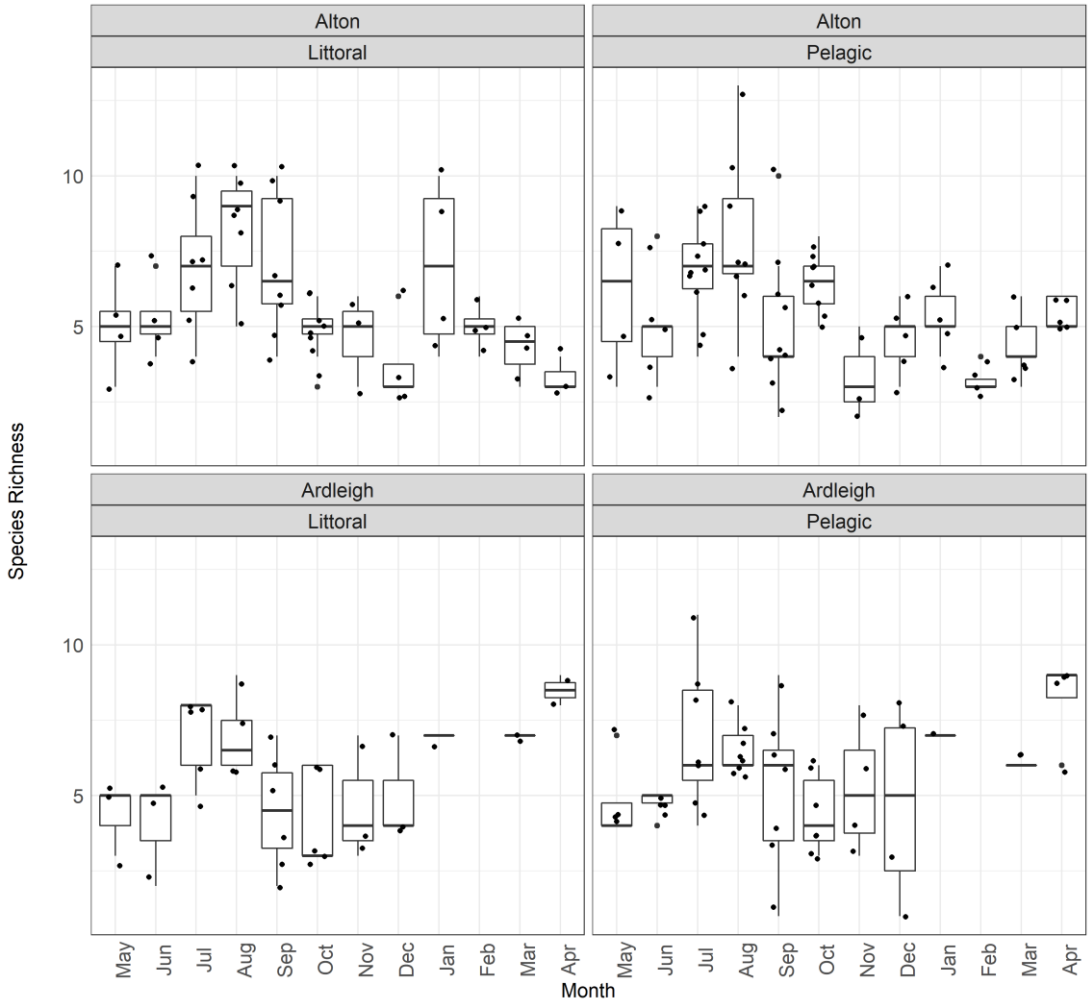

Figure 2.6 Mean species richness in Alton Water and Ardleigh Reservoirs between two habitats (littoral and pelagic) and over a temporal scale of 12 months (May 2017 – April 2018). For each boxplot, the boundary of the box closest to zero indicates the 25th percentile, the black line within the box indicates the median, and the boundary of the box farthest from zero indicates the 75th percentile. Whiskers above and below the box mark the 10th and 90th percentiles while the points above and below the whiskers indicate outliers outside the 10th and 90th percentiles.

Table 2.1 Spearman's rho correlation coefficients of species richness and total abundance for littoral and pelagic habitats in Alton and Ardleigh reservoirs. A coefficient between 1 and 0 indicates a positive correlation, a coefficient at 0 indicates potentially no correlation, and a coefficient between 0 and -1 indicated a negative correlation. The further from zero, the stronger the positive or native relationship. Sig. (2-tailed) is the p-value which identifies the significance of the correlation between the variables.

Spearman's rho			Species Richness	Abundance
Alton Littoral				
	Species Richness	Correlation Coefficient	1.0	-0.386
		Sig. (2-tailed)	.	0.002
		N	8	8
	Abundance	Correlation Coefficient	-0.386	1.0
		Sig. (2-tailed)	0.002	.
		N	8	8
Alton Pelagic				
	Species Richness	Correlation Coefficient	1.0	-0.340
		Sig. (2-tailed)	.	0.003
		N	8	8
	Abundance	Correlation Coefficient	-0.340	1.0
		Sig. (2-tailed)	0.003	.
		N	8	8
Ardleigh Littoral				
	Species Richness	Correlation Coefficient	1.0	-0.205
		Sig. (2-tailed)	.	0.222
		N	8	8
	Abundance	Correlation Coefficient	-0.205	1.0
		Sig. (2-tailed)	0.222	.
		N	8	8
Ardleigh Pelagic				
	Species Richness	Correlation Coefficient	1.0	0.061
		Sig. (2-tailed)	.	0.67
		N	8	8
	Abundance	Correlation Coefficient	0.061	1.0
		Sig. (2-tailed)	0.67	.
		N	8	8

2.2.2.3 Diversity Indices

Both Shannon and Simpson Diversity Indices identified the littoral habitat in Oct (Alton) and Jun (Ardleigh) to have the lowest diversity. In the pelagic, the lowest diversity also occurred in Oct for Alton but in Sep for Ardleigh. Highest Shannon diversity was found in May (Alton) and Dec (Ardleigh) in the littoral and Jul (Alton) and May (Ardleigh) in the pelagic (Fig. 2.7).

A Spearman's correlation coefficient test was used to determine the relationship between Shannon (Fig. 2.8) and Simpson (Fig. 2.9) diversity indices and total abundance in each habitat. In the shallow littoral, analysis revealed a significantly strong negative correlation in both Alton (Shannon; R = -0.669, $P < 0.000$, Simpson; R = -0.631, $P < 0.000$) and Ardleigh (Shannon; R = -0.802, $P < 0.000$, Simpson; R = -0.784, $P < 0.000$). The pelagic also revealed a significantly strong negative correlation in Alton (Shannon; R = -0.726, $P < 0.000$, Simpson; R = -0.661, $P < 0.000$) and a significant negative correlation in Ardleigh (Shannon; R = -0.483, $P < 0.000$, Simpson; R = -0.483, $P < 0.000$).

The relationship between biomass (as chlorophyll-a) and Shannon and Simpson diversity indices were also investigated. However, no correlations were identified in either Alton littoral (Shannon; R = 0.065, $P = 0.618$, Simpson; R = 0.013, $P = 0.916$) or Alton pelagic (Shannon; R = 0.035, $P = 0.771$, Simpson; R = -0.010, $P = 0.932$). In Ardleigh, a weak, negative correlation was found in both habitats however they were not found to be significant (littoral-Shannon; R = -0.390, $P = 0.023$, littoral-Simpson; R = -

0.384, *P* = 0.278, pelagic-Shannon; R = -0.159, *P* = 0.285, pelagic-Simpson; R = -0.169, *P* = 0.254).

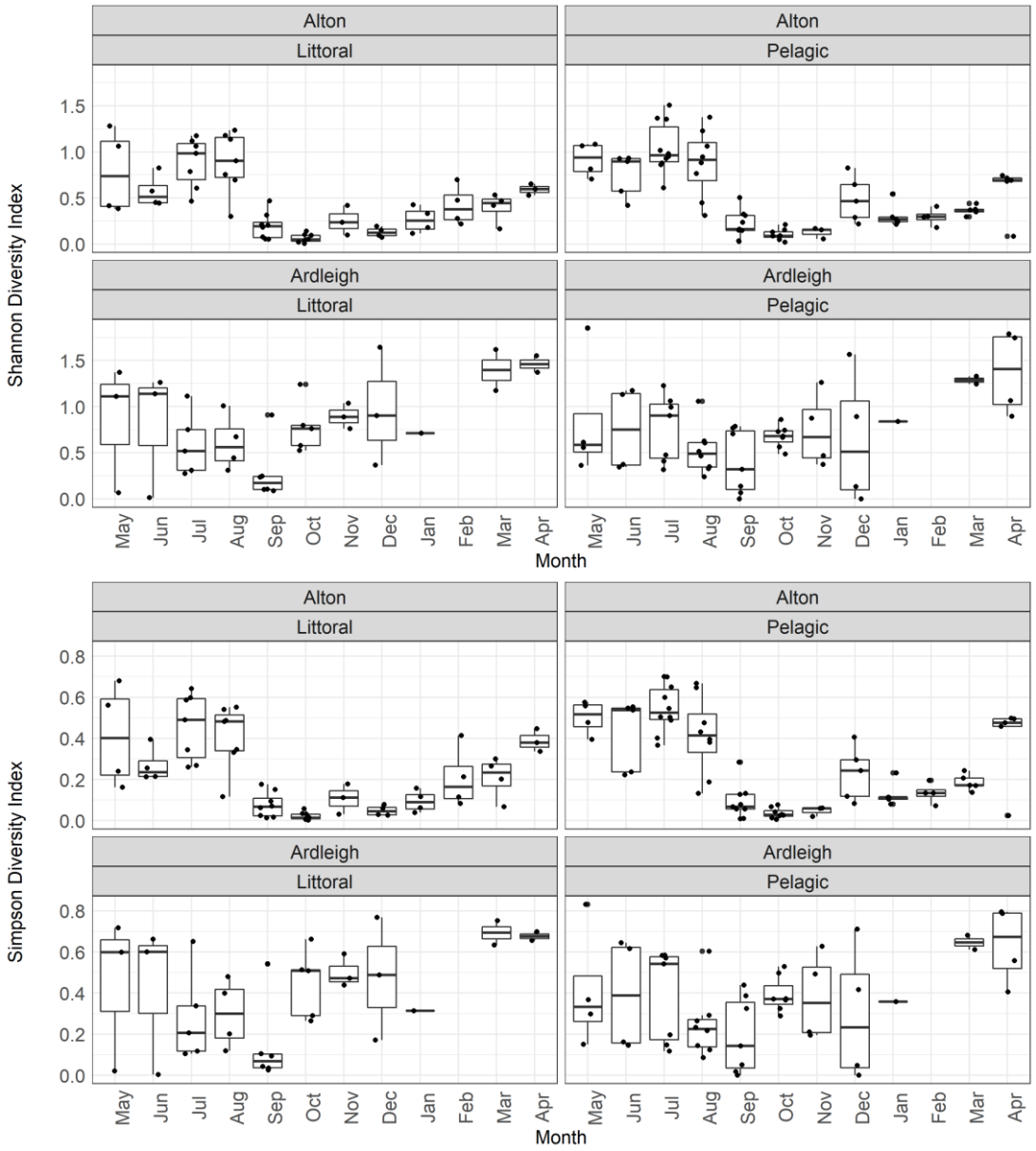

Figure 2.7 Shannon and Simpson diversity indices for Alton and Ardleigh reservoirs between the littoral and pelagic from May 2017 – April 2018. For each boxplot, the boundary of the box closest to zero indicates the 25th percentile, the black line within the box indicates the median, and the boundary of the box farthest from zero indicates the 75th percentile. Whiskers above and below the box mark the 10th and 90th percentiles while the points

above and below the whiskers indicate outliers outside the 10th and 90th percentiles.

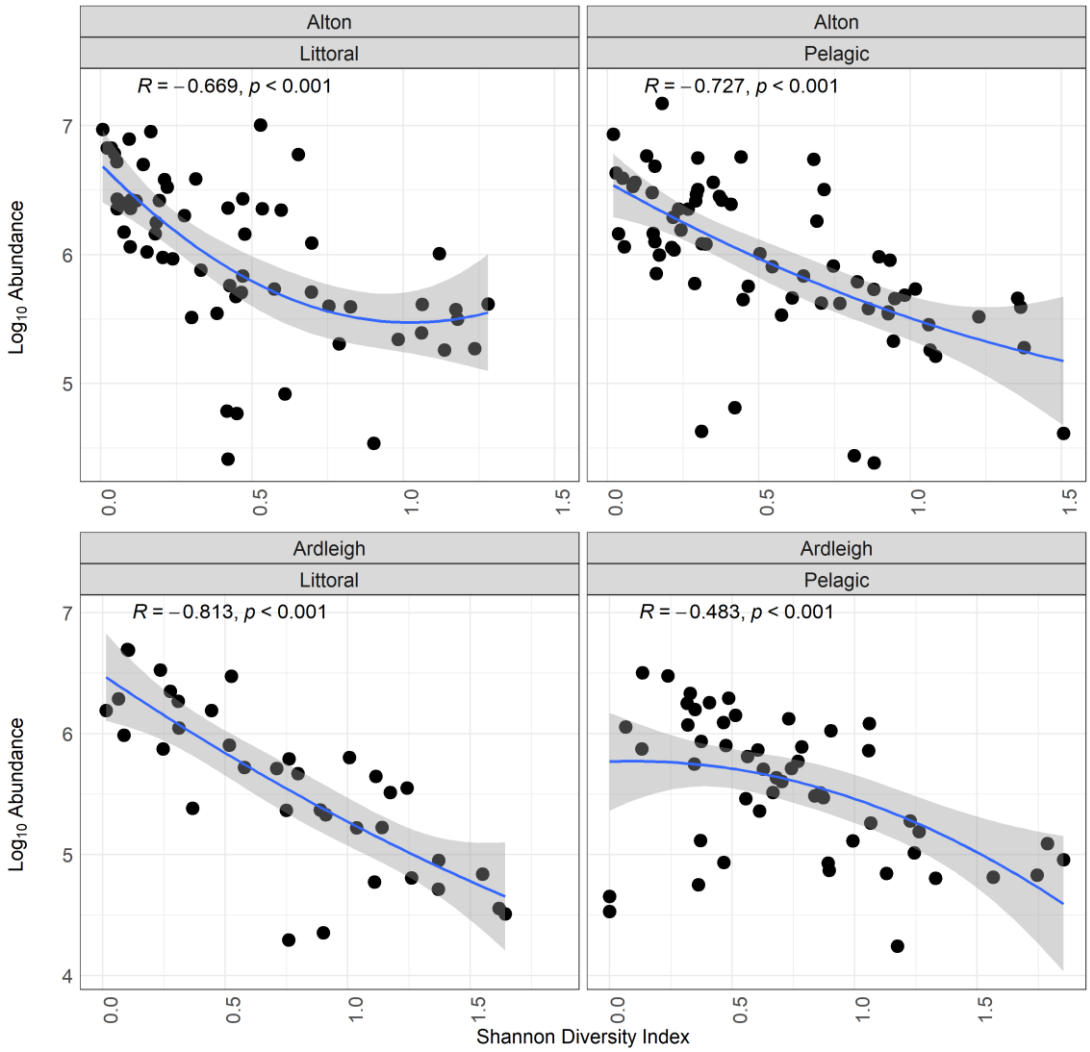

Figure 2.8 The correlation between total abundance and the Shannon diversity index for Alton (top) and Ardleigh (bottom) phytoplankton communities within the littoral and pelagic habitats. Each point represents a single replicate within the habitat from May 2017 – April 2018. The shaded area represents the 95% confidence interval of the fitted linear model. R denotes the Spearman rho correlation coefficient where the *P*-value is the significance of the correlation.

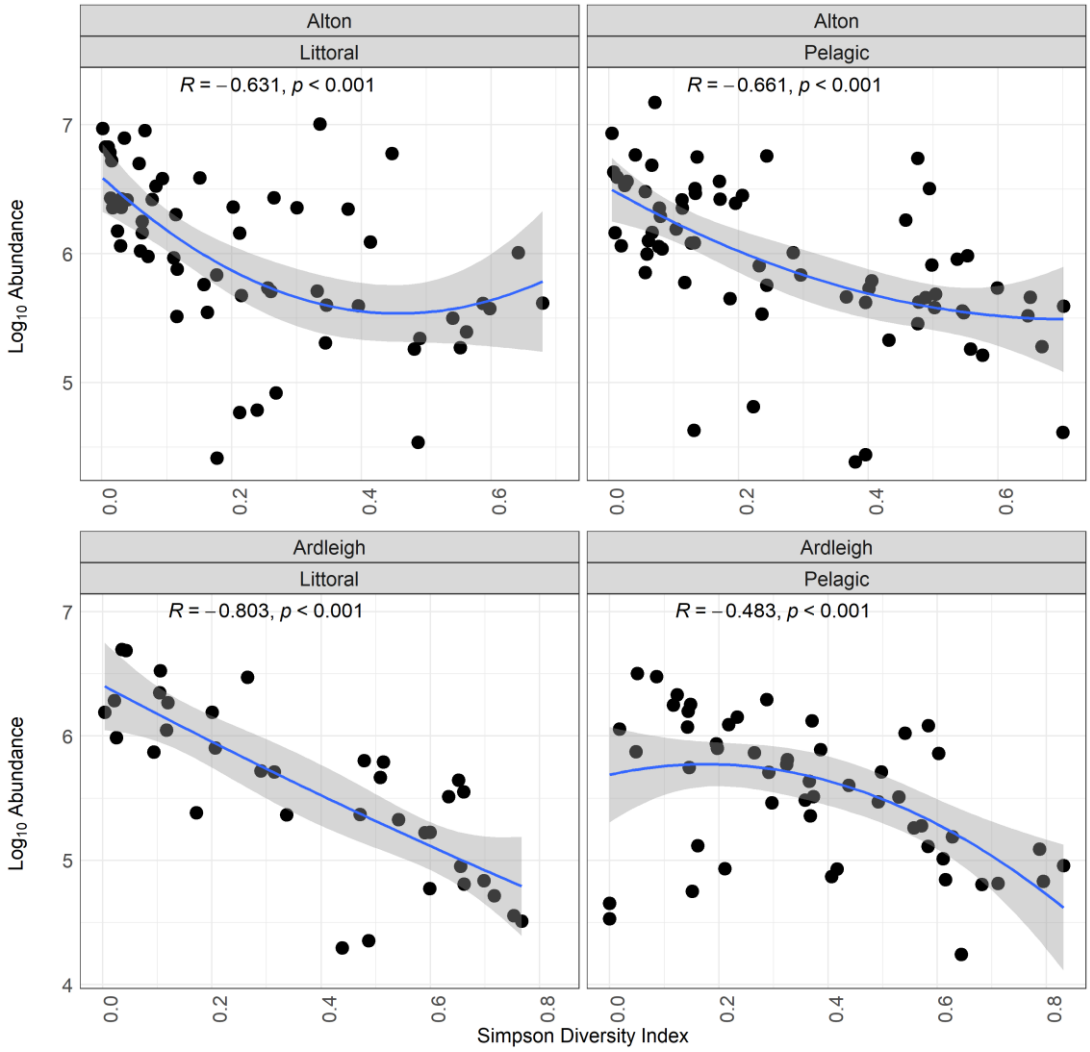

Figure 2.9 The correlation between total abundance and the Simpson diversity index for Alton (top) and Ardleigh (bottom) phytoplankton communities within the littoral and pelagic habitats. Each point represents a single replicate within the habitat from May 2017 – April 2018. The shaded area represents the 95% confidence interval of the fitted linear model. R denotes the Spearman rho correlation coefficient where the *P*-value is the significance of the correlation.

2.2.3 Community Composition

2.2.3.1 Microscopy

At the genus level, *Microcystis spp*. was the dominant species in both the littoral and pelagic habitats of Ardleigh reservoir. It appeared as the most dominant in 10 of the 11 months in the littoral and 8 out of 11 months in the pelagic. In the littoral only Apr was the exception where *Dinobryon spp.* dominated. In the pelagic, the additional dominant species included *Fragilaria spp., Coelastrum spp*., and *Melosira spp.* At the draw-off tower, dominant species varied from the other pelagic sites including *Oscillatoria spp*. in Apr and *Pediastrum spp.* in Jun (Table S2.1).

The least common or rarest species in Ardleigh littoral included *Scenedesmus spp.* (Jan), *Peridinium spp*. (Mar, Aug, Dec), *Chlamydomonas spp*. (Mar, Apr), *Ankyra spp*. (Apr), *Mallomonas spp*. (Apr and Aug), *Closteriopsis spp*. (May), *Bacillariophyceae* (Jun, Aug and Sep), *Staurastrum spp*. (Aug), and *Euglena spp*. (Oct). In the pelagic, the same species were found that were in the littoral with the addition of *Oscillatoria spp*. and *Asterionella spp*. The draw-off tower showed similar species as the pelagic aside from Sep where the least common species was *Stephanodiscus spp*. (Table S2.2).

In Alton, *Aphanizomenon spp*. was the dominant species in both the littoral and pelagic habitats. It appeared as the most dominant 10 of the 12 months in the littoral and 11 out of 12 months in the pelagic. In the littoral only Apr (*Oscillatoria spp.*) and May (*Gomphosphaeria spp*.) were the exception. In the

pelagic, the additional dominant species included *Coelastrum spp*. in May. (Table S2.3).

The least common species in Alton littoral included *Rhodomonas spp.* (Jan and Dec), species (*Bacillariophyceae*) (Jan, Sep, Oct, and Nov), *Stephanodiscus spp.* (Feb), *Closterium* spp. (Mar, Apr), *Gymnodinium spp.* (Mar), *Trachelomonas spp.* (May), *Ceratium spp.* (Jun, Jul), *Chlamydomonas spp*. (Jul), *Euglena spp*. (Jul, Dec), *Closteriopsis spp*. (Jul), *Cosmarium* spp. (Aug), *Mallomonas spp*. (Sep), *Peridinium spp*. (Sep), *Staurastrum spp*. (Sep, Oct). In the pelagic, the same species were found that were in the littoral with the addition of *Oocystis spp.* and *Asterionella spp*. At the draw-off tower, the least common species differed from the pelagic in every month (Table S2.4).

NMDS analysis of microscopy data did not present a clear distinction in community composition between littoral and pelagic habitats in either Alton (Fig. 2.10) or Ardleigh (Fig. 2.11). PERMANOVA analysis, confirmed NDMS visualization and found habitat had no significant effect on community composition (Alton; pseudo-$F_{1, 129} = 0.473$, $R^2 = 0.003$, $P = 0.651$; Ardleigh; pseudo-$F_{1, 87} = 0.484$, $R^2 = 0.005$, $P = 0.564$).

In Alton, NMDS analyses presented potential, reservoir-wide separation of months (Jun and Oct) from the main cluster (Fig. 2.10). PERMANOVA analysis confirmed this dissimilarity in community composition between months was significant (pseudo-$F_{11, 119} = 6.326$, $R^2 = 0.369$, $P = 0.001$). In Ardleigh, NMDS visualization of microscopy data did not present a clear

distinction between months however, PERMANOVA analysis did identify significant dissimilarity in community composition between months (pseudo-$F_{10, 78} = 8.296$, $R^2 = 0.515$, $P = 0.001$) (Fig. 2.11).

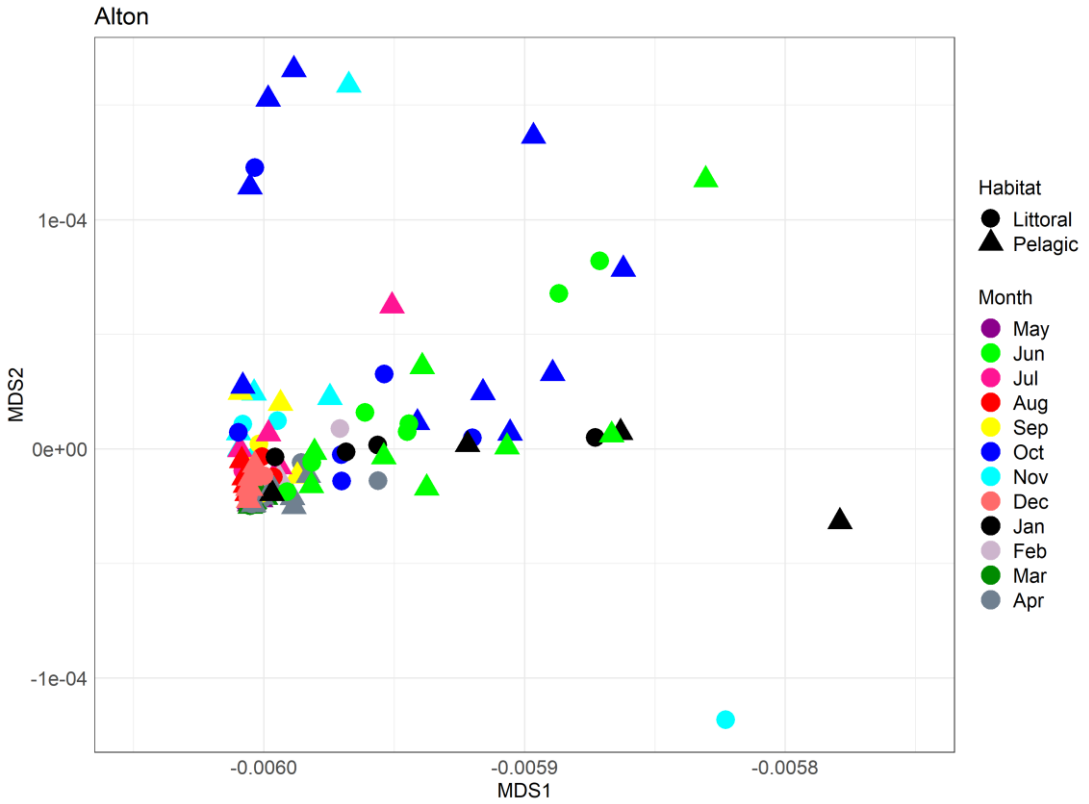

Figure 2.10 Nonmetric multidimensional scaling (NMDS) analysis of microscopy phylum-level phytoplankton communities in Alton Water (2017-2018). Each point represents a single community in each habitat and during a certain month. Points closer together represent more similar communities.

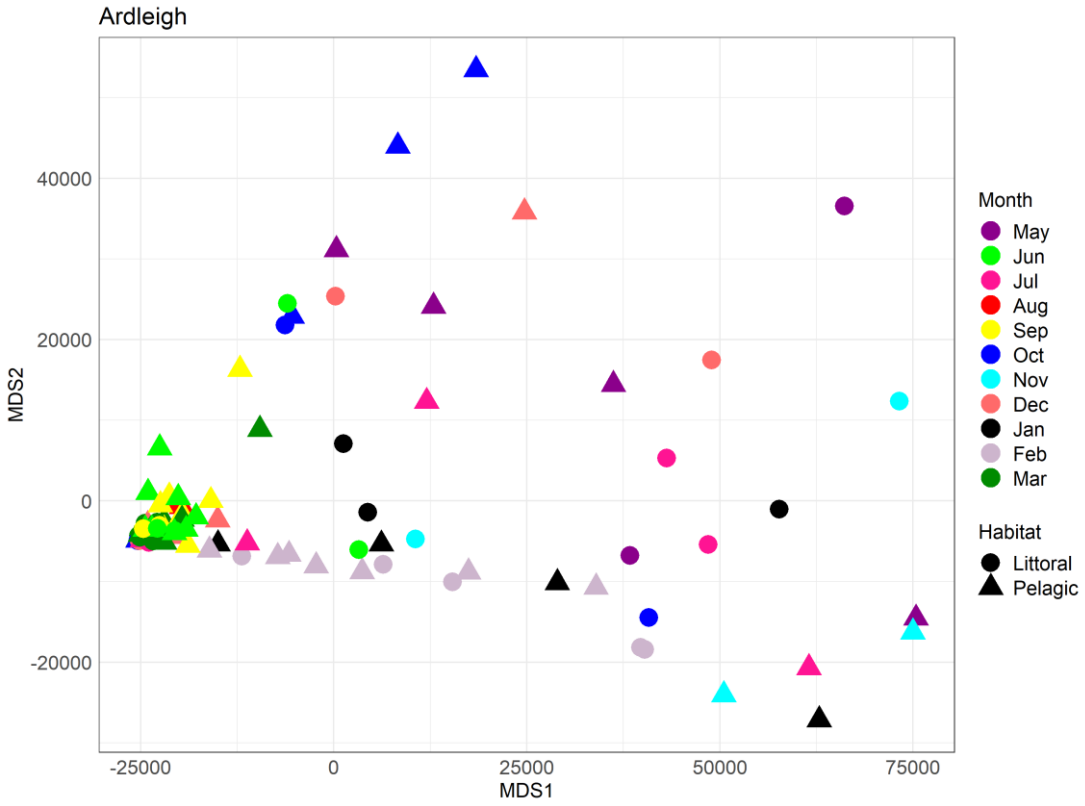

Figure 2.11 Nonmetric multidimensional scaling (NMDS) analysis of microscopy phylum-level phytoplankton communities in Ardleigh reservoir (2017-2018). Each point represents a single community in each habitat and during a certain month. Points closer together represent more similar communities.

2.2.3.2 In situ Fluoroprobe

NMDS analysis of *in situ* fluoroprobe data did not present a clear distinction in community composition between littoral and pelagic habitats in either Alton (Fig. 2.12) or Ardleigh (Fig. 2.13). PERMANOVA analysis, confirmed NDMS, found habitat had no significant effect on community composition (Alton; pseudo-$F_{1, 58} = 2.214$, $R^2 = 0.036$, $P = 0.112$; Ardleigh; pseudo-$F_{1, 47} = 1.418$, $R^2 = 0.029$, $P = 0.243$).

In Alton, NMDS analyses presented potential, reservoir-wide clustering during spring/summer months (May – Aug) and autumn/winter months (Sep – Dec), with a more clear separation in January (Fig. 2.12). PERMANOVA analysis confirmed this dissimilarity in community composition between months was significant (pseudo-$F_{8, 51}$ = 23.789, R^2 = 0.788, P = 0.001). Similarly, reservoir-wide clustering was observed in Ardleigh during the month of July (Fig. 2.13). PERMANOVA analysis confirmed dissimilarity in community composition between months in Ardleigh was also significant (pseudo-$F_{7, 41}$ = 14.265, R^2 = 0.708, P = 0.001).

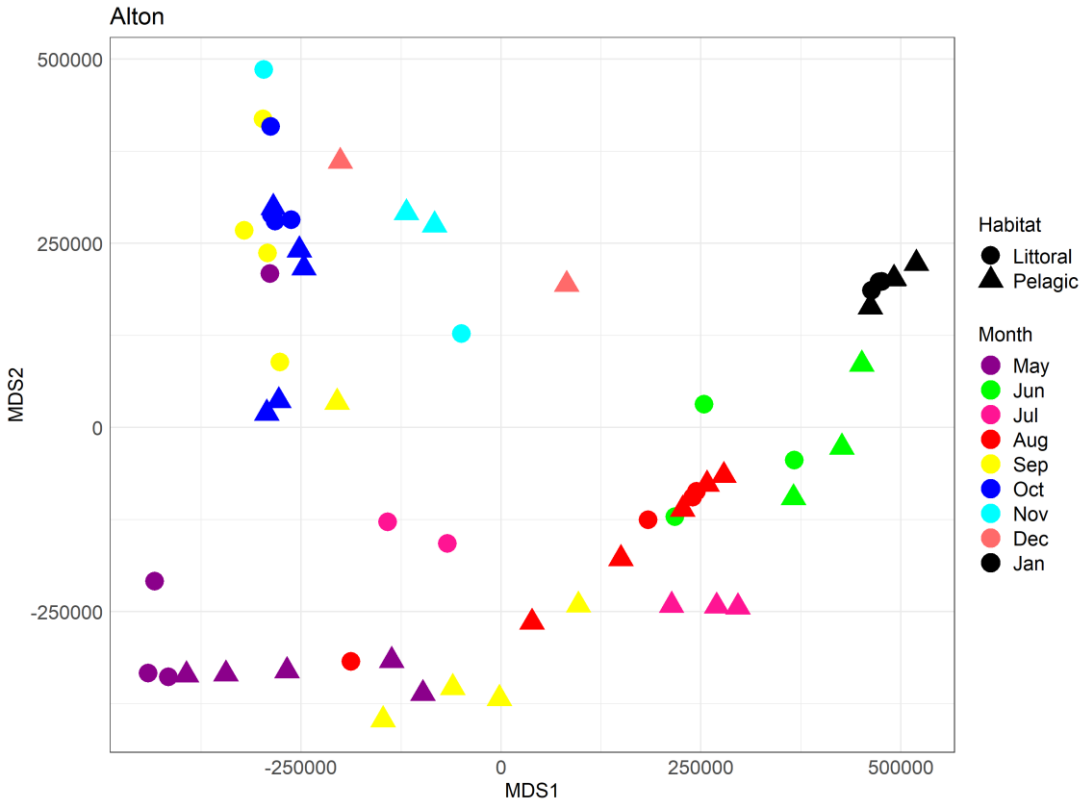

Figure 2.12 Nonmetric multidimensional scaling (NMDS) analysis of *in situ* fluoroprobe phylum-level phytoplankton communities in Alton Water (2017-2018). Each point represents a single community in each habitat and during a certain month. Points closer together represent more similar communities.

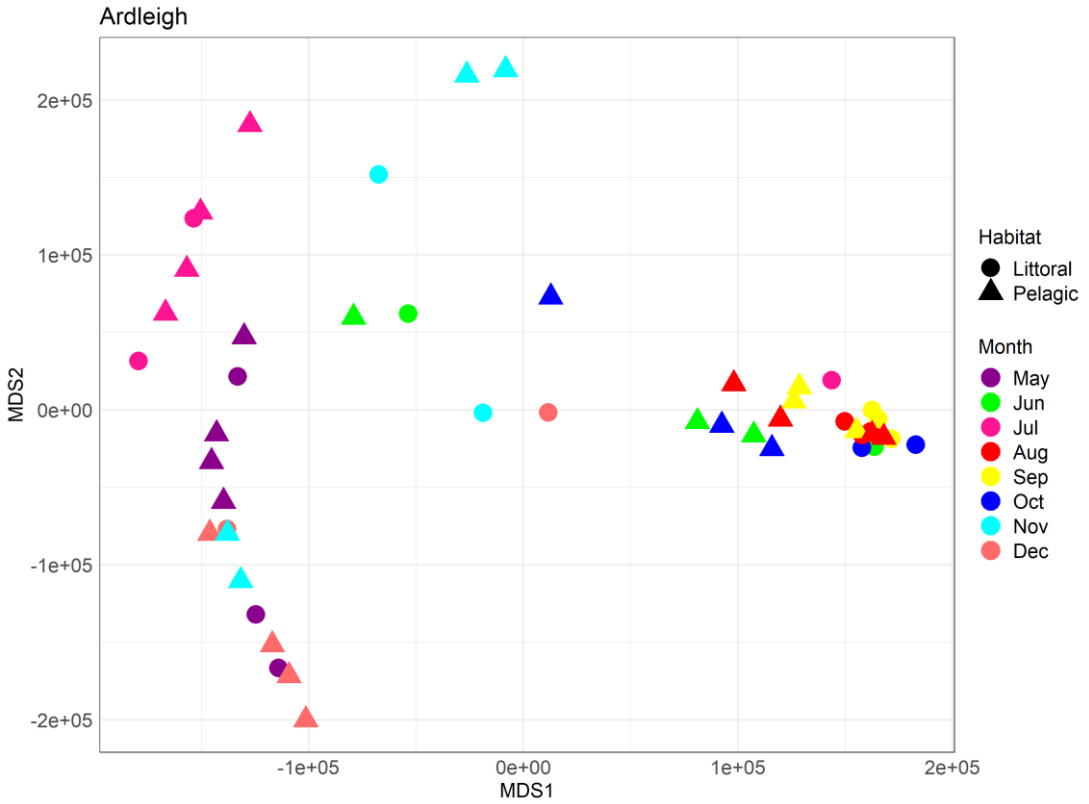

Figure 2.13 Nonmetric multidimensional scaling (NMDS) analysis of in situ fluoroprobe phylum-level phytoplankton communities in Ardleigh Reservoir (2017-2018). Each point represents a single community in each habitat and during a certain month.

2.2.4 Spectrofluorometery versus Microscopy

To compare phytoplankton quantification methods, the percent contribution of each of the four major classes (cyanobacteria, green algae, diatoms, and cryptophyta) to the total community was calculated for each method. For cyanobacteria, microscopy found 52% more cyanobacteria than the fluoroprobe. Diatom's contribution to the total community was 56% lower using microscopy than the fluoroprobe, cryptophyta was 82% lower than the fluoroprobe results, and for green algae, microscopy found 92% less green algae than the fluoroprobe (Fig. 2.14 and Fig. 2.15).

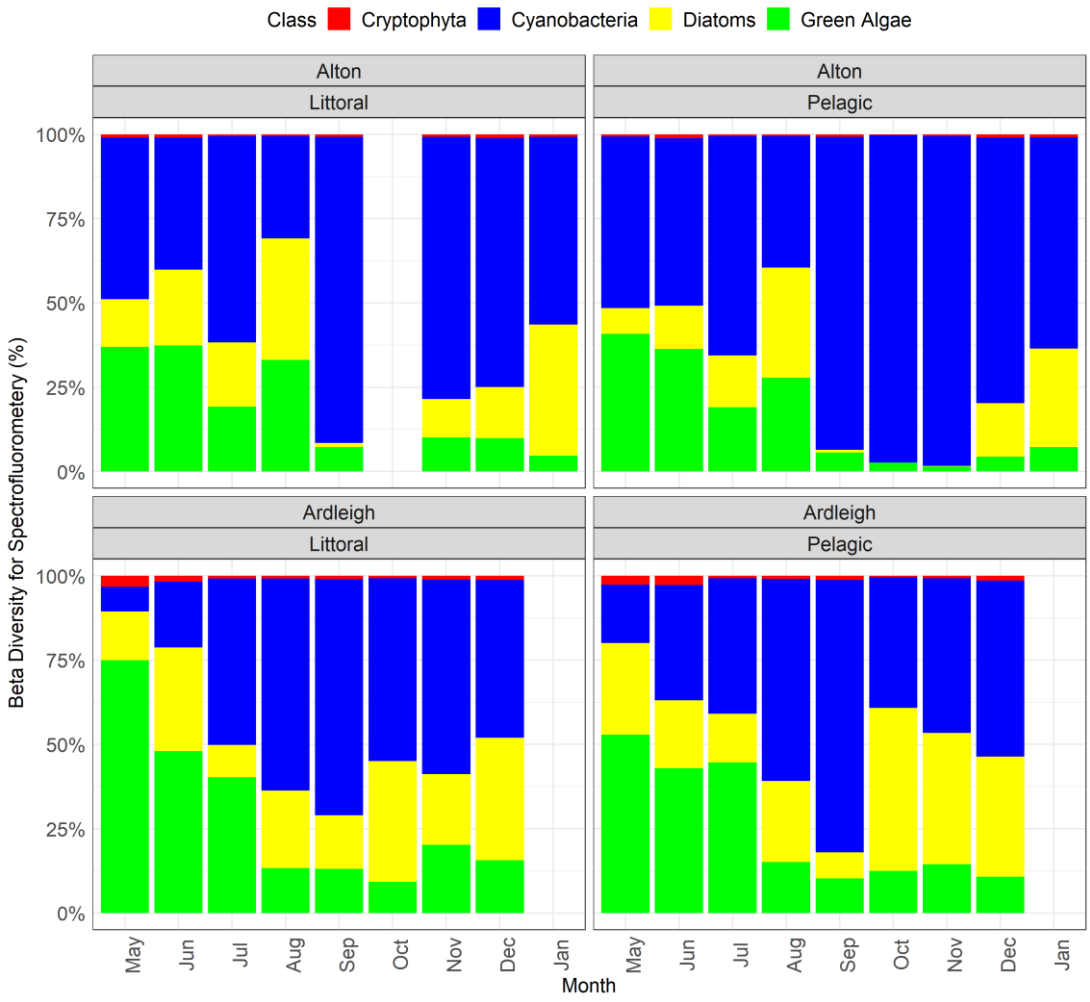

Figure 2.14 Stacked bar chart of fluoroprobe community composition depicting phylum-level contribution (%) to the total community in each habitat and across months. Red bars = cryptophyta, blue bars = cyanobacteria, yellow bars = diatoms, and green bars = green algae. Beta diversity = community composition or relative abundance of a population.

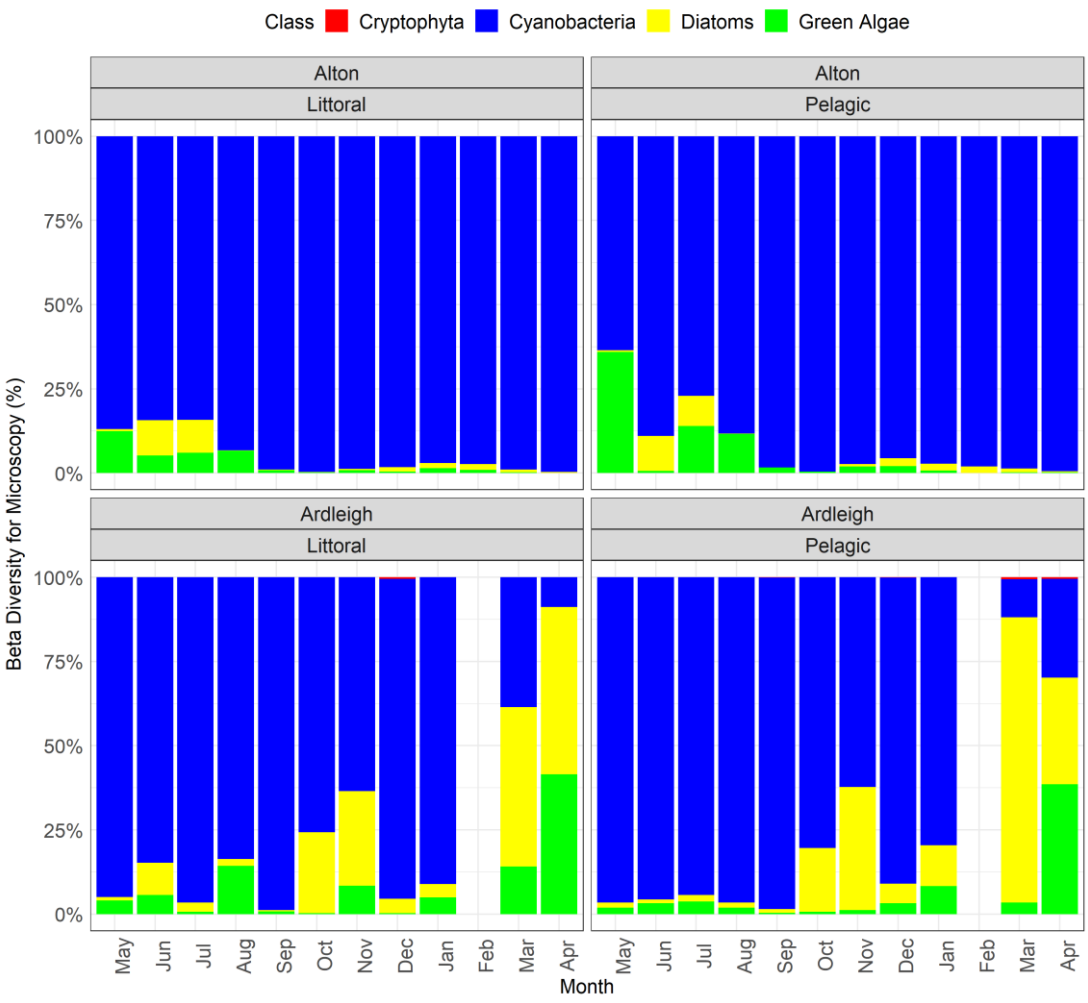

Figure 2.15 Stacked bar chart of community composition by microscopy depicting phylum-level contribution (%) to the total community in each habitat and across months. Red bars = cryptophyta, blue bars = cyanobacteria, yellow bars = diatoms, and green bars = green algae.

2.3 DISCUSSION

2.3.1 Research Question 1: What is the community composition of Alton and Ardleigh and how does it compare to the 1980s and 1990s?

Based on the findings in this study, both reservoirs are quite different now than they were in the 1980s and 1990s. In Ardleigh, species diversity decreased from 58 species (1980s) to 8 (2017) (via microscopy), However, eutrophication and cyanobacteria dominating the summer bloom remains true today. The cyanobacteria *Microcystis* dominated Ardleigh reservoir in both the littoral and pelagic throughout the year. The exception was the spring (Apr) which was dominated by diatoms in the littoral. In addition, the draw off tower showed a different community composition than other pelagic sites in Ardleigh with *Oscillatoria* (cyanobacteria) and *Pediastrum* (green algae) also dominating. As such, a single pelagic sample may overestimate these species, as they were not dominant in any other part of the reservoir.

In Alton, the reservoir was healthier in the 1990s than it is today. In the 90s, the reservoir was in a clear water phase, dominated by macrophytes, and classified as mesotrophic. Today, Alton is dominated by cyanobacteria, experiences almost year-round HABs, and is classified as eutrophic. The cyanobacteria *Aphanizomenon* dominated in almost every month and in both habitats. The exception was spring, which was dominated by another cyanobacteria (*Oscillatoria*). In both reservoirs, habitat was found to have no effect on phytoplankton community composition overall, however, community composition was different temporally.

2.3.2 Research Question 2: Is there a relationship between biomass, abundance, and functional diversity within habitats?

In both Alton and Ardleigh littoral and Alton pelagic, species richness decreased with an increase in total cell counts. In Ardleigh Pelagic, no correlation was identified. The relationship between total abundance and diversity was also negative where diversity within the community decreased with an increase in cell count. This was the case for both habitats and both reservoirs. Among biomass and diversity, no correlation was found in Alton littoral or pelagic. However, in Ardleigh, as biomass increased, diversity decreased. This relationship however was weak. A decrease in biodiversity with an increase in abundance is comparable to an eight-year study of a tropical, shallow reservoir in Brazil where an increase in eutrophication led to a 37% decrease in phytoplankton biodiversity while simultaneously decreasing as cyanobacteria blooms increased (Crossetti et al., 2008).

2.3.2 Research Question 3: Community composition is currently assessed from one sample in the pelagic habitat (draw-off tower), is this sample representative of the reservoir as a whole?

To investigate the validity of a single pelagic sample being representative of the entire reservoir, biomass, total abundance, species richness, and Shannon and Simpson diversity indices were measured on a spatial and temporal scale. In Alton, biomass did not differ between habitats during any month except Aug where the littoral had slightly higher biomass than the pelagic. Ardleigh was spatially and temporally more variable where the littoral had greater biomass in summer and autumn. As with Alton, Aug also had the

largest difference in biomass in any month. Total abundance presented similarly to biomass where no significant difference between habitats was observed in any month or in either reservoir.

Species richness also did not differ between habitats in either reservoir. However, the range in Alton was 3-10 species in the littoral and 2-13 species in the pelagic. These can be regarded as quite similar however; the month of Sep in Alton was a month with the lowest species richness in the pelagic but the highest in the littoral. Therefore, in the month of Sep, sampling only the pelagic would severely underestimate the number of species present in the reservoir.

Amongst phytoplankton diversity, both the littoral and pelagic of Alton were temporally the same when looking into the minimum diversity of the reservoir however, the highest diversity was found in May in the littoral and Jul in the pelagic. Based on this, a single pelagic sample may underestimate phytoplankton diversity at any given time. This is more so the case for Ardleigh where neither high nor low diversity matched temporally in either habitat. Therefore, a pelagic sample should not be used to access phytoplankton biodiversity in Ardleigh reservoir.

2.3.4 Research Question 4: In this study, both microscopy and *in situ* spectrofluorometery were used to assess community composition, how do these methods compare at the phylum level?

Based on this study, spectrofluorometery and microscopy are not comparable. The difference between microscopy community composition and an *in situ* fluoroprobe was significant. Microscopy found over 50% more cyanobacteria than the fluoroprobe but 92% less green algae. Based on these classes alone, microscopy may cause unnecessary management decisions by overestimating cyanobacteria while the fluoroprobe could increase risk by underestimating communities. However, it is not possible to know which method is the most accurate without individual assessment against more advanced methodologies such as real-time qPCR or High Performance Liquid Chromatography (HPLC). In a study of coastal lagoons in the Mediterranean, biomass and phytoplankton group data were found to be significantly correlated to HPLC results under varying tropic states (Garrido et al., 2019). Conversely, in a methods comparison study in US reservoirs, quantitative real-time PCR was able to detect species that microscopy could not while reducing analysis time by 92%, increasing the detection limit, and reducing the limitations of human error and bias (Zamor et al., 2012).

CHAPTER 3

CYANOTOXIN PROFILES AND THE ASSOSCIATED BIOGEOCHEMISTRY OF TWO DRINKING WATER RESERVOIRS IN THE EAST OF ENGLAND

3.0 INTRODUCTION

Cyanobacteria are photosynthetic prokaryotic bacteria (Gupta et al., 1999) best known for producing a variety of potent toxins, commonly referred to as cyanotoxins. Microcystin (MC) is the most common cyanotoxin as well as the most studied (Munoz et al., 2019). Microcystin is a hepatotoxin (i.e. damaging to the liver) and a powerful tumour promoter (Sun et al., 2014) with more than 130 known variants (e.g. MC-LR) (Carmichael and Boyer, 2016). Globally, MC-LR is the most studied of these variants followed by MC-RR (De Figueiredo et al., 2004).

In recent years, cyanotoxin research has expanded from the hepatotoxins to explore those that induce neurotoxicity. Currently, three main cyanobacterial neurotoxins are identified: anatoxin, L-beta-N-methylamino-L-alanine (BMAA), and saxitoxin (Corbel et al., 2014). Anatoxin-a is an alkaloid neurotoxin and powerful agonist of nicotinic acetylcholine (nACh) receptor proteins (found in the central nervous system) (Wonnacott and Gallagher,

2006). Actions against nACh by anatoxin-a may promote tumours, interfere with fetal development, and cause death (Sanchez et al., 2014).

In alkaline waters (i.e. pH > 8), anatoxin-a is very unstable, rapidly transforming from toxic to non-toxic during photochemical degradation (Florczyk et al., 2014). Yet, it is associated with the contamination of drinking water supplies around the world as well as the death of domestic animals (Farrer et al., 2015). In the UK, an outbreak of acute poisoning in Loch Insh, Scotland (1990 and 1991) was the first to identify benthic *Oscillatoria* toxicoses in numerous dog deaths. Associations prior to this discovery link anatoxin-a toxicoses with planktonic cyanobacteria only (Edwards et al., 1992).

Cyanobacteria and their toxins thrive in warm, eutrophic waterbodies (Paerl et al., 2001). When conditions are ideal, cyanobacteria experience rapid increases in biomass on the water's surface forming a visual mat of blue-green scum (Oyama et al., 2015). This accumulation is known as a Harmful Algal Bloom or HAB. HABs may be predominantly toxic or non-toxic depending on the algal community composition. When environmental conditions such as light, temperature, and nutrients are favourable for cell growth (non-limiting), non-toxic strains have been found to out compete toxin-producing strains. Conversely, when environmental conditions did not favour cell/population growth, toxin-producing strains outcompeted non-toxic strains (Briand et al., 2008). In nutrient growth experiments, rates of toxic *Microcystis* strains increased significantly as temperature increased (83% of experiments)

while only 33% of experiments saw an increase in growth rates for non-toxic strains (Davis et al., 2009).

Increased water temperatures are known to correlate with increased growth rates among cyanobacteria where they often thrive in temperatures above 25°C (Paerl and Otten, 2013b). This is a higher tolerance compared to other species such as diatoms or green algae. Cyanobacteria thus gain an advantage over competing phytoplankton as average water body temperatures increase (Paerl and Huisman, 2008). Higher temperatures also create a more stable water column by decreasing vertical mixing. Toxic, buoyant cyanobacteria will out compete non-toxic strains under these conditions, in turn creating blooms that are more likely to be toxic (Johnk et al., 2008). In addition, studies of the Grangent reservoir in France identified toxin-producing genotypes to dominate pre and post bloom while during the bloom, *Microcystis* strains favoured non-toxin forming cells (Briand et al., 2009).

Cyanobacteria dominated blooms are increasing each year as summers become warmer and winters more mild (Paerl and Huisman, 2009). In shallow drinking water reservoirs, these blooms produce taste and odor compounds (Jüttner and Watson, 2007; Medsker et al., 1968), deplete oxygen levels to fish stocks (Rabalais et al., 2010), clog expensive filtration systems (Westrick et al., 2010) and have the potential to negatively affect human health through contaminated fish consumption (Hardy et al., 2015) and direct exposure from recreational activities in or near the water (Chorus et al., 2000). Despite this,

the UK applies a response-based approach to public health where only cell counts are used for management decisions and recreational closures. However, it has been suggested that cell counts do not correlate well with toxicity and do not provide an accurate measure of risk to make informed public health decisions (Turner et al., 2018). To accomplish a risk-based approach, site-specific toxin profiles (identification of the community composition) of the dominant bloom and their driving biogeochemical parameters must be assessed. This is especially true for reservoirs in the East of England which experience multi-stressors from climate change such as the lowest annual rainfall of anywhere in the UK (John C. Rodda, 2006; Todd et al., 2013). Additionally, based on data presented in chapter 2, we know reservoirs in the East of England are shallow, eutrophic, well mixed and exhibit almost uniform biodiversity throughout the waterbody. It was also found the summer blooms in these reservoirs were dominated by cyanobacteria, which may contain neuro and hepato-toxins. To assess the potential risk of these blooms, this study measured the toxicity of summer/ autumn phytoplankton blooms in 2017 (i.e. toxic versus non-toxic strains) of two reservoirs and the biogeochemical parameters that may be driving their community composition. Specifically, the following research questions were studied, (1) How toxic are the summer blooms in the East of England? (2) What is the Microcystin community composition within each bloom and which variants dominate throughout the year? (3) Is there a relationship between reservoir biogeochemistry and bloom toxicity?

3.1 METHODS

3.1.1 Study Sites

The sites for this study include two polymictic reservoirs, which supply drinking water from catchments impacted by climate change (i.e. drought) in the East of England (Cambridgeshire, Essex, Norfolk, and Suffolk). Due to commercial sensitivity, they have not been named.

3.1.2 Sample Collection

Plankton net sample collection procedures follow those presented in Chapter 2, Section 2.2.3.2

3.1.3 Biogeochemical Parameters

3.1.3.1 Environmental

Surface water measurements included pH, conductivity (ppm), temperature (°C), and Secchi depth (as a proxy for turbidity). Surface temperature and pH were collected using a YSI pH meter with internal temperature calibration. The pH probe was submerged for one-minute and the final reading recorded on field data sheets. Conductivity readings were collected using a portable conductivity probe and Secchi depth was measured using a 20 cm black and white disk with pre-marked 50 cm intervals. The disk was lowered off the shaded side of the boat until it could no longer be seen. The disk was then raised until visible again, where the Secchi depth was recorded. For shallow areas where visual depth equals bottom depth, Secchi depth was recorded as bottom depth.

3.1.3.2 Anions

Surface water samples at each replicate site were captured by taking 20 mL from the top one-meter of the water column. Samples were filtered *in situ* using a 20 mL syringe and 25 mm MF300 glass microfiber filter (Fisher brand). Samples were then frozen at -20°C until analysis.

Analysis of dissolved anions (fluoride, acetate, formate, chloride, sulphate, and ascorbic acid) was performed using a Dionex ICS-3000 Ion Chromatography System, ICS-3000 (LabX Model: Dionex-04-0660). Methods for anion quantification followed U.S EPA Method 300.0 (A and B) and 300.1 (A and B) (U.S. Environmental Protection Agency, 1993). To calibrate the ICS and ensure quality chromatograph peaks, a mixed standard of all anions was prepared for each analysis or batch run. A set of five standards were used at 200, 100, 50, 25, and 12.5 µg/L. First, 2.8 mL of mixed standard (1000 mM) was added to 11.2 mL of milli-Q water to acquire 14 mL of a 200 µg/L standard. Then 7 mL of the 200 µg/L standard was added to 7 mL of milli-Q for 14 mL of 100 µg/L standard. This procedure was repeated for the remaining standards.

3.1.3.3 Nutrients

The determination of ammonium (NH_4^+), phosphate (PO_4^{3-}), nitrate (NO_3^-) and nitrite (NO_2^-) was performed on a SEAL Analytical AA3 HR Auto Analyzer tandem JASCO FP-2020 Plus fluorescence detector. For each nutrient, concentrations were measured according to the following methods; ammonia (G-327-05 Rev.6), phosphate (G-297-03 Rev.5), and nitrate and nitrite (G-

172-96 Rev.13). Prior to analysis, all glassware used for phosphate analysis was pre-digested in a 12% HCL acid and MilliQ mixture and autoclaved.

3.1.4 Cyanobacteria Community Composition

Cyanobacteria community composition quantification (via microscopy) follows those methods used for all phytoplankton and are presented in Chapter 2, Section 2.2.3.2.

3.1.5 Microcystin Sample Preparation

Surface samples collected for toxin analysis were filtered in the lab using 47 mm binder-free glass microfiber GF/F filter (GE Whatman 1825-047) and stored in 8 mL borosilicate glass vials containing 90% methanol and stored at -20°C until analysis.

Prior to analysis, cyanobacterial cells were lysed using three rounds of freezing and thawing. The third and final thawing occurred just prior to 1:30 (30 seconds on and 30 seconds off) of sonication. Samples were then centrifuged at 4000 rpm for five minutes. The supernatant was extracted and 1 mL of sample was pipetted into Phenomenex® Verex 2 mL amber glass vials with PTFE/Silicone pre-slit screw top lids (Part No. AR0-9926-13-C, Lot No. 24130859).

3.1.6 Quantification of Microcystin

3.1.6.1 Chemicals and Reagents

Mobile phases were prepared using LC-MS-grade acetonitrile (Fisher Optima, ThermoFisher, Greater London, UK) and deionized water (DI). All other reagents used were HPLC grade. Calibration curve standards were obtained from Enzo Life Sciences, Exeter, UK and the Institute of Biotoxin Metrology, National Research Council Canada (NRCC, Halifax, Canada) (Table 3.1).

Reference standards received as solid films were dissolved in 50% aqueous methanol to form stock solutions. The NRCC standard of [Dha^{7}]-MC-LR was received at a certified concentration of 9.4 µg/mL. A mixed stock solution was subsequently prepared by combining aliquots of each stock solution comprising of each analyte at 500 ng/mL, followed by further dilutions to create a dilution series of working calibration standard between 0.50 ng/mL to 500 ng/mL per toxin (*Andy Turner, CEFAS*).

Table 3.1 Microcystin calibration curve standards. All standards except [Dha7] MC-LR were obtained from Enzo Life Sciences, Exeter, UK. A certified standard of [Dha7] MC-LR was obtained from the Institute of Biotoxin Metrology, National Research Council Canada (NRCC, Halifax, Canada).

Analyte	Product Number	Lot
MC-RR	ALX-350-043	C30197
MC-LA	ALX-350-096	L30140
[Dha^{7}]-MC-LR	CRM-dmMCLR	201501
[Asp3] MC-LR	ALX-350-173	L30137
MC-LF	ALX-350-081	L30189
MC-LR	ALX-350-012	L30209
MC-LY	ALX-350-148	L30200
MC-HilR*	ALX-350-177	L30204
MC-LW	ALX-350-080	L30187
MC-YR	ALX-350-044	L30213
MC-HtyR	ALX-350-174	L30194
MC-WR	ALX-350-167	L30218

3.1.6.2 UHPLC-MS/MS Analysis

Chemical analysis of cyanotoxins was conducted using a Waters Acquity UHPLC system (Manchester, UK) coupled to a Waters Xevo TQ tandem quadrupole mass spectrometer (MS/MS). Chromatographic separation was completed through a 1.7 µm, 2.1 × 50 mm Waters Acquity UPLC BEH C18

column in combination with a Waters BEH C18 guard cartridge. Column conditions are presented in Table 3.1. The column was held at +60 °C, and a 5 µL injection volume utilized, together with mobile phase flow rate of 0.6 mL/min.

The UHPLC gradient started at 98% A1, dropping to 75% A1 at 0.5 min holding until 1.5 min, dropping further to 60% A1 at 3.0 min, decreasing further to 50% A1 at 4 min, before a sharp drop to 5% A1 at 4.1 min, holding until 4.5 min before increasing back to 98% A1 for column equilibration at 5 min for a further 0.5 min (Table 3.2). Each instrumental sequence started with a series of instrumental blanks (100% methanol), followed by toxin calibration standards and a microcystin chromatographic retention time marker solution.

Table 3.2 UPLC Gradient

Time (min)	Mobile Phase A	Mobile Phase B
0	98%	2%
0.5	75%	25%
1.5	75%	25%
3.0	60%	40%
4.0	50%	50%
4.1	5%	95%
4.5	5%	95%
5.0	98%	2%
5.5	98%	2%

The Waters Xevo TQ tune parameters were as follows: 150°C source temperature, 600°C desolvation temperature, 600 L/hr desolvation gas flow, 0.15 mL/min collision gas flow. Capillary voltage was held at 1.0 kV. Selected Reaction Monitoring (SRM) transitions were built into the MS/MS method using positive mode acquisition for each toxin. Parent and daughter ions, as well as cone and collision voltages were optimized following experiments whereby pure standards were infused into the mass spectrometer in the mobile phase (Table 3.3). The majority of toxins exhibited unique SRM transitions and chromatographic retention times, resulting in good separation of cyanotoxins over the 5 min run time. The exception was [Dha7]-MC-LR and

[Asp3] MC-LR, which shared the same transitions and could not be completely resolved. These two analytes are therefore reported together (Figure 3.1).

The LC-MS/MS microcystin detection method involved the direct quantitation of cyanotoxin toxins against working standards available as certified reference standards. Quantitation was performed using external calibration and results calculated in terms of µg/L of cultures.

Table 3.3 Positive ion mode SRM transitions used for MC detection and quantitation

Analyte	SRM transitions	Cone, V	CE, eV
MC-RR*	519.9 > **134.9**; 126.9; 102.8	30	30; 50; 70
MC-LA	910.1 > **135.1**; 106.9	35	70: 80
[Dha^{7}]-MC-LR	981.5 > **135.0**; 106.8	75	75: 80
[Asp3] MC-LR	981.5 > **134.9**; 106.9	75	70; 80
MC-LF	986.5 > **213.0**; 135.0	35	60; 65
MC-LR	995.6 > **135.0**; 127.0	60	70; 90
MC-LY	1002.5 > **135.0**; 106.9	40	70; 90
MC-HilR*	1009.7 >**134.9**; 126.9; 106.9	75	75; 90; 80
MC-LW	1025.5 > **134.9**; 126.8	35	65; 90
MC-YR	1045.6 > **135.0**; 126.9	75	75; 90
MC-HtyR	1059.6 > **134.9**; 106.9	75	70; 90
MC-WR	1068.6 > **134.9**; 106.9	80	75; 100

CE = Collision energy. *3 SRM transitions used for detection and conformation. Primary SRM transitions for quantification are shown in bold.

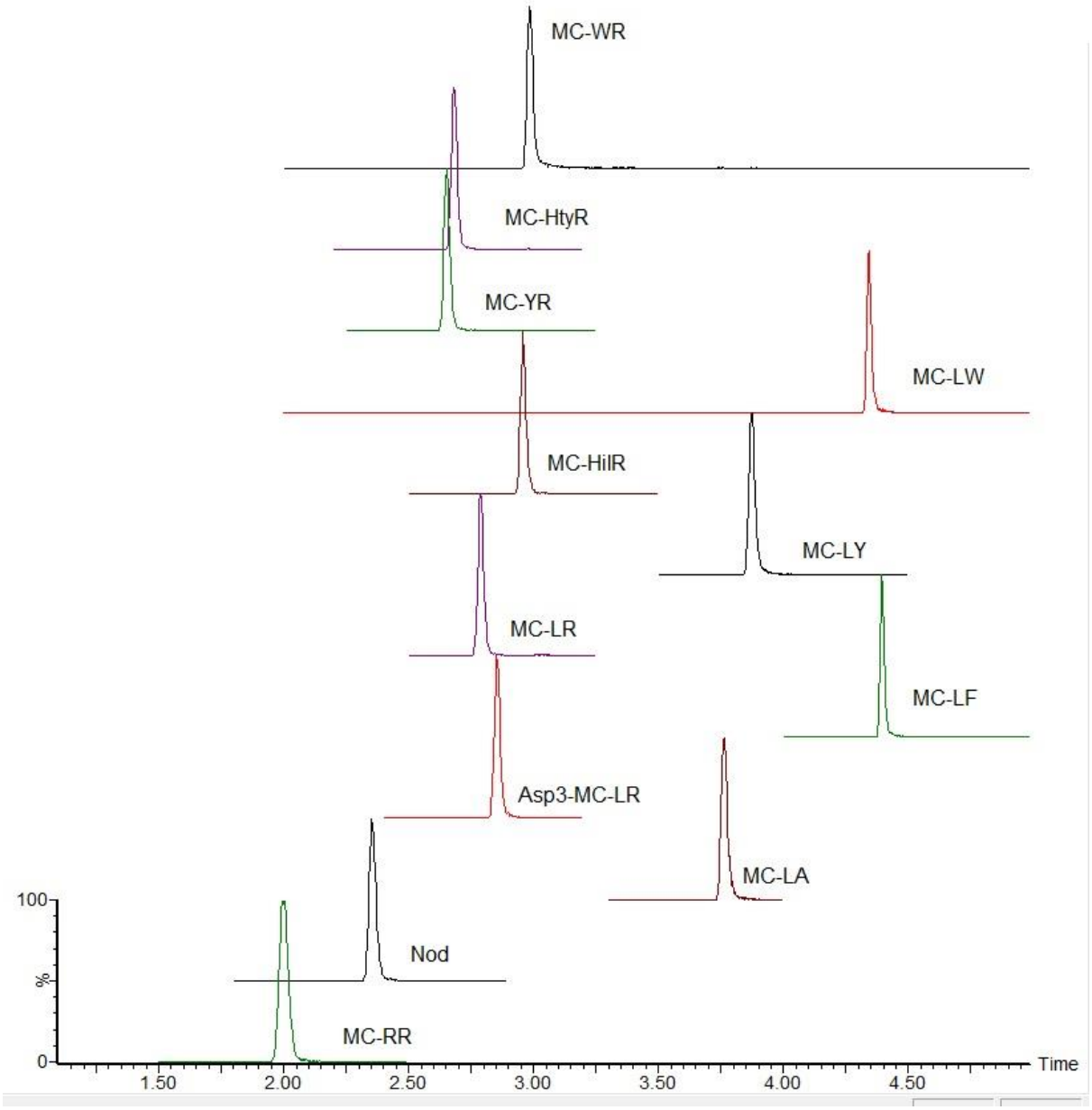

Figure 3.1 Representative ion chromatogram constructed from summed SRM traces depicting toxin analytes and their elution times.

3.1.6.3 Quantifying Results

The identification and quantitation of microcystin analytes were conducted using Waters TargetLynx software. The primary SRM transition for each analyte was used to generate calibration curves, with the secondary SRMs

used for qualification purposes. Calibration curves for each analyte were used to generate linear regressions, with the gradient and intercept used to calculate the concentration of analytes in each sample. This calculation was performed automatically within the TargetLynx software once calibration standard and sample peak areas had been generated and checked.

Calculated concentrations of each toxin analyte in every sample and standard are then exported to Excel, where they are tabulated. Two laboratory analysts are involved in this step for quality control purposes.

3.1.7 Statistical Analysis

3.1.7.1 Biochemistry

Principal component analysis (PCA) was performed on environmental, nutrient, and anion explanatory variables in each reservoir. Using PC1 scores for each, the top three variables contributing to PC1 were used for further analysis. Dimensionality reduction is an important tool to identify the explanatory variables contributing the most to the independent variable(s).

3.1.7.2 Toxicity

To test for statistical differences between toxin producing and non-producing strains, one-way analysis of variance (ANOVA) models were performed to test whether these variables were significantly different from each other and in each reservoir. Two-way ANOVA models were also performed with toxicity, month, and their interaction as explanatory variables. Post hoc Tukey tests

then examined which combinations, if any, were significant and driving the model output.

3.1.7.3 Toxicity and Biochemistry

To evaluate the relationships among toxicity and the top three explanatory variables in each reservoir, Spearman rho rank-based correlation coefficient tests were applied to each pair of variables. Individual tests were run for toxin producers and non-producers within the two reservoirs. From the rho values, statistical significance testing was performed to determine if the correlation could be accepted.

3.1.7.4 Software

Analysis for this chapter was conducted using R Statistical Software (R Core Team, 2020) with figures produced using the package 'ggplot2' version 3.3.1 (Wickham, 2016). Analysis packages include: 'dplyr' (Hadley et al., 2020), 'tidyverse' (Wickham and Henry, 2020).

3.2 RESULTS

3.2.1 Biogeochemistry

3.2.1.1 Environmental variables

Among environmental explanatory variables in Reservoir A, pH was alkaline ranging from 9.04 in Feb (2018) to 7.84 in Dec (2017). During summer months, pH increased from Jul (2017) (8.44) – Sep (2017) (8.84) becoming more alkaline with each month. Mean surface water temperatures ranged from of 20.6 °C in May (2017) to 2.5 °C in Mar (2018). Between May and Jun

there was a decrease in mean temperature of 0.8 °C before increasing again in Jul to 20.4 °C. After Jul, water temperatures continued to drop each month until the following spring. For Reservoir B, pH was alkaline ranging from 9.00 in Sep to 7.54 in Mar. During summer months, pH also increased from Jul (8.71) – Sep (9.00) becoming more alkaline with each month. Mean surface water temperatures ranged from of 20.9 °C in Jul to 3.0 °C in Mar (2018). Between May and Jul, there was an increase of 4.1 °C after which a continued drop in water temperature occurred until the following spring (Fig. 3.2).

3.2.1.2 Nutrients

Four key nutrients were measured between May 2017 through Apr 2018. In Reservoir A, ammonia concentrations ranged from 2347 (µg/L) (Nov) to undetectable (Feb, Jan, and May), nitrate ranged from 222 (µg/L) (Feb) to undetectable (Oct), nitrite ranged from 3.04 (mg/L) (Dec) to undetectable (Feb and Oct), and orthophosphate ranged from 0.01 (mg/L) (Sep) to undetectable (Apr, Feb, Jan, Jun, Mar, Nov, and Oct). In Reservoir B, ammonia concentrations ranged from 639 (µg/L) (Nov) to undetectable (Dec, Jan, and May), nitrate ranged from 269 (µg/L) (Jan) to 2.6 (mg/L) (Aug), nitrite ranged from 5.93 (mg/L) (Oct) to undetectable (Dec), and orthophosphate ranged from 0.02 (mg/L) (Sep) to undetectable (Apr, Dec, Mar, Oct, and Nov) (Fig. 3.3).

3.2.1.3 Anions

Six anions were measured between May 2017 through Apr 2018. In Reservoir A, acetate concentrations ranged from 0.14 (mg/L) (Aug) to undetectable (Dec and Jan), ascorbic acid ranged from 0.13 (mg/L) (Jul) to undetectable (Apr, Dec, Feb, Jan, Mar, and Nov), chloride ranged from 134.38 (mg/L) (Oct) to 10.24 (mg/L) (Jan), fluoride ranged from 0.28 (mg/L) (Oct) to 0.01 (mg/L) (Jan), formate ranged from 0.05 (mg/L) (Jul) to undetectable (Mar and Oct), and sulphate ranged from 145.97 (mg/L) (Oct) to 15.16 (mg/L) (Jan). In Reservoir B, acetate concentrations ranged from 0.13 (mg/L) (Sep) to 0.002 (mg/L) (Nov), ascorbic acid ranged from 0.13 (mg/L) (Aug) to undetectable (Apr, Dec, Jan, Mar, Nov, Oct), chloride ranged from 136.36 (mg/L) (Oct) to 19.61 (mg/L) (Aug), fluoride ranged from 0.38 (mg/L) (Oct) to 0.05 (mg/L) (Mar), formate ranged from 0.06 (mg/L) (Apr) to undetectable (Oct), and sulphate ranged from 155.70 (mg/L) (Jan) to 29.09 (mg/L) (Mar) (Fig. 3.4).

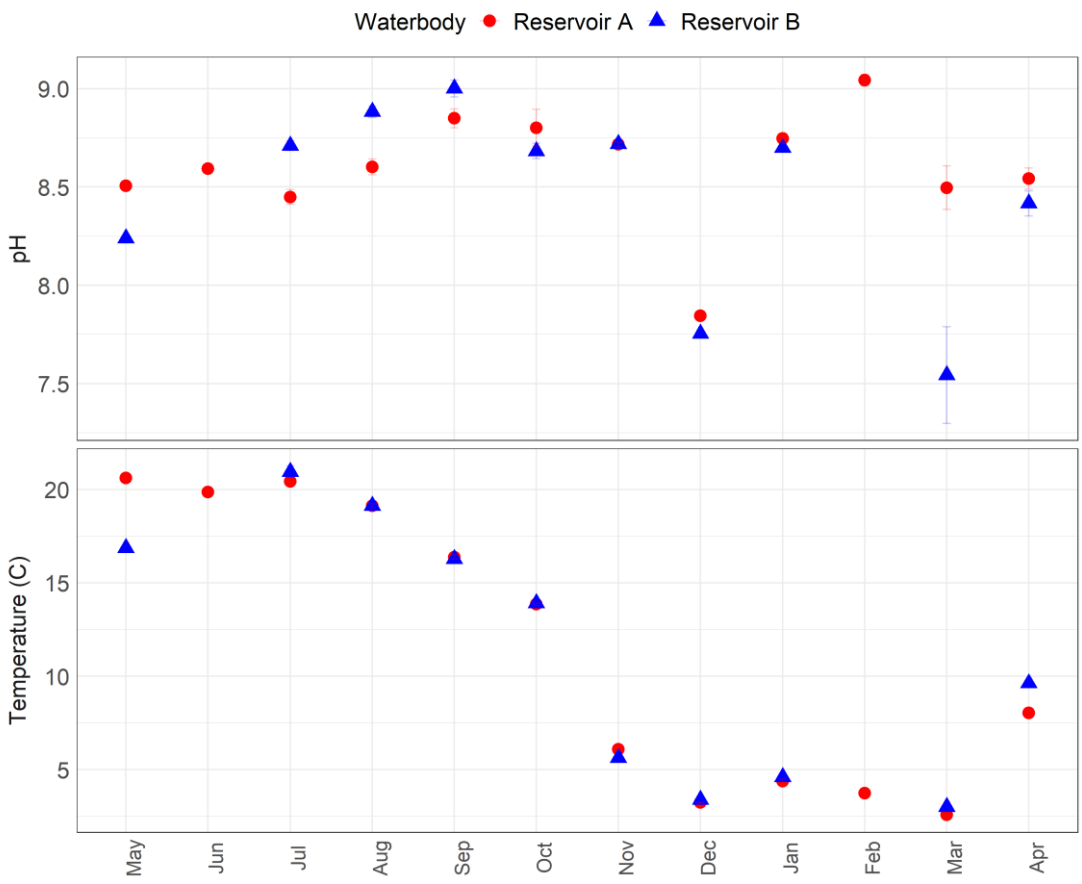

Figure 3.2 Mean pH (top) and temperature (°C) (bottom) in Reservoirs A and B. For both variables, May (Reservoir A; n=21, Reservoir B; n=23), Jun (Reservoir A; n=17), Jul (Reservoir A; n=25, Reservoir B; n=26), Aug (Reservoir A; n=30, Reservoir B; n=24), Sep (Reservoir A; n=32, Reservoir B; n=17), Oct (Reservoir A; n=34, Reservoir B; n=23), Nov (Reservoir A; n=13, Reservoir B; n=14), Dec (Reservoir A; n=12, Reservoir B; n=16), Jan (Reservoir A; n=19, Reservoir B; n=8), Feb (Reservoir A; n=16), and Mar (Reservoir A; n=13, Reservoir B; n=3). Error bars indicate SE between replicates.

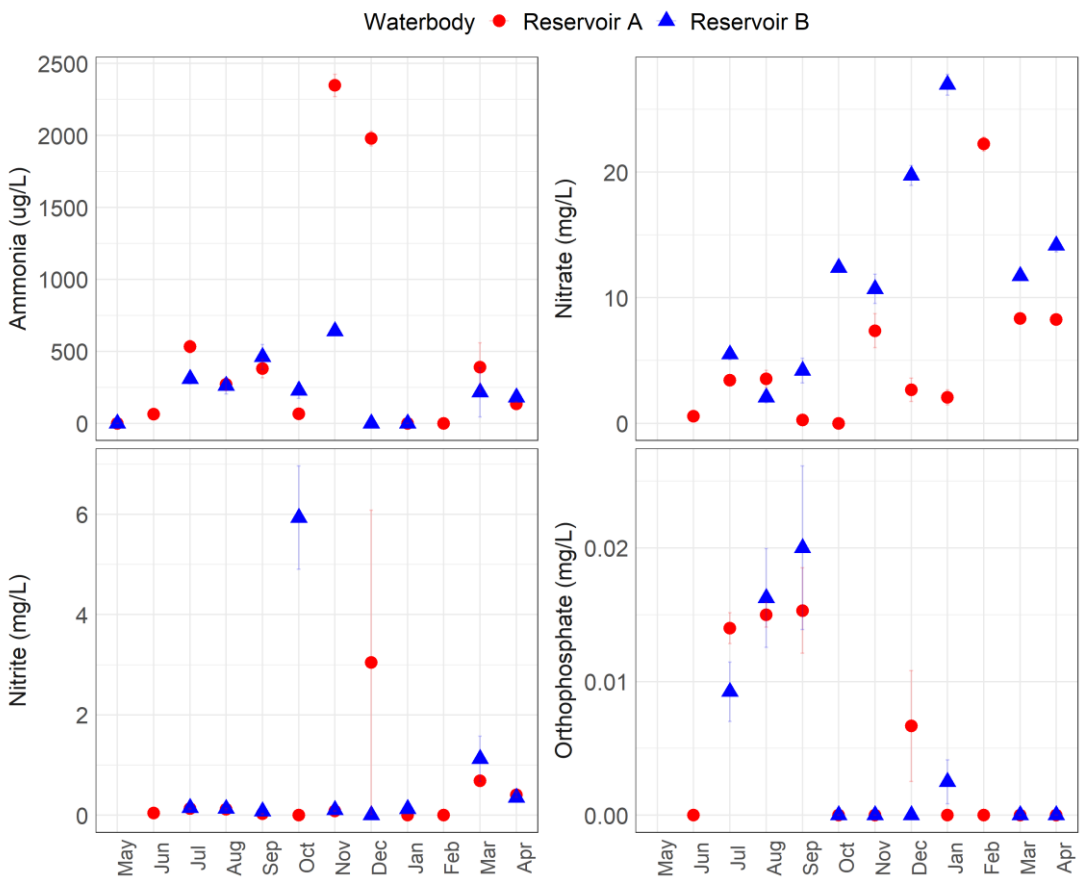

Figure 3.3 Mean ammonia (µg/L) (top-left), nitrite (mg/L) (top-right), nitrate (mg/L) (bottom-left), and orthophosphate (mg/L) (bottom-right) in Reservoirs A and B. For all variables, Jun (Reservoir A; n=17), Jul (Reservoir A; n=25, Reservoir B; n=26), Aug (Reservoir A; n=30, Reservoir B; n=24), Sep (Reservoir A; n=32, Reservoir B; n=17), Oct (Reservoir A; n=34, Reservoir B; n=23), Nov (Reservoir A; n=13, Reservoir B; n=14), Dec (Reservoir A; n=12, Reservoir B; n=16), Jan (Reservoir A; n=19, Reservoir B; n=8), Feb (Reservoir A; n=16), Mar (Reservoir A; n=13, Reservoir B; n=3) and May ammonia (Reservoir A; n=21, Reservoir B; n=23). Error bars indicate SE between replicates.

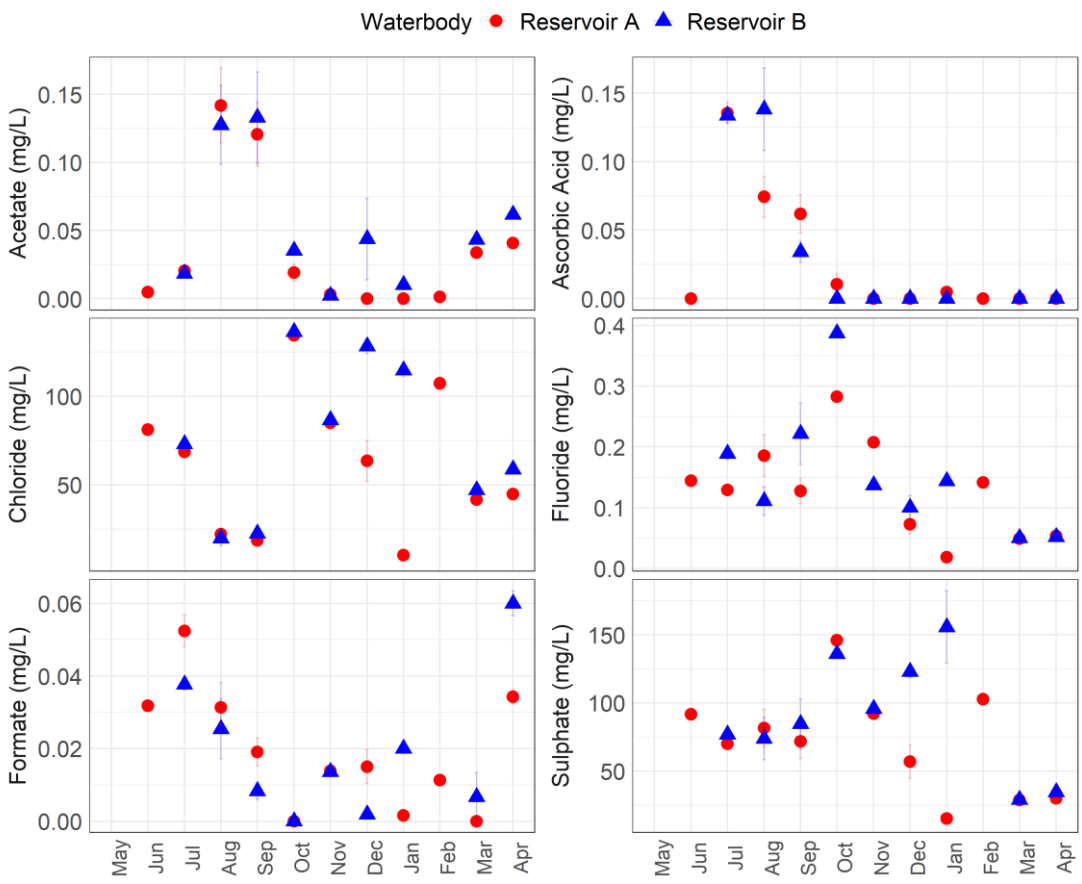

Figure 3.4 Mean acetate (mg/L) (top-left), ascorbic acid (mg/L) (top-right), chloride (mg/L) (middle-left), fluoride (mg/L) (middle-right), formate (mg/L) (bottom-left), and sulphate (mg/L) (bottom-right) in Reservoirs A and B. For all variables, Jun (Reservoir A; n=17), Jul (Reservoir A; n=25, Reservoir B; n=26), Aug (Reservoir A; n=30, Reservoir B; n=24), Sep (Reservoir A; n=32, Reservoir B; n=17), Oct (Reservoir A; n=34, Reservoir B; n=23), Nov (Reservoir A; n=13, Reservoir B; n=14), Dec (Reservoir A; n=12, Reservoir B; n=16), Jan (Reservoir A; n=19, Reservoir B; n=8), Feb (Reservoir A; n=16), Mar (Reservoir A; n=13, Reservoir B; n=3) and May ammonia (Reservoir A; n=21, Reservoir B; n=23). Error bars indicate SE between replicates.

Using the 12 explanatory variables discussed, Principle Component Analysis (PCA) extracted two main components (PC1 and PC2) accounting for 52.26% and 12.01% of the variation in Reservoir A biogeochemistry respectively (Fig. 3.5). In dimension 1, the highest contributions were found with fluoride, chloride, and sulphate whereas the highest contributions in dimension 2 were nitrite, temperature, and formate. PCA extracted two main components (PC1 and PC2) accounting for 51% and 15.9% of the variation in Reservoir B biogeochemistry, respectively (Fig. 3.6). In dimension 1, the highest contributions were found with fluoride, chloride, and nitrate whereas the highest contributions in dimension 2 correlated to pH, temperature, and ammonia. For both reservoirs, the three variables contributing the most to PC1 were used for subsequent modelling.

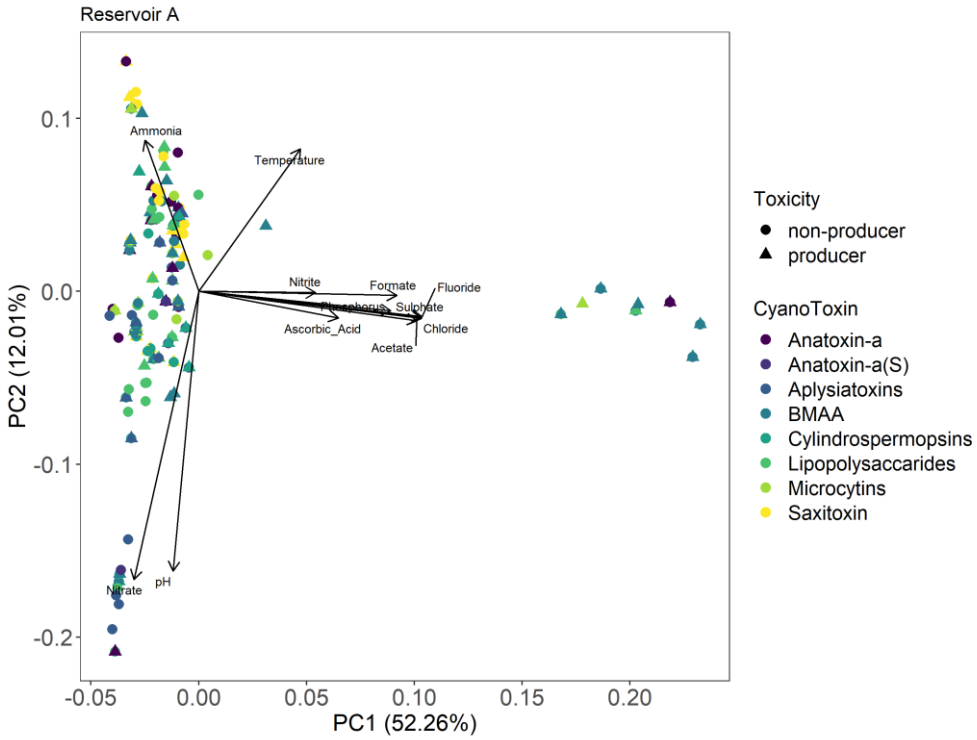

Figure 3.5 A biplot of Principal Component Analyses (PCA) of biogeochemical explanatory variables relative to eight cyanotoxins and their potential toxicity (producer, non-producer) in Reservoir A from May 2017 to Apr 2018. Explanatory variables include temperature, pH, ammonia, fluoride, acetate, formate, chloride, nitrite, nitrate, sulphate, ascorbic acid, and orthophosphate. Circles represent non-producers, triangles represent producers and each circle represents a cyanotoxin in ordination space while black arrows indicate PCA loadings for all variables.

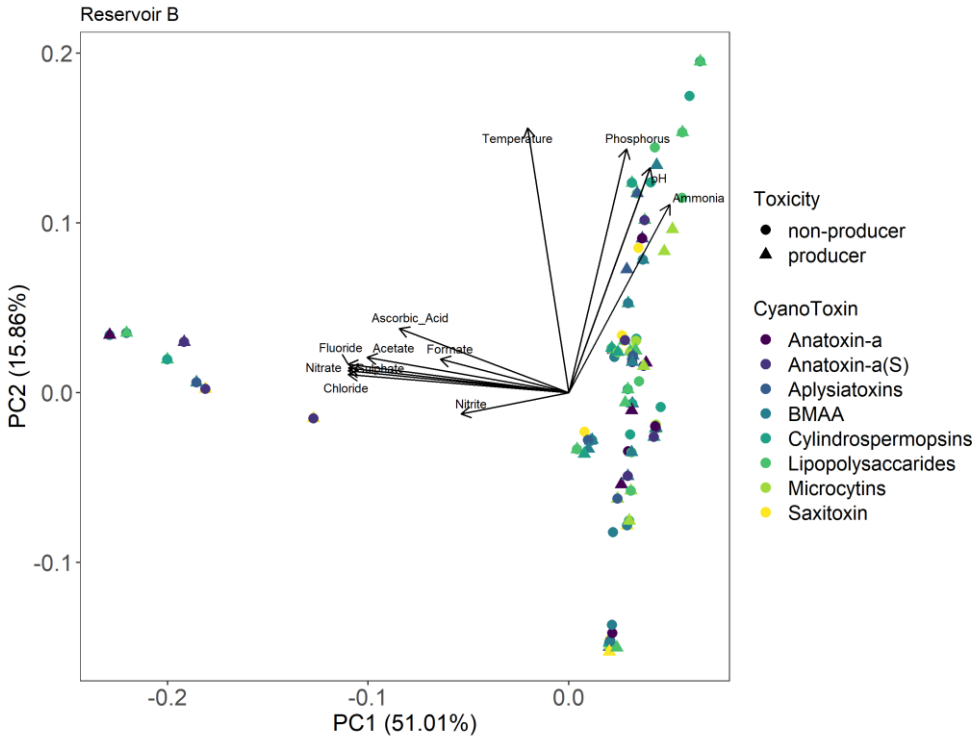

Figure 3.6 A biplot of Principal Component Analyses (PCA) of biogeochemical explanatory variables relative to eight cyanotoxins and their potential toxicity (producer, non-producer) in Reservoir B from May 2017 to Apr 2018. Explanatory variables include temperature, pH, ammonia, fluoride, acetate, formate, chloride, nitrite, nitrate, sulphate, ascorbic acid, and orthophosphate. Circles represent non-producers, triangles represent producers and each circle represents a cyanotoxin in ordination space while black arrows indicate PCA loadings for all variables.

3.2.2 Toxicity

Total abundance of toxin producing phytoplankton ranged from 2.05 billion - 405,600 cells in Reservoir A and 597million - 45,067 cells in Reservoir B. Among non-toxin producers, total abundance ranged from 2.07 billion - 2.3

million cells in Reservoir A and 627 million - 360,533 cells in Reservoir B. Annually, mean total abundance of toxin producers ranged from 1.1 billion cells (Reservoir A; Apr) to 8.0 million (Reservoir A; May) and 228 million cells (Reservoir B; Aug) to 2.4 million (Reservoir B; Mar). Among non-toxin producers, abundance ranged from 944 million cells (Reservoir A; Mar) to 72 million (Reservoir A; Jun) and 228 million cells (Reservoir B; Aug) to 14 million (Reservoir B; Sep). In Reservoir A, the late-winter/early-spring months of Feb, Mar, and Apr expressed the highest abundance of cyanotoxin producing and non-producing species whereas Reservoir B experienced its most abundant cyanotoxin cell counts in the summer months of Jul, Aug, and Sep (Fig. 3.7).

Analysis of Variance tests identified a significant difference in total abundance between cyanotoxin producers and non-producers (Reservoir A; *pseudo-F*$_{1, 244}$ = 3.994, P = 0.04, Reservoir B; *pseudo-F*$_{1, 164}$ = 22.07, P < 0.000). However, in Reservoir A there was no significant difference between toxicity for any month (*pseudo-F*$_{11, 222}$ = 1.816, P = 0.052) whereas in Reservoir B, the difference in toxicity between months was significant (*pseudo-F*$_{9, 146}$ = 2.599, P = 0.008). In addition, total abundance of cyanotoxin cells was found to be significant overall between months (Reservoir A; *pseudo-F*$_{11, 222}$ = 3.499, P < 0.000, Reservoir B; *pseudo-F*$_{9, 146}$ = 4.413, P < 0.000). Post hoc Tukey tests identified the significant difference between total abundance in each month occurred between the following: Reservoir A: May-Feb, Nov-Feb, Mar-Jan, May-Mar, and Nov-Mar and Reservoir B: Dec-Aug, May-Aug, Jul-Dec, and Oct-Dec.

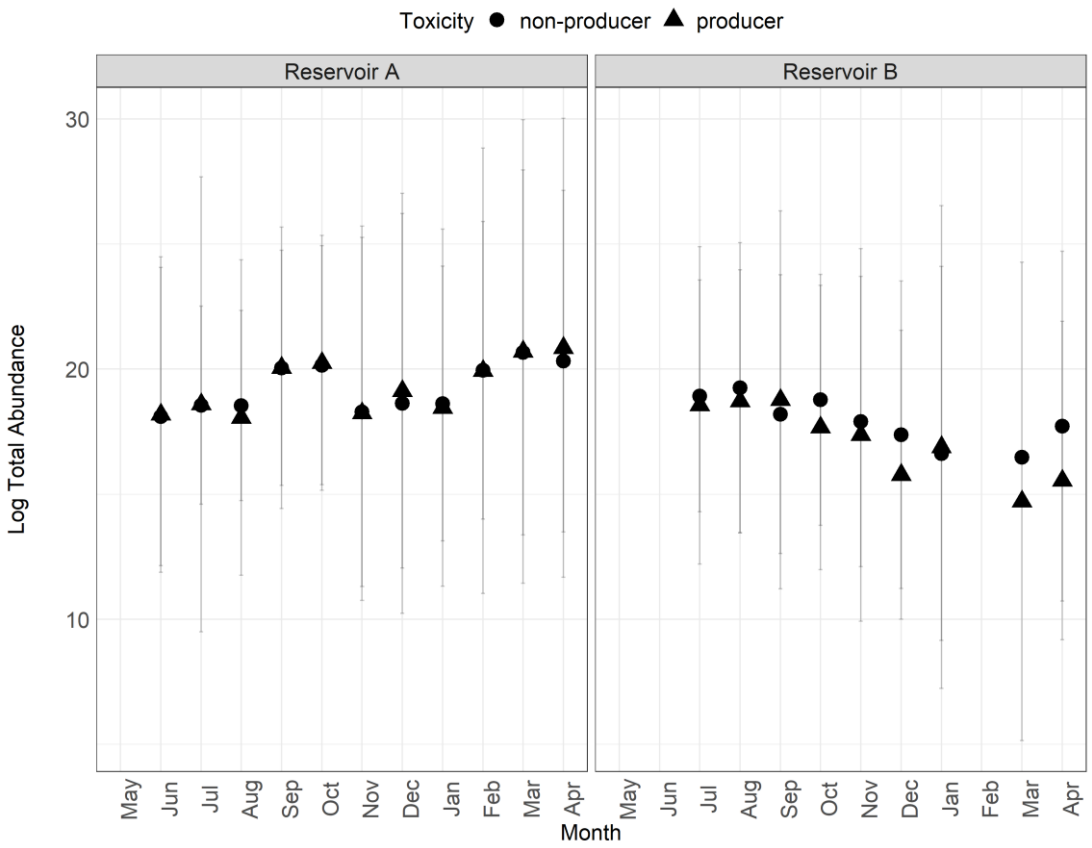

Figure 3.7 Mean log abundance (cells/mL) of cyanotoxin producers and non-producers in Reservoir A and Reservoir B between May 2017 and Apr 2018. Reservoir A producers (May n=12, Jun n=8, Jul n=4, Aug n=8, Sep n=13, Oct n=16, Nov n=6, Dec n=7, Jan n=7, Feb n=5, Mar n=5, Apr n=5). Reservoir A non-producers (May n=9, Jun n=9, Jul n=21, Aug n=22, Sep n=19, Oct n=18, Nov n=7, Dec n=5, Jan n=12, Feb n=11, Mar n=8, Apr n=9). Reservoir B producers (May n=12, Jul n=9, Aug n=13, Sep n=6, Oct n=10, Nov n=5, Dec n=8, Jan n=3, Mar n=2, Apr n=6). Reservoir B non-producers (May n=11, Jul n=17, Aug n=11, Sep n=11, Oct n=13, Nov n=9, Dec n=8, Jan n=5, Mar n=1, Apr n=6). Error bars indicate SE between replicates.

3.2.3 Toxicity-Biochemistry Relationship

A Spearman's correlation coefficient test was used to determine the relationship between the top three explanatory variables in each reservoir based on PCA ordination presented in section 3.2.2 and toxicity total abundance. Reservoir A and Reservoir B shared two of the three variables (fluoride and sulphate) while Reservoir A's third variable was chloride and Reservoir B's was nitrate. Among fluoride concentrations (mg/L), analysis revealed a nonsignificant negative correlation between mean total abundance and fluoride in both Reservoir A producers ($R = -0.455$, $P = 0.163$) and non-producers ($R = -0.409$, $P = 0.214$). In Reservoir B, the relationship between total abundance of toxin producers was positive but that relationship was not significant ($R = 0.417$, $P = 0.27$). Non-producers however, had a significantly strong positive relationship with fluoride ($R = 0.717$, $P = 0.037$) (Fig. 3.8). Sulphate concentrations (mg/L) revealed a nonsignificant, weak negative correlation between mean total abundance and sulphate in both Reservoir A producers ($R = -0.364$, $P = 0.273$) and non-producers ($R = -0.264$, $P = 0.435$). In Reservoir B, no correlation was found between toxin producer and non-producer abundance and sulphate (Fig. 3.9). Chloride was also found to have no correlation with Reservoir A abundance in either producers or non-producers (Fig. 3.10). In Reservoir B, nitrate was negatively correlated to abundance in non-producers but that relationship did not prove to be significant ($R = -0.394$, $P = 0.087$) whereas as the negative relationship among producer abundance was significant ($R = -0.466$, $P = 0.04$) (Fig. 3.11).

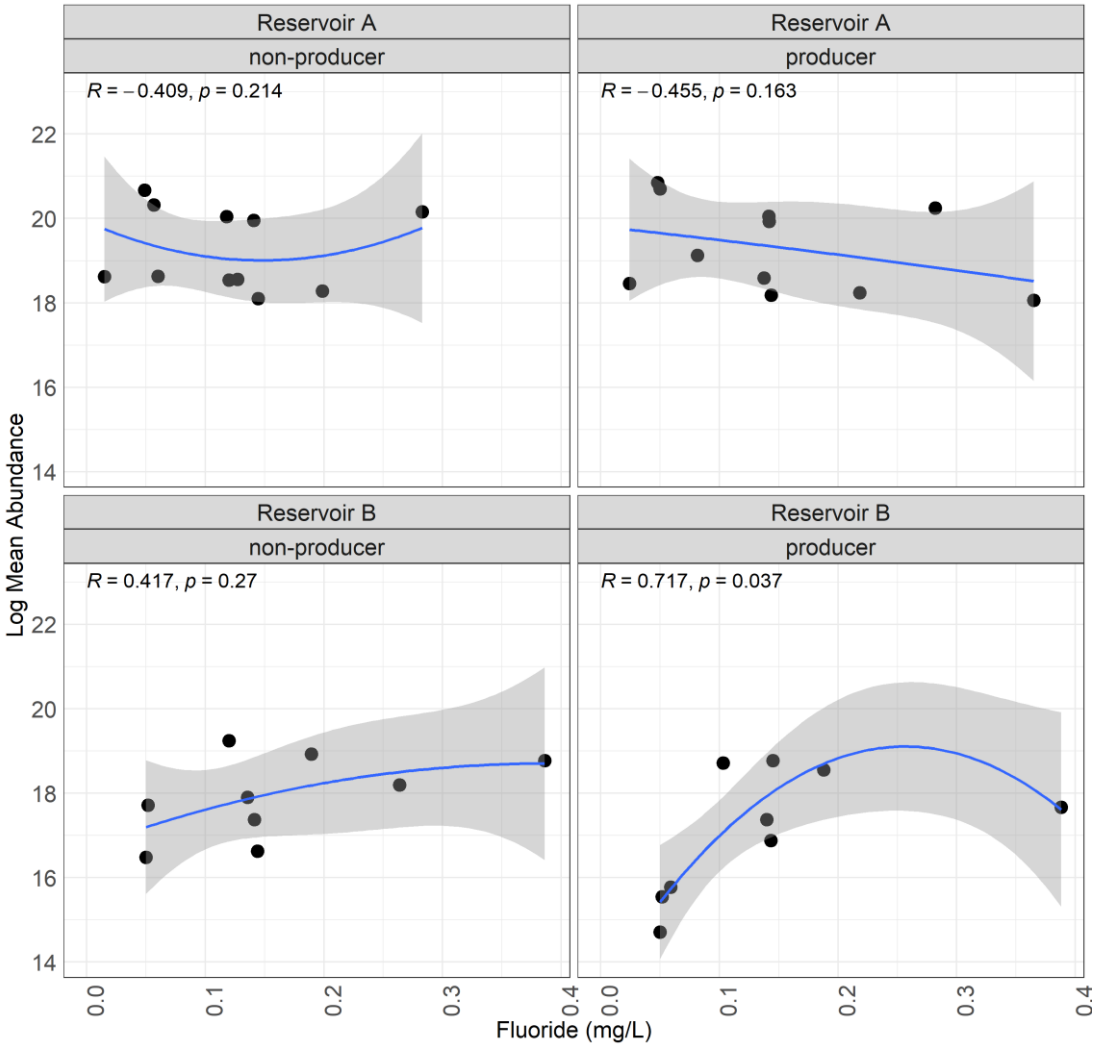

Figure 3.8 Correlation plots of mean log abundance and fluoride concentrations (mg/L) for Reservoir A (top) and Reservoir B (bottom) toxin producing and non-producing cyanobacteria communities. Each point represents a monthly mean from May 2017 – Apr 2018. The shaded area represents the 95% confidence interval of the fitted linear model. R denotes the Spearman rho correlation coefficient where the P-value is the significance of the correlation.

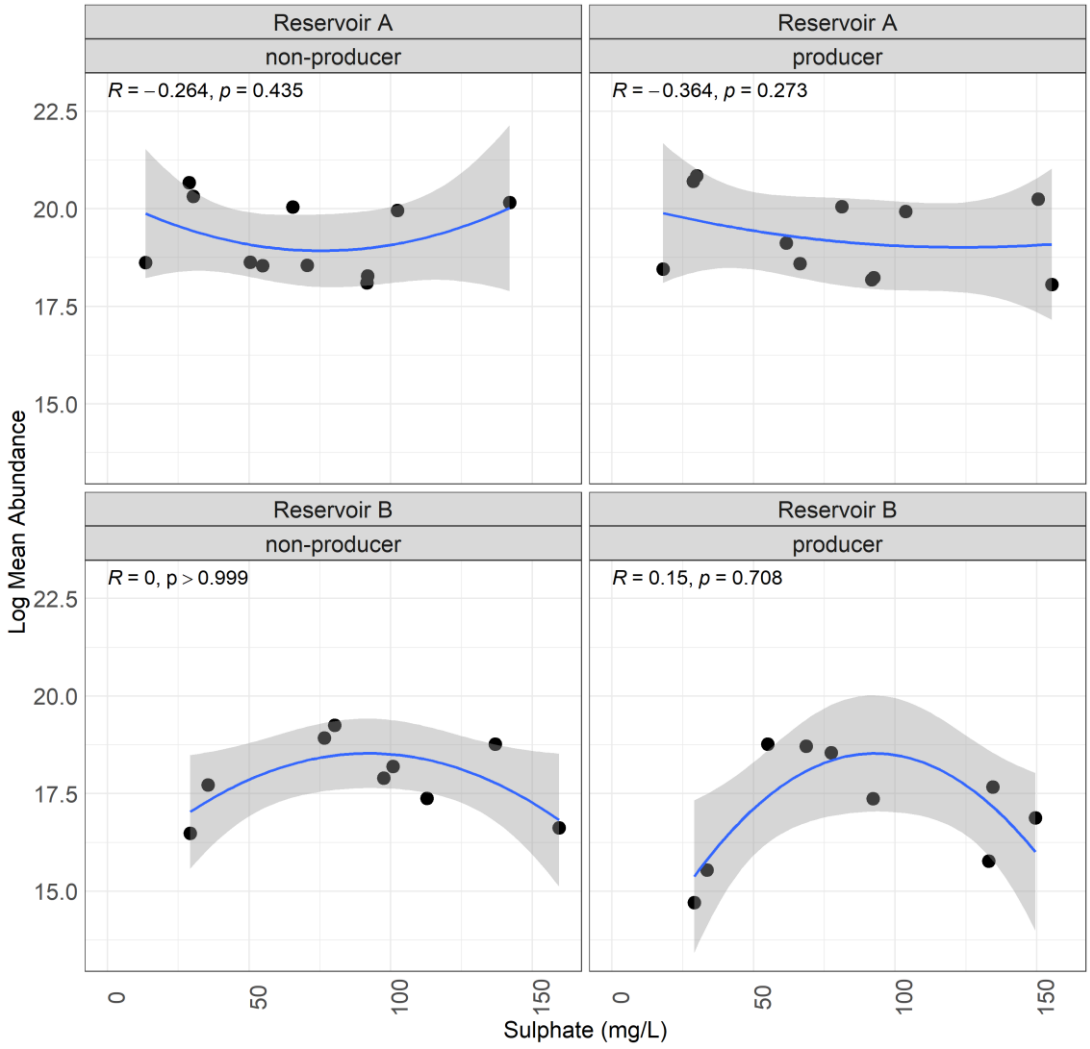

Figure 3.9 Correlation plots of mean log abundance and sulphate concentrations (mg/L) for Reservoir A (top) and Reservoir B (bottom) toxin producing and non-producing cyanobacteria communities. Each point represents a monthly mean from May 2017 – Apr 2018. The shaded area represents the 95% confidence interval of the fitted linear model. R denotes the Spearman rho correlation coefficient where the P-value is the significance of the correlation.

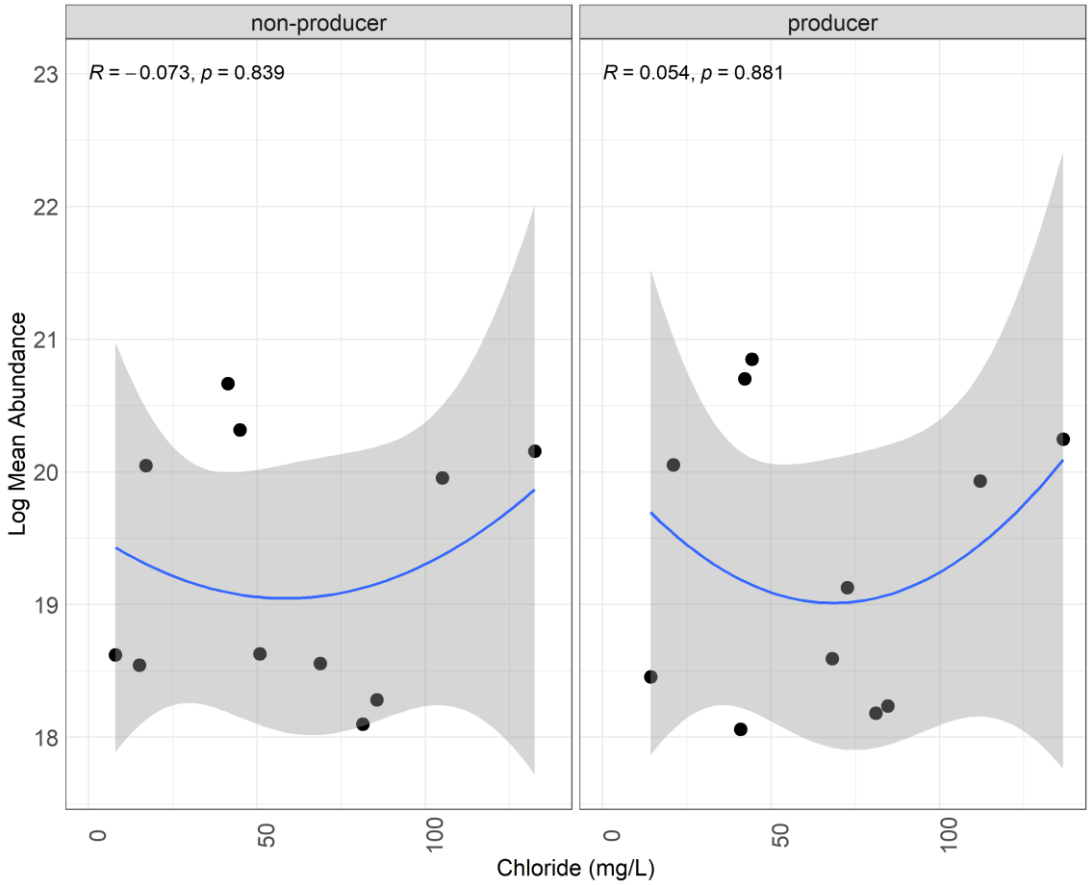

Figure 3.10 Correlation plots of mean log abundance and chloride concentrations (mg/L) for Reservoir A toxin producing and non-producing cyanobacteria communities. Each point represents a monthly mean from May 2017 – Apr 2018. The shaded area represents the 95% confidence interval of the fitted linear model. R denotes the Spearman rho correlation coefficient where the P-value is the significance of the correlation.

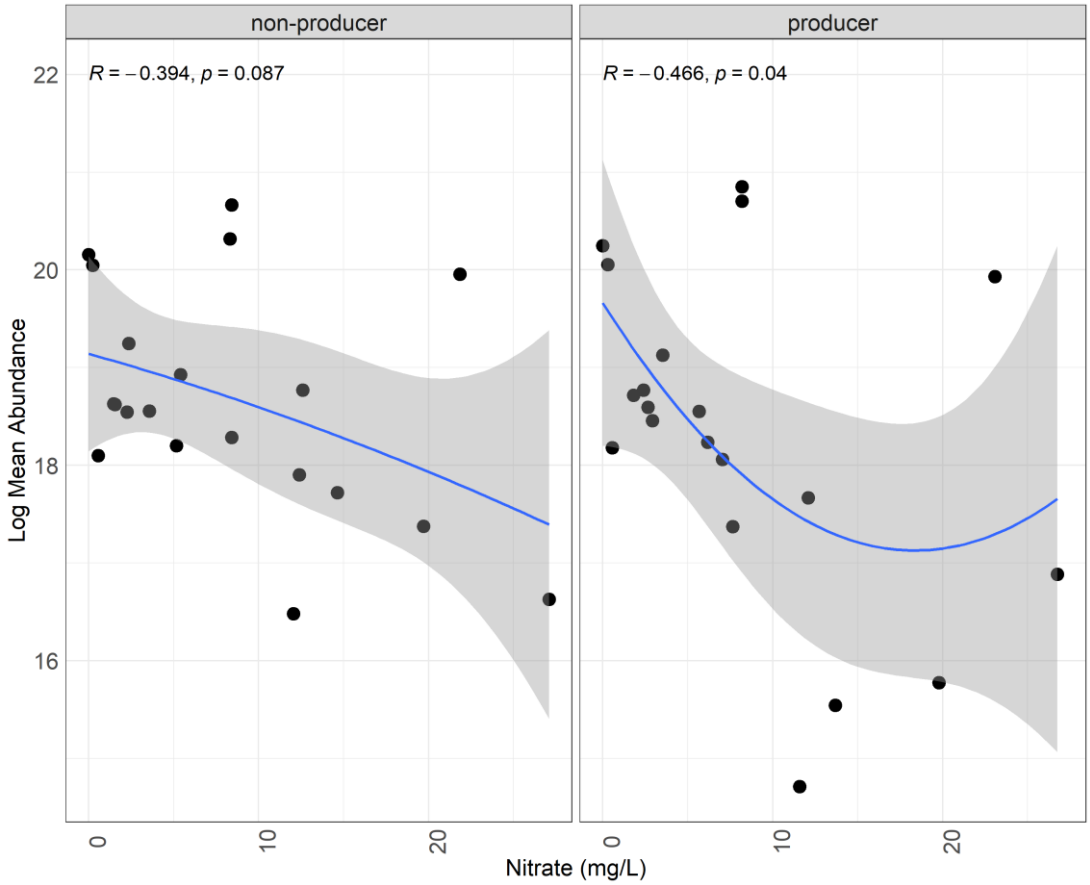

Figure 3.11 Correlation plots of mean log abundance and nitrate concentrations (mg/L) for Reservoir B toxin producing and non-producing cyanobacteria communities. Each point represents a monthly mean from May 2017 – Apr 2018. The shaded area represents the 95% confidence interval of the fitted linear model. R denotes the Spearman rho correlation coefficient where the P-value is the significance of the correlation.

3.2.4 Microcystin bloom profiles

Total microcystin contained concentrations from the 12 analytes presented in section 3.1.6. The highest mean concentration of total microcystin was found in Aug in Reservoir B (7.63 µg/L) (Fig. 3.12) while the highest mean concentration in Reservoir A was 2.59 µg/L in Oct (Fig. 3.13). Within a single

sample, 94.19 µg/L was the largest total MC concentration in the study (Aug-Reservoir B). By comparison, the highest total MC in a single sample in Reservoir A was 9.99 µg/L, which also occurred in Aug.

MC-LR was the highest recorded variant in a single sample at 47.40 µg/L (Aug-Reservoir B). This was followed by MC-RR, the second most abundant single sample concentration in the study at 24.41 µg/L (Aug-Reservoir B). Among individual variants, MC-RR* was the dominant variant in Reservoir A accounting for 89 percent of the total MC profile in Oct. Sep had the second largest concentrations for a single variant where MC-RR* accounted for 86 percent of the toxin profile for that month. This was followed by Nov, which too was dominated by MC-RR* at 85 percent of the MC profile. In Reservoir B (Fig. 3.14), MC-LF was the dominant variant accounting for 83 percent of the total MC profile in Apr. Mar contained the next highest concentration for a single variant MC-RR at 88 percent of the microcystin profile.

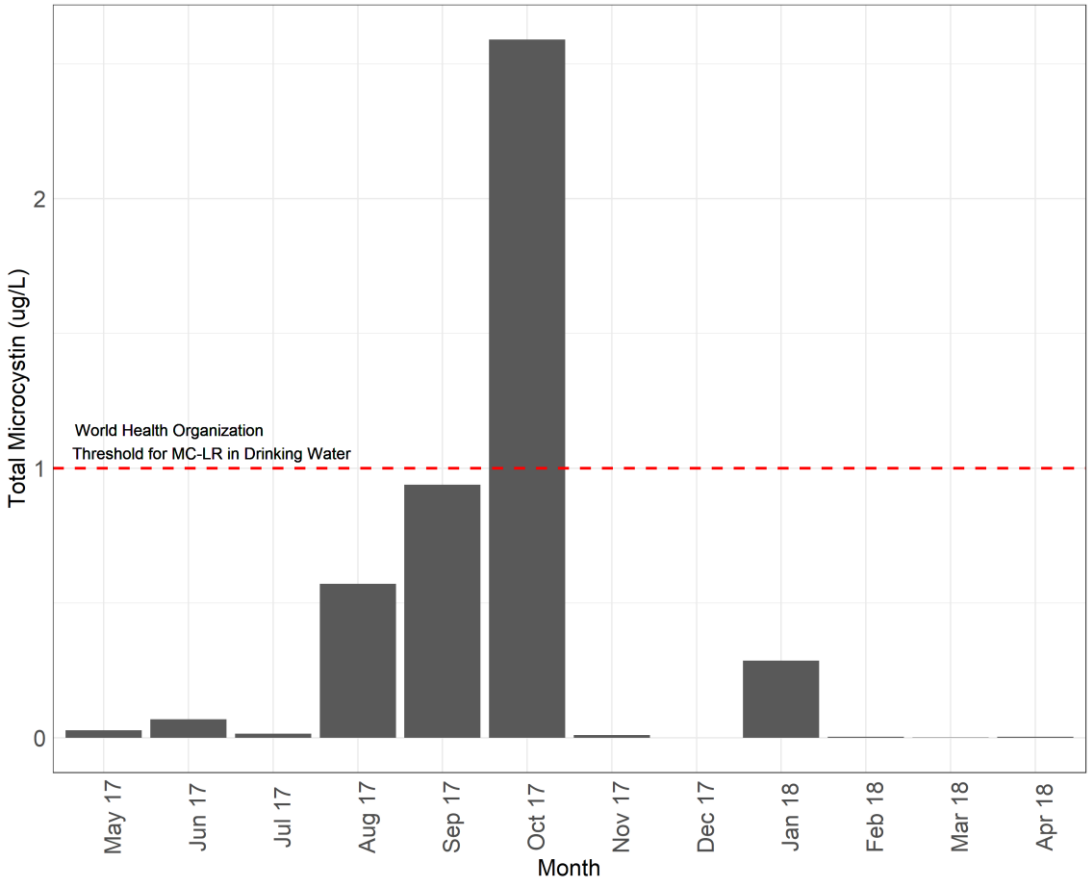

Figure 3. 12 Box plot of the mean log total microcystin concentrations (µg/L) in Reservoir A between May 2017 and Apr 2018. Red dashed line notes the World Health Organization's threshold for MC-LR in drinking water (1 µg/L).

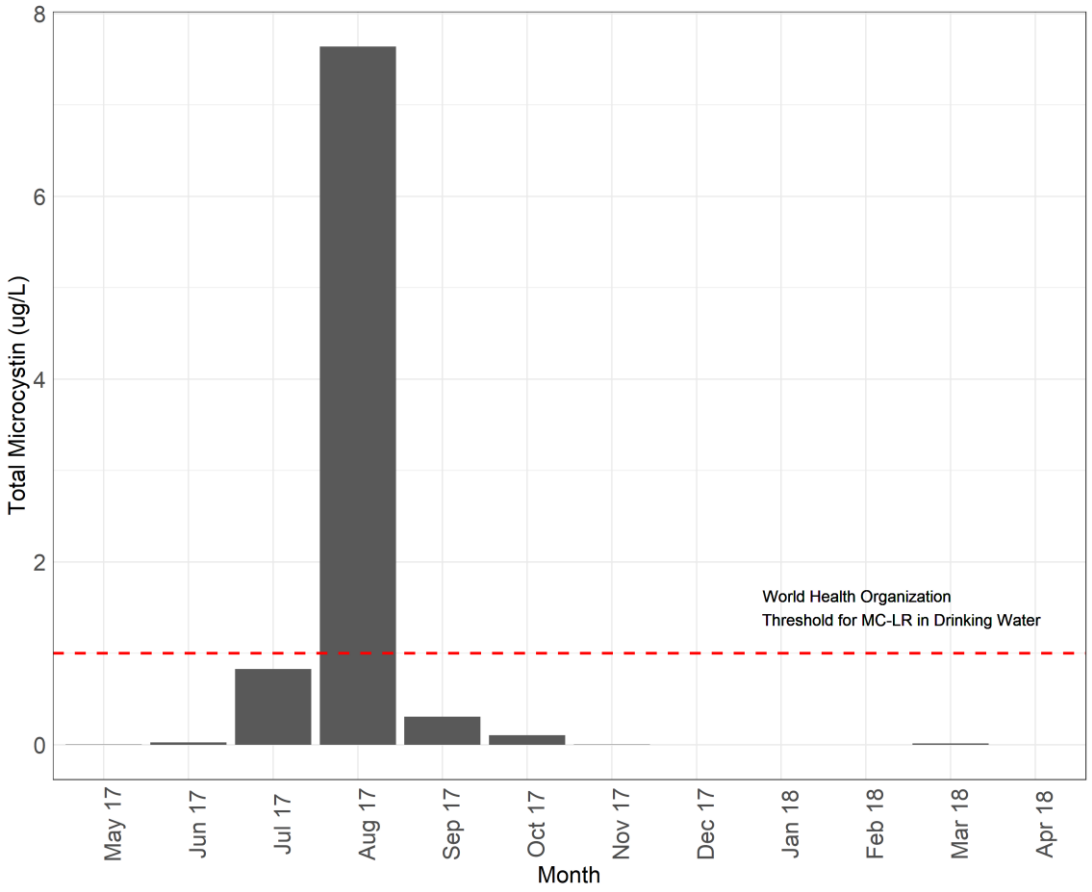

Figure 3.13 Box plot of the mean log total microcystin concentrations (µg/L) in Reservoir B between May 2017 and Apr 2018. Red dashed line notes the World Health Organization's threshold for MC-LR in drinking water (1 µg/L).

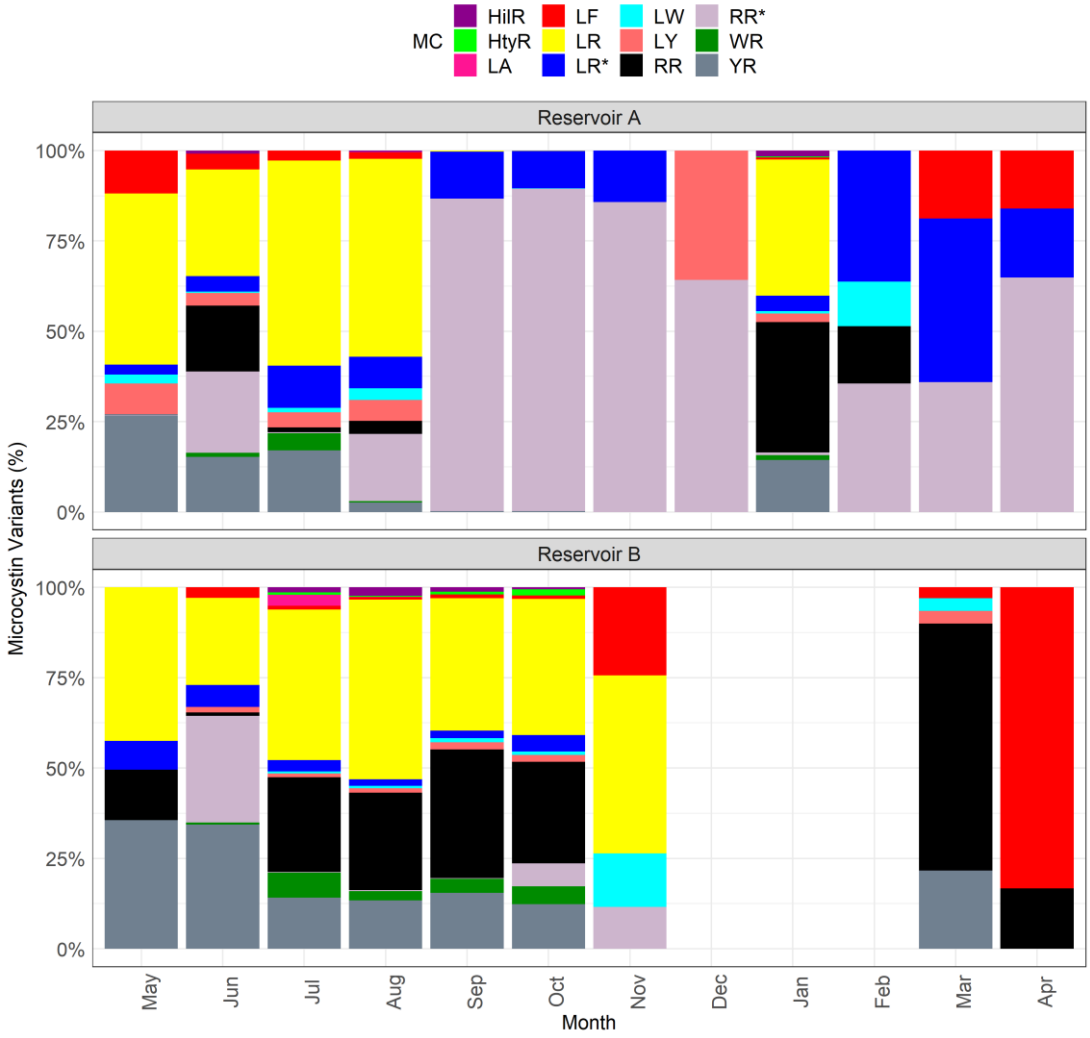

Figure 3.14 Microcystin (%) toxin profile for Reservoir A and Reservoir B from May 2017 - Apr 2018. Burgundy = $C_{50}H_{76}N_{10}O_{12}$ (Microcystin-HilR), neon-green = $C_{53}H_{74}N_{10}O_{13}$ (Microcystin-HtyR), neon-pink = $C_{46}H_{67}N_7O_{12}$ (Microcystin-LA), Red = $C_{52}H_{71}N_7O_{12}$ (Microcystin-LF), Yellow = $C_{49}H_{74}N_{10}O_{12}$ (Microcystin-LR), Blue = $C_{48}H_{72}N_{10}O_{12}$ (Microcystin-LR desmethylated), Teal = $C_{54}H_{72}N_8O_{12}$ (Microcystin-LW), Orange = $C_{52}H_{71}N_7O_{13}$ (Microcystin-LY), Black = $C_{49}H_{75}N_{13}O_{12}$ (Microcystin-RR), Pink = $C_{48}H_{73}N_{13}O_{12}$ (Microcystin-RR desmethylated), Green = $C_{54}H_{73}N_{11}O_{12}$ (Microcystin-WR), and Grey = $C_{52}H_{72}N_{10}O_{13}$ (Microcystin-YR).

3.3 DISCUSSION

3.3.1 Research Question 1. How toxic are the summer blooms in the East of England?

Reservoir A was dominated by toxin producer's pre bloom and non-producers post-bloom while at the height of the summer bloom, toxin producers dominated. In Reservoir B, non-producers dominated pre-bloom and during its peak while toxin producers dominated post-bloom. This contradicts studies conducted in France on dominance of toxic and non-toxic strains where they found toxic strains dominated pre and post blooms with toxic strains dominating during the bloom (Briand et al., 2009). Reservoir B was also the least toxic of the two reservoirs where non-producers outcompeted toxin-producing strains in every month except Sep, which was directly following the peak summer bloom and Jan in the middle of winter. This supports competition experiments, which identified toxin producers outcompeting non-producers under favourable conditions and non-producers beating out toxin producers during unfavourable conditions (Briand et al., 2008). In Sept when conditions were favourable in the East of England (warm and bright) toxins dominated in Reservoir B whereas, non-producers dominated during unfavourable months (i.e. winter). Based on this we can say Reservoir B is most at risk directly following the summer bloom die-off. In Reservoir A, toxin and non-toxin producing strains fluctuated between months however; toxin-producing cells outcompeted non-produces in most cases identifying risk as being unpredictable.

3.3.2 Research Question 2. What is the Microcystin community composition within each bloom and which variants dominate throughout the year?

Microcystin was found in both reservoirs and in every month except the winter in Reservoir B. Reservoir B was also more diverse in variant composition compared to Reservoir A. This was especially true of summer and autumn bloom months where Reservoir A was dominated by MC-RR. In both reservoirs, the early spring was less variable than the summer. These profiles and their respective distribution bring into question the appropriateness of the World Health Organization's (WHO) thresholds for drinking and recreational thresholds. Currently, those concentrations are set to 1 µg/L for the LR variant only. Based on the reservoirs presented in this study, we know MC-LR is a dominant variant in both reservoirs but is more so in the early summer. In reservoir A, the summer bloom contained only negligible concentrations of MC-LR. If a management decision is formed solely on WHO guidelines, there is potential for serious risk. As an alternative to WHO guidelines, some countries (i.e. Oregon, US) have adopted multiple variant thresholds for their local waterbodies to reduce risk and provide robust guidance for water managers (Farrer et al., 2015) which may be an effective approach for the East of England. Another example of proactive response and management of cyanobacteria is Australia. As a country, they provide national guidance, alert systems, monitoring and action plans to all states and territories.

3.3.3 Research Question 3. Is there a relationship between reservoir biogeochemistry and bloom toxicity?

Since Alfred Redfield first published his finding in 1958, the ratio (16:1) of nitrogen (N) to phosphorus (P) for phytoplankton remains the standard in phytoplankton nutrient assessments (Redfield, 1958) (Hillebrand et al., 2013). However, a great amount of research has since studied the ratio's variability to gain a more accurate assessment of N:P for phytoplankton. Recent studies have found cyanotoxins have a varied response to ratios of nitrogen versus phosphorus (Harke and Gobler, 2013). In a study of more than 100 freshwater lakes in Germany, total biovolume increased as nitrogen increased, telling us there may be a nitrogen limitation in phosphorus-rich waters. Germany's findings are particularly noteworthy as two abundant toxin producers appeared in waters with high nitrogen versus phosphorus concentrations (Dolman et al., 2012). This association was also seen in Reservoirs A and B, where nitrogen was significantly higher than phosphorus, signifying potential phosphorus limitation and increased biovolume. Additionally, among all nutrients, only nitrate was found to be correlated to abundance and this was only in Reservoir A and among toxin-producers. That relationship was significantly positive, telling us as nitrogen increases abundance also increases.

Among all other anions and environmental variables, no significant correlations were found in either toxin producers or non-producers in either reservoir. Based on this, there may be explanatory variables not investigated in this study driving reservoir toxicity (i.e. predation). In a study of 134 lake

across the United Kingdom, total phosphorous and water retention time were borderline significant explanatory variables of cyanobacteria blooms. Nutrient concentrations did not prove to be explanatory while watercolour and alkalinity were the most significant variables (Carvalho et al., 2011). In Reservoirs A and B, neither pH (alkalinity) nor water colour (dissolved organic matter) identified as important.

CHAPTER 4

INTERNAL LOADING OF LEGACY PHOSPHORUS MAY SUPPORT SUMMER PHYTOPLANKTON BLOOMS

4.0 INTRODUCTION

In the 1990s, Alton Water was investigated for the availability of phosphorus (P) and its role in supporting large summer phytoplankton blooms. A strong chlorophyll-*a* gradient from the reservoir inlet to the downstream extraction point and its correlation to total phosphorus were identified (Perkins and Underwood, 2000). By 2017, that gradient was no longer detectable with field assessments describing a 52.8% decrease in mean annual Chlorophyll-*a* (2010-2017) compared to previous years (1981-1994) (Parris, 2017). Over this same period, P inputs also declined, while P output concentrations were found to be higher than historically known. Controlling for P in Alton has been a key management strategy since 1983 when ferric dosing was first introduced to the pumped input (Perkins and Underwood, 2002). However, despite significant declines in catchment P entering the system and ferric binding (ferric sulphate added to the reservoir to precipitate dissolved particulate and orthophosphate), summer phytoplankton blooms continue to afflict the reservoir year after year. This suggests P may have a legacy effect, transferring from a stored, metal-bound state in sediments to the water column with internal loading subsidising growth (Gonsiorczyk et al., 1998; Nürnberg and LaZerrte, 2016; Søndergaard et al., 2003).

Internal loading is an intricate process involving simultaneous biological, chemical, and physical processes (Fig. 4.1) (Steinman and Spears, 2020). The sediment phosphorus pool driving these processes is composed of several forms including Soluble Reactive Phosphorus (SRP), inorganic and organic forms as well as legacy P fractions including labile P, Fe and Mn bound reductant soluble P, and Ca bound apatite P (Spears et al., 2007). While SRP is considered readily available for uptake, legacy P fractions slowly release into the water column serving as a long-term nutrient source for algae and plays a pivotal role in the sorption and desorption mechanics of internal loading (Orihel et al., 2017).

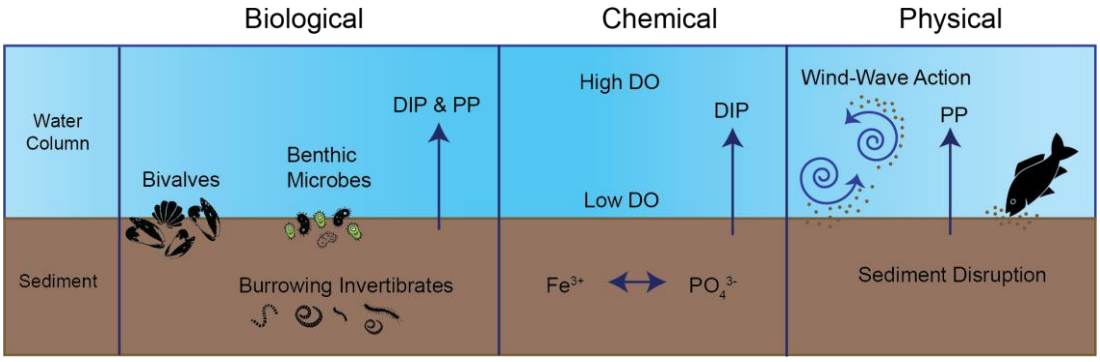

Figure 4.1 A simple schematic diagram of the biological, chemical, and physical processes attributed to internal P loading in freshwater systesms. PP = Particulate Phosphorus and DIP = Dissolved Inorganic Phosphorus. Modified from (Steinman and Spears, 2020). Figure credit: Amie L. Parris.

Reservoir sediment has the ability to act as a source or a sink for SRP (Tye et al., 2016). Water column biochemistry may propel these states where redox potential (Smolders et al., 2017), temperature (Jensen and Andersen, 1992),

and dissolved oxygen (Mei-Lin et al., 2014) are some of the major driving forces. Equilibrium Phosphorus Concentrations or EPC_0 can help identify the state of sorption kinetics (i.e. sink or source) by identifying the concentration at which there is no net uptake or release of SRP by the sediment (Hartikainen et al., 2010; Taylor and Kunishi, 1971). When EPC_0 > SRP in the water column, the reservoir sediment will release phosphorus and become a source. Conversely, when EPC_0 < SRP of the water column the sediment becomes a sink and adsorbs phosphorus from the overlying water (Palmer-Felgate et al., 2009; Roberts and Cooper, 2018). EPC_0 is derived from data points at 24 hours of incubation in phosphorus adsorption capacity experiments (Tye et al., 2016). To calculate the EPC_0, a plot is produced where the y-axis represents the concentration of SRP sorbed after 24 hours relative to the initial concentration of the solution (in mg PO_4 L) and the x-axis represents the remaining SRP in the solution after 24 hours. These concentrations are then fitted to either Freundlich or Langmuir adsorption capacity isotherm models depending on model best fit. From the isotherm fitted data points, EPC_0 is the x intercept when y = 0 (House et al., 1995; House and Denison, 2000) (Fig. 4.2).

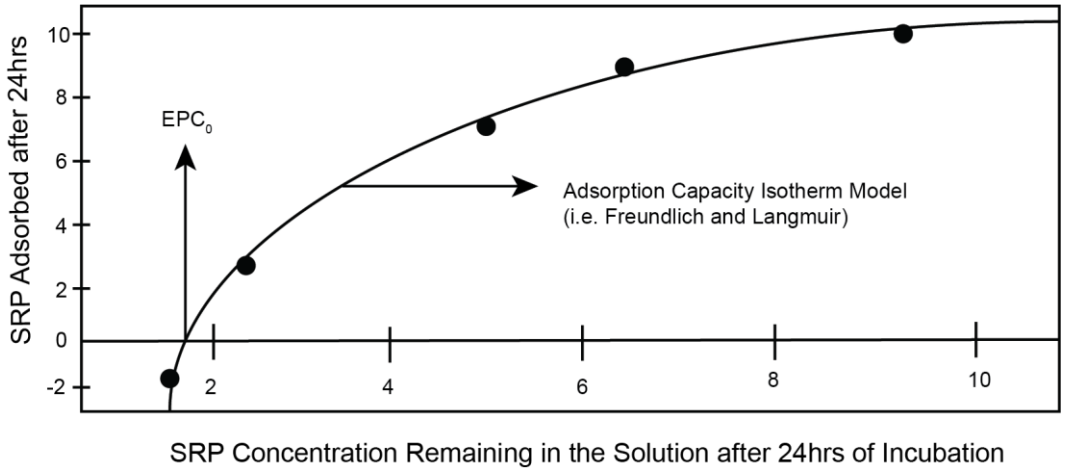

Figure 4.2 Example plot of SRP data points fitted to an adsorption capacity isotherm model along with the EPC_0. Figure credit: Amie L. Parris.

Freundlich and Langmuir isotherm models fitted to adsorption capacity experiments are the most widely used methods for determining sorption and desorption kinetics in reservoir sediment (Pierzynski and Sharpley, 2009). More specifically, the Langmuir isotherm (Li et al., 2007; Tang et al., 2014; Yin et al., 2016) provides values for the P sorption maximum and constant coefficients associated with the bonding energy of P (Dari et al., 2015). Whereas the Freundlich isotherm (Hwang et al., 1976; Skopp, 2009) is an empirical model to quantify the variation in energy with focus on sorption thermodynamics and the heterogeneity of the sediment surface (Skopp, 2009). Each model may be used in linear or non-linear form depending on which best fit the data (Dari et al., 2015). In the Langmuir model however, the linear form is more commonly applied for its simplicity, as the non-linear form requires specialised optimisation based on multiple site-specific datasets (Bolster and Hornberger, 2007).

The current study explored the phosphorus gradient from the reservoir inlet to the main basin by identifying the role of internal sediment phosphorus and the current effectiveness of sediment metals, (Fe, Al, and Ca) to bind P. Specifically; the following research questions were studied. (1) What is the role of legacy P in supporting reservoir wide phytoplankton blooms? (2) Is Alton Water sediment a source or sink for bound phosphorus? (3) Can water chemistry help explain trends in metal-bound P fractions? (4) How effective is the bund wall in holding locked-P in the reservoir inlet?

4.1 METHODS

4.1.1 Study Sites

A detailed description of Alton Water can be found in Chapter 2 section 2.1. For this study, sample locations included a four-point gradient down the length of the reservoir from north to south. Sampling sites follow this gradient where Site 1 is located at the reservoir inlet and just inside the bund. Site 2 lies immediately outside the bund where the summer depth is approximately 2-3 m. Site 3 is located south along the reservoir gradient and opposite Lemon Hill Bridge. Finally, Site 4 is near the reservoir's deepest point in the main basin (Fig. 4.3).

Figure 4. 3 Alton Water located in the East of England, UK (top right) and four sample sites within the reservoir. Site 1 is located inside the bund, site 2 directly outside the bund, site 3 south of a motorist bridge and site 4 is located in the middle of the main basin. Figure Credit: Amie L. Parris.

4.1.2 Water Chemistry

For all sites, vertical depth profiles of the water column were captured *in situ* using a YSI EXO^2 multi-parameter sonde (SKU 599502-00) for the following: pH, ORP - redox potential (mV), water temperature (°C), conductivity (µs), turbidity (NTU), total dissolved solids (mg/L), dissolved oxygen (mg/L), and fluorescent dissolved organic matter (µg/L). Data stored in the EXO^2 was exported under YSI International 2015 KorExo software version 2.2.0.1.

4.1.3 Nutrients

Surface water samples of 500mL were collected in the top 2-meters of the water column for each site. Surface samples were analysed for Total Nitrogen (TN), Inorganic Nitrogen (IN) (sum of nitrate, nitrite, and ammonia), Total Phosphorus (TP) Orthophosphate (OP), Organic Phosphate (OrgP) (TP minus IP), Total Carbon (TC), Inorganic Carbon (IC), Organic Carbon (OC) (TC minus IC) and Silicate (Si). Sample preparation for each variable used the following protocols: ammonia (Method 4500-NH_3. APHA, 2017), nitrate (Method 4500-NO_2 APHA, 2017), nitrite (Method 4500-NO_2 APHA, 2017), TP (Method 4500-P J. APHA, 2017) and OP (Method 4500-P E. APHA, 2017) and were analysed using a SEAL Analytical AA3 HR AutoAnalyzer tandem JASCO FP-2020 Plus fluorescence detector. Sample preparation and analysis for the auto analyser used the following methods by Seal Analytical: ammonia (Method-No. G-327-05 Rev. 6), nitrate (Method-No. G-172-96 Rev. 13 (Multitest MT 19)), nitrite (Method-No. G-173-96 Rev. 9 (Multitest MT 18)), phosphorus (Method-No. G-297-03 Rev. 5 (Multitest MT 19)), and silicate (Method-No. G-177-96 Rev. 10 (Multitest MT 19)). TC and IC were analysed

using a Skalar® Formacs^{HT} Total Organic Carbon high temperature catalytic combustion system. TN was analysed using a Skalar® Formacs^{TN} Analyser with ND25 Total Nitrogen detector.

4.1.4 Sediment Coring

Sediment cores were collected in triplicate at each of four sample sites during September and October 2018. Cores were captured using a UWITEC® 90mm hammer-action ball corer enclosing a 60 cm x 59.5 mm PVC core tube (Fig. 4.S0). The corer and tube were lowered to the reservoir bottom where a suspended 7kg galvanized steel weight was released allowing the corer to "hammer" into the sediment. This action captured both sediment and the overlying water. The corer was then lifted out of the water where the tube and intact core were removed from the corer. The over-lying water was extracted from the tube *in situ* using a 50 mL syringe, placed in 500 mL Nalgene bottles and stored on ice for transport. Sediment water was analysed together with surface water samples and followed the sample methods outlined in section 4.1.3. Cores were dissected in the laboratory where the top 6 cm of the core was sliced off using a UWITEC® core cutter with extension sleeve (Fig. 4.S1). From the 6 cm slicing, a sub-core was extracted using the barrel of a 10 mL syringe. The sub-corers were then placed in acid-washed crucibles, weighed, and dried at 85°C for 24 hours. Remaining sediment from the cut section was placed in 250 mL wide-mouth plastic pots with screw top lids and placed in -20°C storage.

4.1.5 Phosphorus Adsorption Capacity

Phosphorus adsorption capacity experiments followed the methods of (Perkins and Underwood, 2001). Each wet sub-sample was weighed and oven dried at 80 °C for 24 hours for the determination of percent water content. Additional wet sub-samples equivalent to 0.5 g dry weight were placed in 250 mL conical flasks containing 100 mL of a spiked KH_2PO_4 solution. KH_2PO_4 concentrations of 0.5, 1, 5 and 10 mg/L were incubated at 20 °C with continuous shaking. At one-hour intervals over 24 hours, 1.25 mL of the overlying water was extracted and centrifuged at 13,400 rpm for 5 minutes prior to PO_4^{3-} quantification following (Method 4500-P E. APHA, 2017).

4.1.6 Freundlich and Langmuir adsorption equations

Freundlich and Langmuir isotherm models were fit to data points in adsorption capacity experiments using the following equations.

Freundlich equation (linear form): $\log S = \log K + 1/n * \log C$

Where:

- S = The total amount of P sorbed (y-axis)
- C = Concentration of P after 24 hours (x-axis)
- K = In a plot of log S against log C, log K is the intercept
- n = In a plot of log S against log C, n is the slope

Langmuir equation (linear form): $C/S = (1/kS_{max}) + C/S_{max}$

Where:

- S = The total amount of P sorbed (y-axis)
- C = Concentration of P after 24 hours (x-axis)
- K = bonding energy (constant)
- Smax = Phosphorus sorption maximum

4.1.7 EPC_0 Calculations

Using the adsorption experiments above, phosphorus concentrations were extracted to construct adsorption capacity isotherms where phosphorus adsorbed after 24-hours (S) is a function of the remaining concentration after 24-hours (C) (Fig 4.6). A fitted linear trend line of the data identifies the x-intercept when y = 0 and phosphorus uptake and release are equal.

4.1.8 Sequential Extraction of Metal-Bound Phosphorus

Labile phosphorus and three fractions of phosphorus bound to sediment metals (i.e. Ca-P, Al-P, and Fe-P) were extracted following the modified methods of (Barik et al., 2016; Psenner et al., 1988). Labile-P was extracted first using NH_4Cl (pH 7) as the extractant. The sample was then mixed for two hours at 25 °C and centrifuged at 4000 rpm for 15 minutes. The supernatant was extracted and processed for PO_4^{3-} quantification (Method 4500-P E. APHA, 2017) and the remaining pellet was processed for the remaining bound fractions (Fig. 4.4).

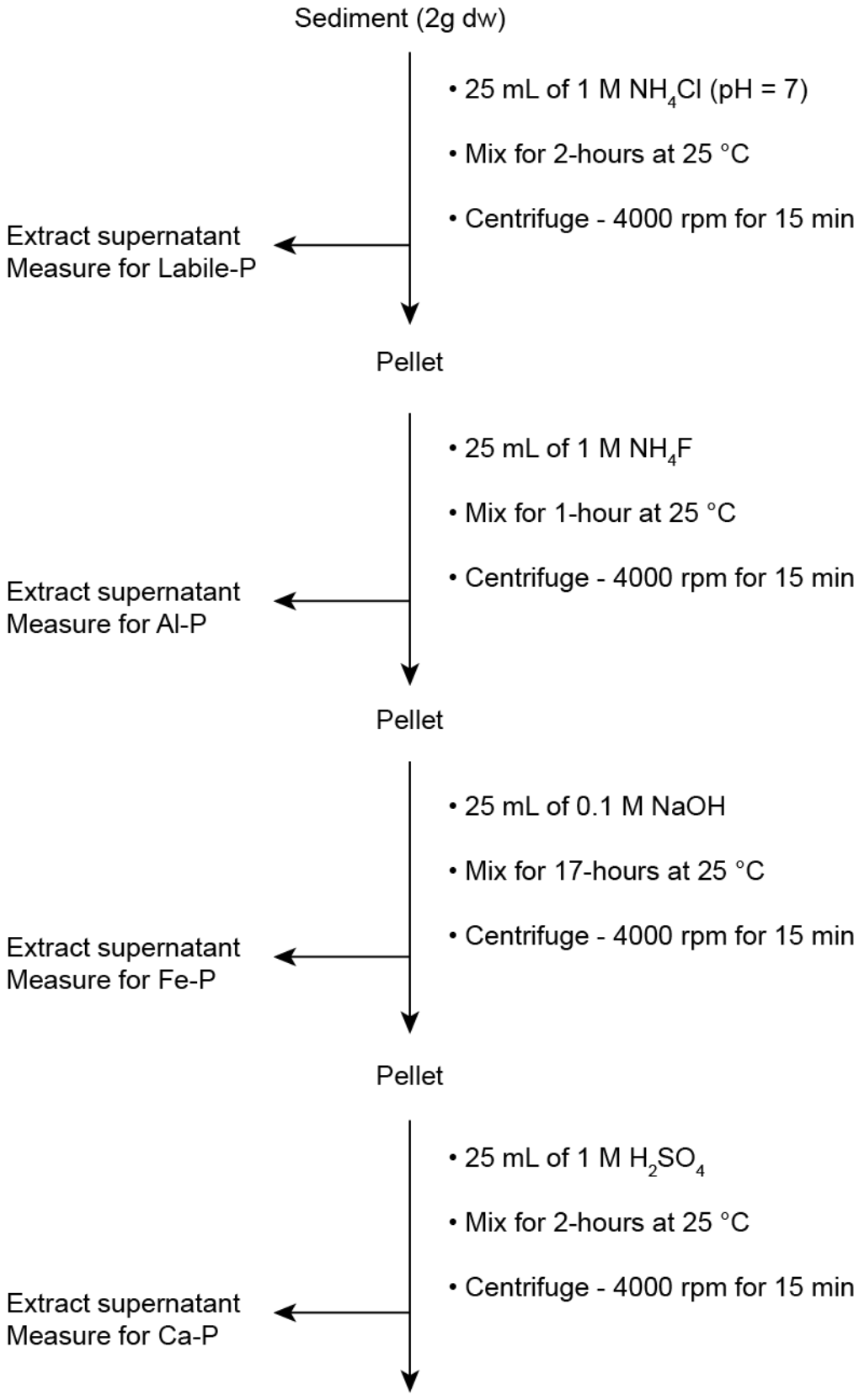

Figure 4.4 Sequential extraction method for determining four fractions of bound phosphorus in sediment. Figure Credit: Amie L. Parris.

4.1.9 Statistical Analysis

4.1.9.1 Water Chemistry and Nutrient Impact

Principal component analysis (PCA) was performed on both water chemistry and nutrient datasets (Table. 4.1). Each set of variables (water chemistry: 14; nutrients: 6) were reduced into the single variable, water chemistry impact and nutrient impact, by extracting the PC1 scores for each site. Creating a single impact variable for each dataset through dimensionality reduction avoids statistical errors associated with non-independent variables.

4.1.9.2 Phosphorus Adsorption Capacity

To test for statistical differences in adsorption capacity at equilibrium (24-hours), one-way analysis of variance (ANOVA) models were performed to test whether adsorption capacity was significantly different between sites 1 and 3. One-way ANOVA models were also performed between adsorption capacity at equilibrium (24-hours) and the experimental concentrations (0.5, 1, 5, and 10 mg/L). Post hoc Tukey tests then examined which combinations, if any, were significant and driving the model output.

4.1.9.3 Metal-bound Phosphorus Fractions

To test for statistical differences in each metal-bound P fraction (labile-P, Ca-P, Fe-P, and Al-P), one-way analysis of variance (ANOVA) models were performed to test whether metal bound P was significantly different between sites. For fractions where significance was identified, post hoc Tukey tests were used to examine which combinations were significant and driving the model output.

4.1.9.4 Impact Factors on bound P Fractions

To assess the effect of water chemistry and nutrients on metal-bound P concentrations, multivariate analysis of variance (MANOVA) was used to model the difference of impact factor on labile, Fe, Ca, and Al bound P fractions across the four sites.

4.1.9.5 Software

All analyses were conducted in the R statistical language (R Core Team, 2019), using the following packages: 'dplyr' (Hadley et al., 2020), 'tidyr' (Wickham and Henry, 2020), 'ggplot2' (Wickham, 2016) and 'PUPAIM' (John et al., 2020).

4.1.9.6 Figures

Figures 4.0, 4.1, 4.2, and 4.3 were made using Adobe Illustrator software (version 23.1) and Adobe Lightroom software (version 3.4) from Adobe Inc. under personal Creative Cloud license ADB001443181EDU.

4.2 RESULTS

4.2.1 Water Chemistry

Redox potential, total dissolved solids, and conductivity decreased in concentration from inside the bund down the reservoir gradient and into the main basin. Dissolved oxygen and pH were highest outside the bund then decreased through the mid reservoir and into the main basin. Turbidity increased down the reservoir before falling to its lowest mean in the main basin. Dissolved organic matter showed a reverse trend to turbidity and

decreased from inside the bund and down the reservoir before increasing again in the main basin. Temperature also fluctuated throughout the reservoir with the highest water temperature in the main basin followed by site 2, site 3 and coolest inside the bund (Table 4.1).

Table 4. 1 Mean water chemistry variables (± SE) across sites 1-4 in Alton Water from September and October 2018. Variables include: pH, redox potential (ORP), water temperature (Temp), conductivity (Cond), turbidity (Turb), total dissolved solids (TDS), dissolved oxygen (DO), and fluorescent dissolved organic matter (fDOM).

Parameter	Unit	Year	Site 1	Site 2	Site 3	Site 4
pH		2018	7.02 ± (0.01)	7.27 ± (0.01)	7.19 ± (0.01)	7.08 ± (0.00)
DO	(mg/L)	2018	9.47 ± (0.12)	11.92 ± (0.14)	8.38 ± (0.12)	6.28 ± (0.03)
Temp	(°C)	2018	14.98 ± (0.24)	16.54 ± (0.13)	16.20 ± (0.07)	16.84 ± (0.03)
ORP	(mV)	2018	125.72 ± (7.72)	108.83 ± (6.46)	45.77 ± (5.62)	56.88 ± (1.62)
Turb.	(NTU)	2018	20.90 ± (8.41)	33.02 ± (5.49)	58.21 ± (7.91)	20.67 ± (2.91)
fDOM	(µg/L)	2018	64.40 ± (1.35)	51.23 ± (1.12)	47.61 ± (0.76)	50.92 ± (0.24)
TDS	(mg/L)	2018	608.68 ± (2.77)	475.45 ± (4.33)	422.12 ± (1.37)	407.38 ± (1.04)
Cond	(µs)	2018	756.17 ± (2.21)	613.32 ± (5.83)	539.53 ± (1.29)	528.80 ± (1.37)

Principle Component Analysis (PCA) extracted two main components (PC1 and PC2) accounting for 65.49% and 23.7% of the variation in reservoir water chemistry, respectively (Fig. 4.5). For site 2 (outside the bund), dissolved organic matter, total dissolved solids, conductivity, and redox potential presented the greatest impact whereas temperature had the least impact. Temperature had a greater impact on site 3 (mid reservoir) and site 4 (main

basin) appeared to be the least impacted by water chemistry variables overall. For each site, PCA scores were extracted to create a new variable called water chemistry impact.

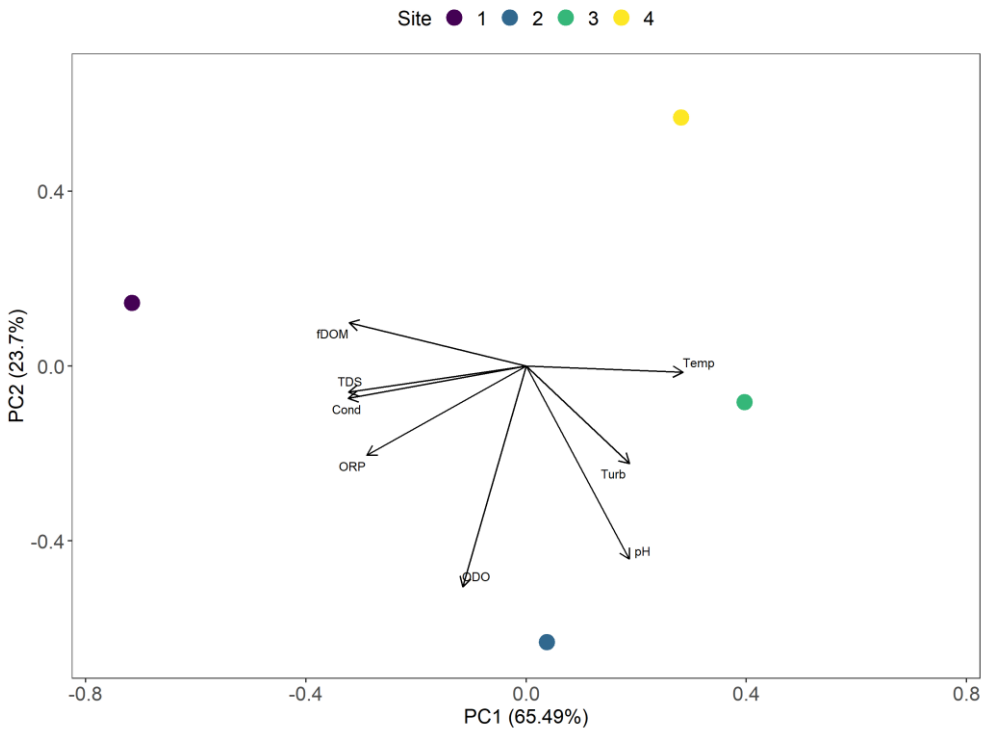

Figure 4.5 A biplot of Principal Component Analyses (PCA) on water chemistry variables across the four reservoir sites. The water chemistry variables shown include fluorescent Dissolved Organic Matter (fDOM), Total Dissolved Solids (TDS), Conductivity (Cond), Redox Potential (ORP), Dissolved Oxygen (DO), pH, Turbidity (Turb), and Temperature (Temp). Each circle represents a reservoir site in ordination space while black arrows indicate PCA loadings for all water chemistry variables.

4.2.2 Nutrients

At the surface, nitrate, nitrite, and total nitrogen decreased in concentration from inside the bund down the reservoir gradient and into the main basin while

ammonia, silicate, and orthophosphate increased from the inlet to the main basin. Organic phosphorus, total phosphorus, and organic carbon increased down the reservoir before decreasing in the main basin. Conversely, inorganic nitrogen, inorganic carbon, and total carbon showed a reverse trend and decreased from inside the bund and down the reservoir before increasing again in the main basin. In the sediment, nitrate, inorganic nitrogen, inorganic carbon, and total carbon decreased in concentration from inside the bund down the reservoir gradient and into the main basin while ammonia and silicate increased from the inlet to the main basin. Organic phosphorus, total phosphorus, and organic carbon were more variable increasing from inside to outside the bund, decreasing in the mid reservoir then increasing again in the main basin. Orthophosphate had the opposite trend and decreased from inside to outside the bund, increased in the mid reservoir before decreasing again in the main basin. Nitrite was highest outside the bund then decreased through the mid reservoir and into the main basin whereas total nitrogen decreased down the reservoir before increasing again in the main basin (Table 4.2).

Table 4.2 Mean surface and sediment-water nutrients (± SE) across sites 1-4 in Alton Water from September and October 2018. Variables include: nitrate (NO_3), nitrite (NO_2), ammonia (NH_3), total nitrogen (TN), inorganic nitrogen (IN), total phosphorus (TP), orthophosphate (OP), organic phosphate (OrgP), total carbon (TC), inorganic carbon (IC), and organic carbon (OC), and Silicate (Si).

Parameter	Collection Site	Unit	Year	Site 1	Site 2	Site 3	Site 4
NO3	Surface	(µg/L)	2018	5.14 ± (0.09)	1.04 ± (0.17)	0.25 ± (0.03)	0.13 ± (0.03)
NO2	Surface	(µg/L)	2018	0.11 ± (0.01)	0.10 ± (0.01)	0.08 ± (0.01)	0.06 ± (0.01)
NH3	Surface	(µg/L)	2018	0.18 ± (0.02)	0.21 ± (0.05)	0.43 ± (0.06)	0.72 ± (0.09)
IN	Surface	(µg/L)	2018	5.44 ± (0.13)	1.36 ± (0.11)	0.76 ± (0.11)	0.92 ± (0.11)
TN	Surface	(µg/L)	2018	5.92 ± (0.38)	2.20 ± (0.30)	1.54 ± (0.12)	1.48 ± (0.14)
Si	Surface	(µg/L)	2018	12.97 ± (0.80	14.69 ± (1.15)	15.34 ± (1.01)	15.95 ± (1.12)
OP	Surface	(µg/L)	2018	0.06 ± (0.00)	0.09 ± (0.01)	0.15 ± (0.02)	0.19 ± (0.02)
OrgP	Surface	(µg/L)	2018	0.13 ± (0.01)	0.29 ± (0.08)	0.41 ± (0.10)	0.35 ± (0.11)
TP	Surface	(µg/L)	2018	0.20 ± (0.01)	0.39 ± (0.09)	0.56 ± (0.12)	0.54 ± (0.13)
IC	Surface	(mg/L)	2018	72.41 ± (1.38)	44.65 ± (2.17)	37.27 ± (0.62)	38.92 ± (2.21)
OC	Surface	(mg/L)	2018	6.79 ± (0.15)	11.09 ± (0.04)	11.54 ± (0.45)	10.53 ± (0.49)
TC	Surface	(mg/L)	2018	79.21 ± (1.34)	55.75 ± (2.28)	48.81 ± (0.30)	49.45 ± (2.02)
NO3	Sediment	(µg/L)	2018	5.12 ± (0.10)	2.15 ± (0.22)	0.79 ± (0.16)	0.14 ± (0.02)
NO2	Sediment	(µg/L)	2018	0.12 ± (0.06)	0.13 ± (0.01)	0.12 ± (0.02)	0.06 ± (0.01)
NH3	Sediment	(µg/L)	2018	0.16 ± (0.02)	0.43 ± (0.17)	0.60 ± (0.05)	0.89 ± (0.14)
IN	Sediment	(µg/L)	2018	5.41 ± (0.14)	2.73 ± (0.17)	1.52 ± (0.14)	1.09 ± (0.15)
TN	Sediment	(µg/L)	2018	5.93 ± (0.55)	2.75 ± (0.11)	1.79 ± (0.11)	1.98 ± (0.25)
Si	Sediment	(µg/L)	2018	12.94 ± (0.78)	14.54 ± (0.95)	15.58 ± (1.09)	16.23 ± (1.05)
OP	Sediment	(µg/L)	2018	0.07 ± (0.00)	0.06 ± (0.01)	0.14 ± (0.02)	0.11 ± (0.01)
OrgP	Sediment	(µg/L)	2018	0.52 ± (0.22)	0.67 ± (0.21)	0.41 ± (0.08)	0.66 ± (0.16)
TP	Sediment	(µg/L)	2018	0.59 ± (0.22)	0.73 ± (0.22)	0.56 ± (0.09)	0.78 ± (0.16)
IC	Sediment	(mg/L)	2018	73.90 ± (2.21)	57.49 ± (0.94)	45.56 ± (1.53)	39.69 ± (1.20)
OC	Sediment	(mg/L)	2018	11.45 ± (1.91)	13.19 ± (1.60)	11.91 ± (0.74)	13.93 ± (1.68)
TC	Sediment	(mg/L)	2018	85.35 ± (3.89)	70.69 ± (2.04)	57.48 ± (0.96)	53.63 ± (2.10)

Principle Component Analysis (PCA) extracted two main components (PC1 and PC2) accounting for 89.75% and 9.75% of the variation in reservoir

nutrients, respectively (Fig. 4.6). Site 1 appeared to be most impacted by total and inorganic carbon, total and inorganic nitrogen, and nitrate but less impacted by silicate and organic phosphorus. Whereas ammonia and orthophosphate showed the greatest impact on site 4, silicate, organic phosphorus and organic carbon appears to impact site 3. Among all four sites, site 2 (outside the bund) showed to be the least effected by nutrients. For each site, PCA scores were extracted to create a new variable called nutrient impact.

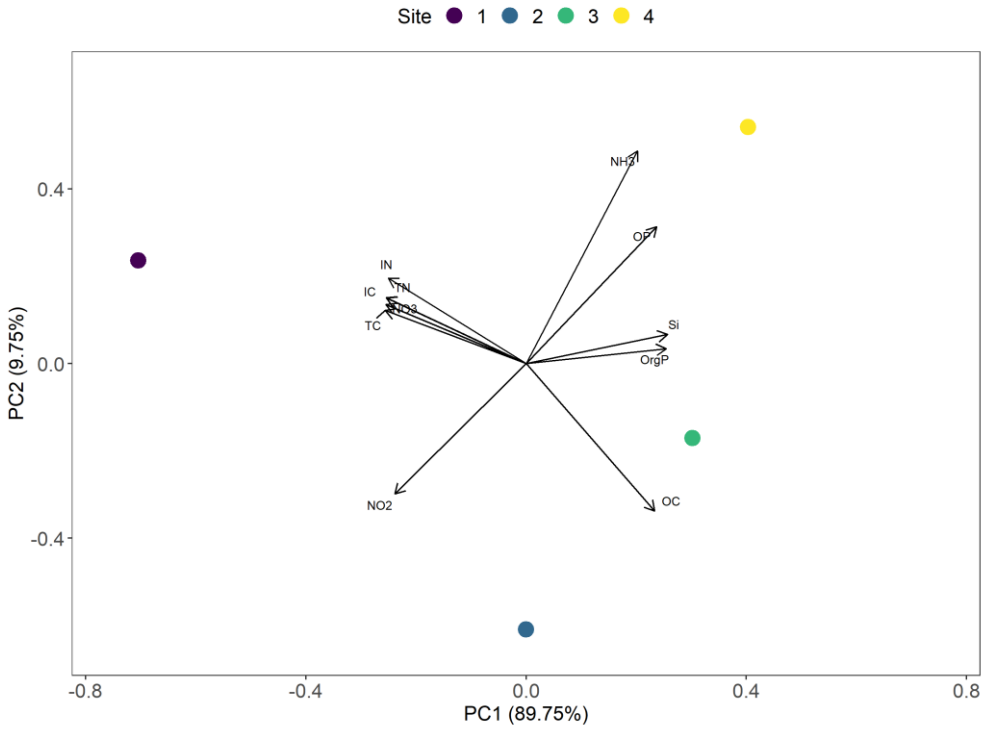

Figure 4.6 A biplot of Principal Component Analyses (PCA) on nutrient variables across the four reservoir sites. The nutrient variables shown include Total Organic Carbon (TOC), Inorganic Carbon (IC), Organic Carbon (OC), Total Phosphorous (TP), Organic Phosphorus (OP), Orthophosphate (OP), Total Nitrogen (TN), Ammonium (NH_4), Nitrate (NO_3), Nitrite (NO_2), and

Silicate (Si). Each circle represents a reservoir site in ordination space while black arrows indicate PCA loadings for all nutrient variables.

4.2.3 Phosphorus Adsorption Capacity

Sediment from site 1 (high ferric site) and site 3 (low ferric site) underwent adsorption capacity experiments to examine the potential for phosphorus release into the water column. Site 1 sediments were the most successful, adsorbing 84% over the overlying phosphorus across all incubations after 2 hours (Fig. 4.7.A). Within 24 hours, that adsorbance increased to 91% across all incubations with a maximum of 96% at 10 mg/L. Adsorption efficiency also increased with an increase in concentration where the lowest phosphorus addition (0.5 mg/L) yielded an 86% adsorption rate and 10 mg/L yielded 96% (Table 4.2).

Site 3 sediments were far less efficient, adsorbing 55% of the overlying phosphorus across all incubations after 2 hours (Fig. 4.7.B). Within 24 hours, that adsorbance increased to 65% with a maximum of 82% in the lowest incubation (0.5 mg/L). However, contrary to site 1, site 3 adsorption efficiency decreased with an increase in concentration where the lowest addition (0.5 mg/L) yielded an 82% adsorption rate and 10 mg/L yielded only 54% (Table 4.3).

Analysis of variance of adsorption capacity at equilibrium (24-hours) as a function of sites 1 and 3 proved statistically significant (pseudo-$F_{1, 22} = 8.422$, $P = 0.008$). Analysis of variance also identified a significant difference

between concentrations after 24-hours between 10 and 0.5 mg/L (pseudo-$F_{3, 20}$ = 4.519, P = 0.01) and between 10 and 1 mg/L (pseudo-$F_{3, 20}$ = 4.519, P = 0.02).

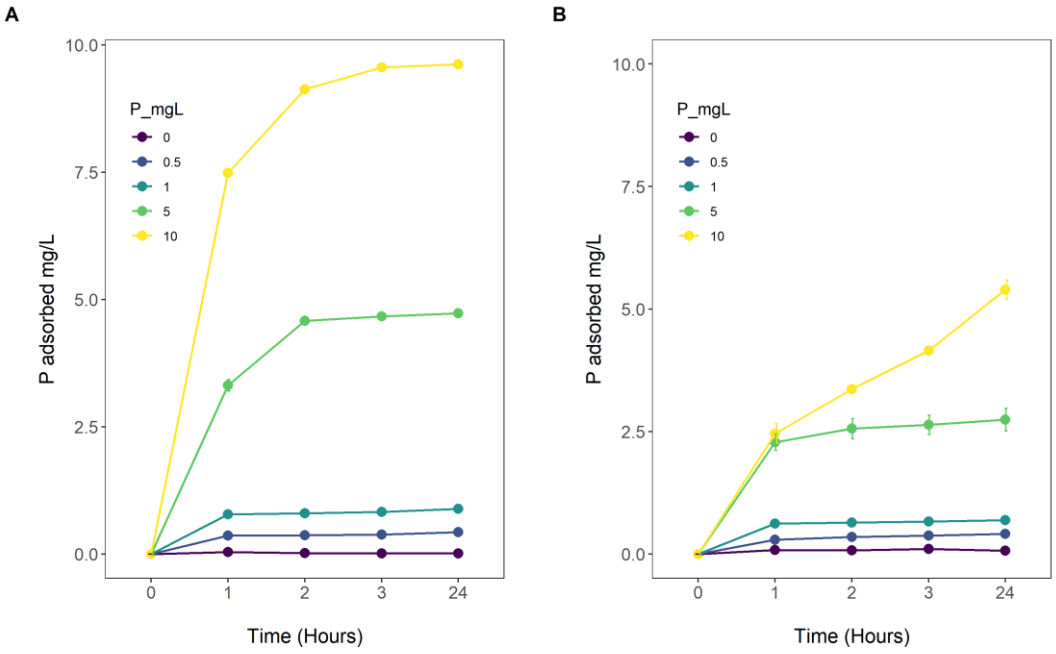

Figure 4.7 Mean phosphorus (mg/L) adsorbed over 24 hours of incubation by site 1 (A) and site 3 (B) sediments collected in September and October 2018.

Table 4.3 Mean Phosphorus (± SE) adsorbed after 24 hours as a percentage of the initial phosphorus added for Sites 1 and 3 in September and October 2018. n = 3

Initial Concentration mg $P\text{-}PO_4$ L	Site 1 Adsorption (%) at 2 Hours	Site 1 Adsorption (%) at 24 Hours	Site 3 Adsorption (%) at 2 Hours	Site 3 Adsorption (%) at 24 Hours
0.5	74 ± 0.00	86 ± 2.09	70 ± 0.01	82 ± 0.00
1.0	80 ± 0.02	89 ± 0.46	65 ± 0.01	69 ± 0.02
5.0	92 ± 0.02	95 ± 0.25	51 ± 0.20	55 ± 0.23
10.0	91 ± 0.00	96 ± 0.08	34 ± 0.04	54 ± 0.19

4.2.4 Freundlich and Langmuir adsorption equations

Site 1 (high ferric site) and site 3 (low ferric site) data points corresponding to 24-hours of incubation were fitted to Freundlich and Langmuir isotherm models. Both the linear and non-linear forms of each model were applied to identify best fit. For both sites 1 and 3, the Freundlich linear model best fit the data supported by both the R^2 and AIC scores (Table 4.4). The fitted data was then plotted and the linear equation of the isotherm extracted (Fig. 4.8).

Table 4.4 Fitted Freundlich and Langmuir isotherm models with model coefficients for sites 1 and 3 sediment collected in September - October 2018.

Sample Site	Isotherm Model	Fitted adsorption capacity isotherm	R^2	*P* -value	AIC
Site 1	Freundlich	S = 1.7 + 1.8 * C	0.962	< 0.000	-13.92
Site 1	Langmuir	S = -0.28 + 0.16 * C	0.849	< 0.000	14.76
Site 3	Freundlich	S = 0.24 + 0.65 * C	0.970	< 0.000	-21.42
Site 3	Langmuir	S = 0.37 + 0.2 * C	0.916	< 0.000	7.98

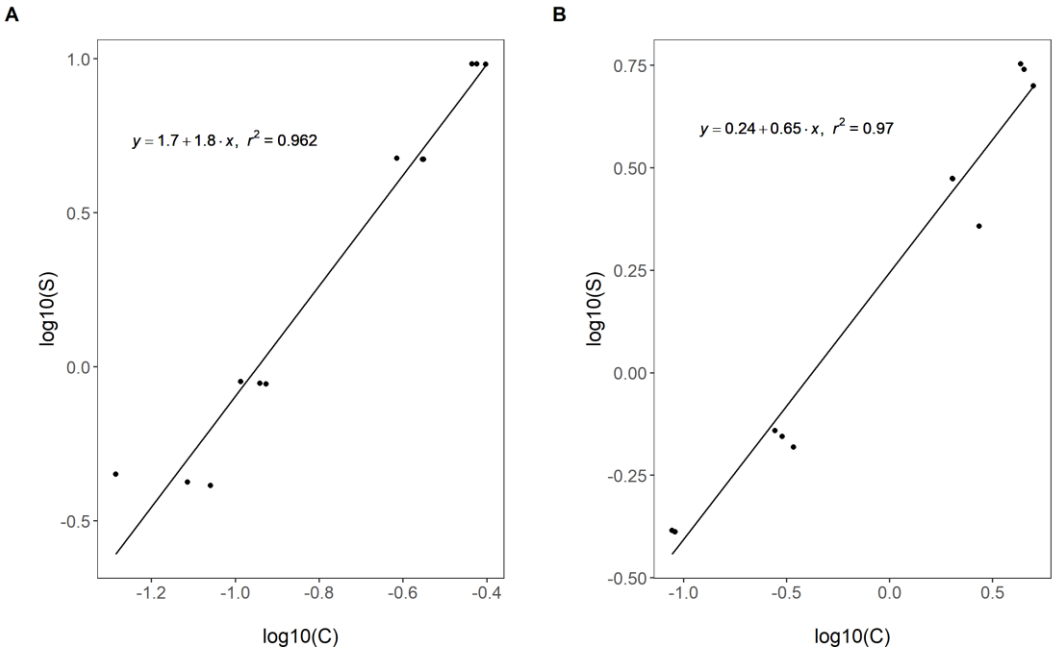

Figure 4.8 Freundlich adsorption capacity isotherms constructed for sites 1 (A) and 3 (B) for Alton Water in September and October 2018. S is the phosphorus adsorbed (mg/L) after 24 hours of incubation and C is the phosphorus concentration (mg/L) after 24 hours of incubation. The linear model and R^2 coefficient for isotherm's A and B are displayed in each plot.

4.2.5 Equilibrium Phosphorus Concentrations (EPC_0)

EPC_0 concentrations varied from 0.24 mg P L^{-1} at site 3 to 1.7 mg P L^{-1} at site 1. Compared to the overlying sediment-water, the EPC_0 for site 1 was 24x great whereas site 3 was only 1.6x greater (Table 4.5).

Table 4.5 Equilibrium Phosphorus Concentrations (EPC_0) derived from fitted adsorption capacity isotherms for sites 1 and 3 sediment collected in September and October 2018.

Sample Site	Isotherm Model	EPC_0 mg P- PO_4 L	Overlying Water mg P- PO_4 L
Site 1	Freundlich (linear)	1.7	0.07
Site 3	Freundlich (linear)	0.24	0.15

4.2.6 Metal-bound Phosphorus Fractions

4.2.6.1 Labile-P

The highest concentration of Labile P in Alton Water was found inside the bund (1.87 mg P/g dw). Concentrations then decreased from inside to outside the bund (1.14 mg P/g dw) before increasing in the mid reservoir (1.24 mg P/g dw) and again in the main basin (1.27 mg P/g dw) (Table. 4.5). Analysis of variance models determined labile-P did not differ significantly between any site combinations (Fig. 4.9).

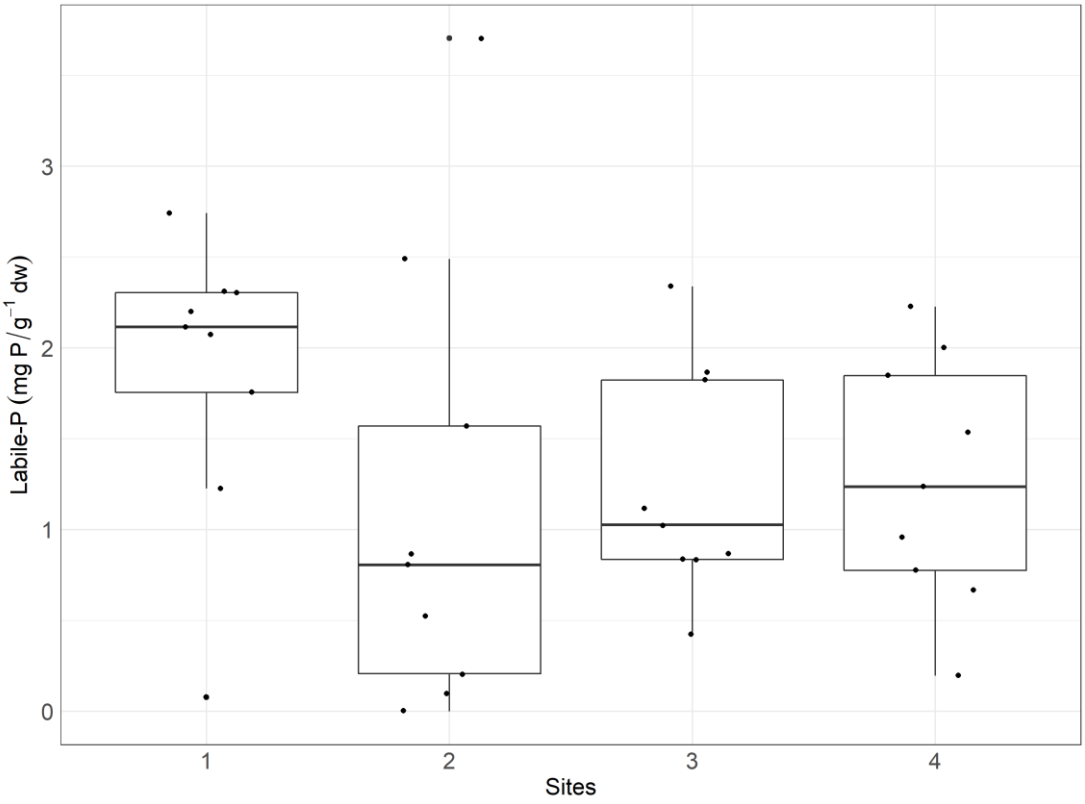

Figure 4.9 Labile-P (mg P/g dw) in Alton Water across sites 1, 2, 3, and 4 in September and October 2018. For each boxplot, the boundary of the box closest to zero indicates the 25th percentile, the black line within the box indicates the median, and the boundary of the box farthest from zero indicates the 75th percentile. Whiskers above and below the box mark the 10th and 90th percentiles while the points above and below the whiskers indicate outliers outside the 10th and 90th percentiles.

4.2.6.2 Iron bound P

Iron-bound phosphorus (Fe-P) in Alton Water has accumulated in greatest concentrations outside the bund (17.11 mg P/g dw). Concentrations then show a large decrease in the mid reservoir (0.25 mg P/g dw) and decrease further again in the main basin (0.22 mg P/g dw) (Table. 4.5). While there is

a noticeable difference in Fe-P from the upper reservoir to the deeper waters analysis of variance models found Fe-P did not differ significantly between any site combinations (Fig. 4.10).

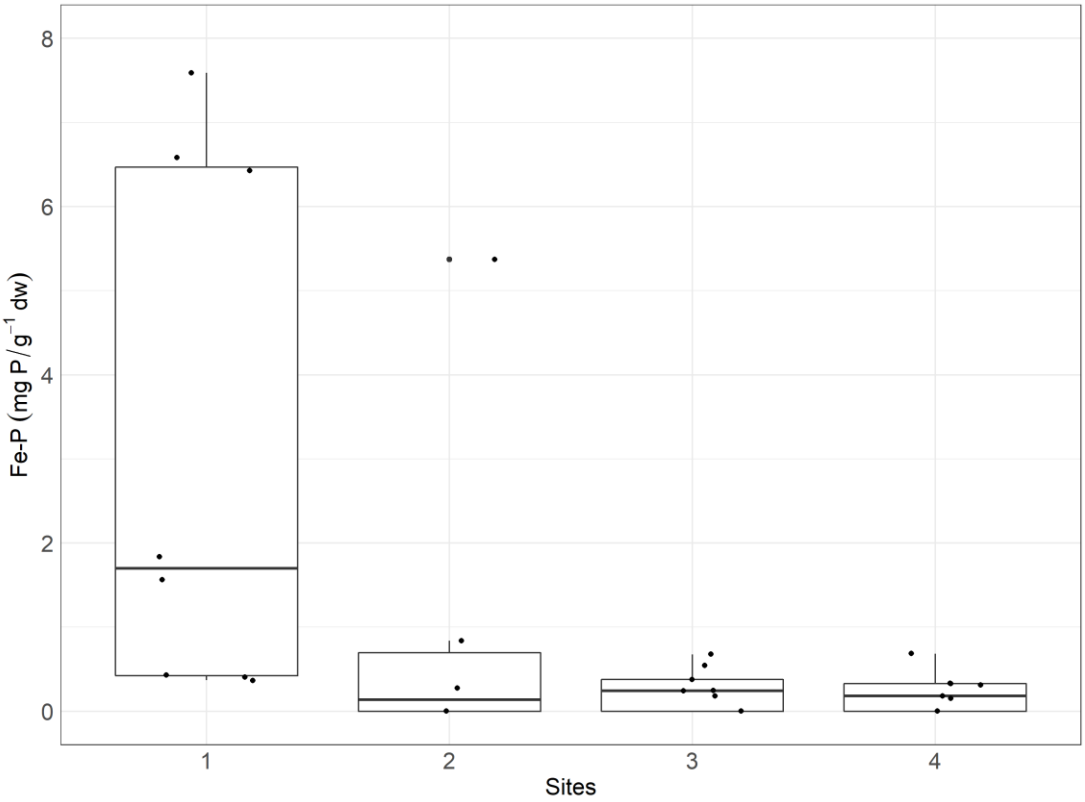

Figure 4.10 Fe-P (mg P/g dw) in Alton Water across sites 1, 2, 3, and 4 in September and October 2018. For each boxplot, the boundary of the box closest to zero indicates the 25th percentile, the black line within the box indicates the median, and the boundary of the box farthest from zero indicates the 75th percentile. Whiskers above and below the box mark the 10th and 90th percentiles while the points above and below the whiskers indicate outliers outside the 10th and 90th percentiles.

4.2.6.3 Calcium bound P

Concentrations of calcium bound phosphorus (Ca-P) decreased down the reservoir gradient from the inlet to the main basin with the highest concentrations inside the bund (53.20 mg P/g dw) (Table. 4.5). Analysis of variance models found Ca-P differed significantly between sites 1-2 ($F_{3, 32}$ = 7.741, P = 0.03), sites 1-3 ($F_{3, 32}$ = 7.741, P = 0.002), and sites 1-4 ($F_{3, 32}$ = 7.741, P < 0.000). For all other site interactions, no significant difference in Ca-P concentrations was found (Fig. 4.11).

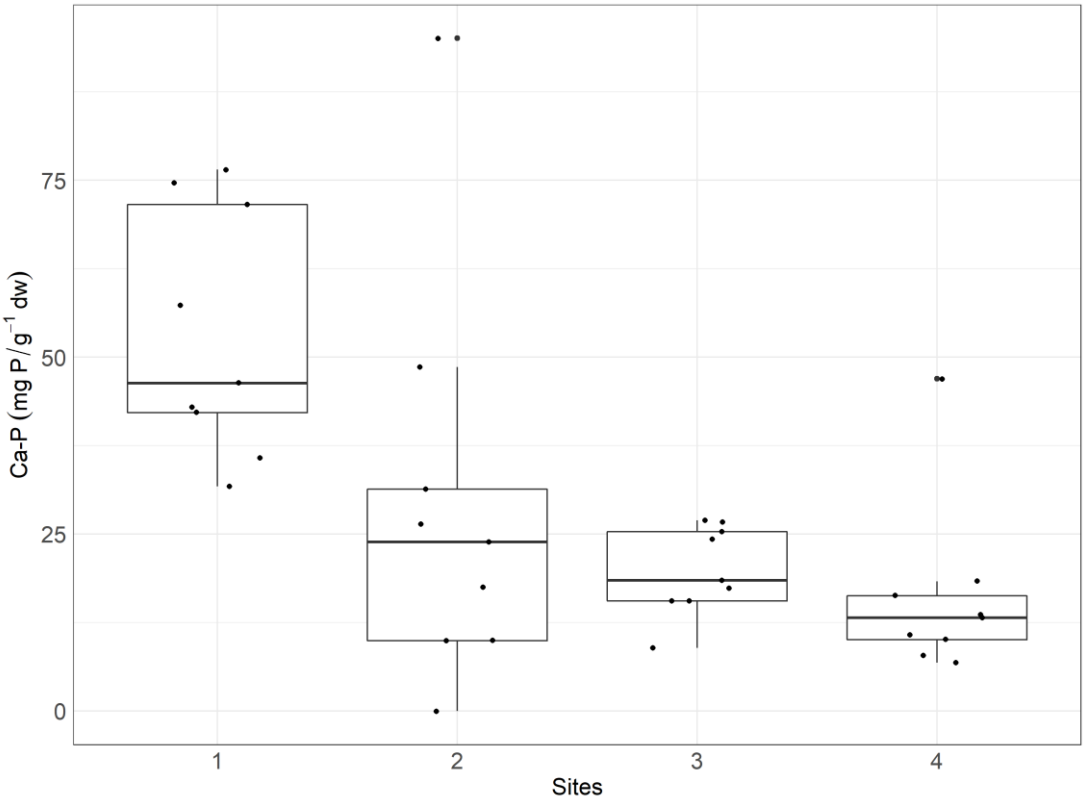

Figure 4.11 Ca-P (mg P/g dw) in Alton Water across sites 1, 2, 3, and 4 in September and October 2018. For each boxplot, the boundary of the box closest to zero indicates the 25th percentile, the black line within the box indicates the median, and the boundary of the box farthest from zero indicates the 75th percentile. Whiskers above and below the box mark the 10th and 90th percentiles while the points above and below the whiskers indicate outliers outside the 10th and 90th percentiles.

4.2.6.4 Aluminum bound P

Aluminium bound phosphorus (Al-P) was found is concentrations approaching the limit of detection. These concentrations remained equivalent throughout the reservoir until the main basin where it was not detected (Table.

4.6). Analysis of variance models found Al-P did not differ significantly between any site combinations (Fig. 4.12).

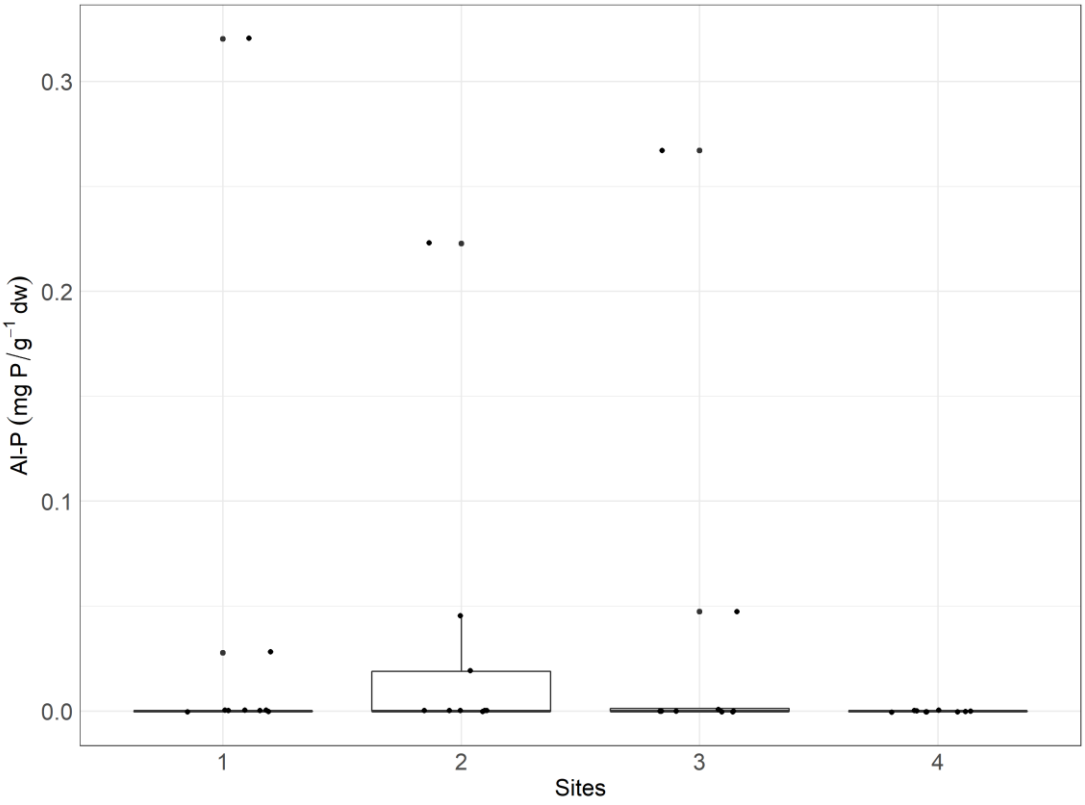

Figure 4.12 Al-P (mg P/g dw) in Alton Water across sites 1, 2, 3, and 4 in September and October 2018. For each boxplot, the boundary of the box closest to zero indicates the 25th percentile, the black line within the box indicates the median, and the boundary of the box farthest from zero indicates the 75th percentile. Whiskers above and below the box mark the 10th and 90th percentiles while the points above and below the whiskers indicate outliers outside the 10th and 90th percentiles.

Table 4.6 Mean sediment iron (Fe-P), calcium (Ca-P), aluminium (Al-P), and Labile-P fractions (mg of P per gram of dw sediment) in the top 6cm of Alton Water (Sep – Oct 2018). ND indicated non-detection.

Site	Labile-P *n* =9	Fe-P *n* =9	Ca-P *n* =9	Al-P *n* =9
1	1.87 ± (0.26)	12.81 ± (9.71)	53.20 ± (5.76)	0.04 ± (0.03)
2	1.14 ± (0.42)	17.11 ± (9.30)	29.19 ± (9.49)	0.03 ± (0.02)
3	1.24 ± (0.21)	0.25 ± (0.08)	19.89 ± (2.08)	0.04 ± (0.03)
4	1.27 ± (0.26)	0.22 ± (0.07)	15.97 ± (4.06)	ND

4.2.7 Water and Nutrient Impact on bound P

Nutrient and water chemistry impact variables were created from PCA scores as discussed in section 4.3.1 and 4.3.2. Multivariate analysis (MANOVA) identified a significant effect of nutrients on calcium bound P concentrations ($F_{1,32}$ = 22.96, P < 0.000) but not on any other bound fraction. Similarly, multivariate analysis further identified a significant effect of water chemistry on calcium bound P concentrations ($F_{1,33}$ = 23.65, P < 0.000) but not on any other bound fraction. There was also no significant difference of this effect between sites.

4.3 DISCUSSION

4.3.1 Research Question 1. What is the role of legacy P in supporting reservoir wide phytoplankton blooms?

Labile P is the bound fraction that diffuses the fastest from the sediment and becomes readily available for uptake by phytoplankton. In Alton Water, labile P was found in a near uniform distribution throughout the length of the reservoir. This confirms a steady supply of nutrients to the water column to support growth. Calcium bound P (Ca-P) was also found is supply throughout

the reservoir but in much higher concentrations inside the bund. This may be attributed to calcite/calcium-carbonate entering the system from the inlet where catchment waters carry chalk rich groundwater to the reservoir (Lloyd et al., 1981). Iron bound P (Fe-P) was highest in the upper reservoir compared to negligible concentrations in lower reservoir. This distribution is expected as ferric dosing to bind P is dispensed inside the bund. Inside the bund, the ratio of Fe-P to Ca-P is 1:4. Studies have found a ratio of iron to calcium bound P less than 0.5 releases more P when water chemistry pH is less than 7 (acidic) (Huang et al., 2005). Therefore, monitoring pH in the upper reservoir may help identify increases in water column P (from internal loading) despite little P entering the system. This is also true for the rest of the reservoir as the ratio of Fe-P to Ca-P in the lower reservoir was 1:76 (0.01). Aluminium bound P (Al-P) was found in very low concentrations from the inlet through to the main reservoir before it was undetectable in the main basin. We can therefore say Al-P is unlikely to be a major source of internal loading in Alton.

4.3.2 Research Question 2. Is Alton Water sediment a source or sink for bound phosphorus?

Equilibrium phosphorus concentrations based on adsorption capacity experiments and isotherm modelling found both sites 1 and 3 were a source for phosphorus to the water column. Sediment inside the bund was 24x greater than the overlying water column whereas sediment in the mid reservoir was 1.6x greater than the water column. While both sites are contributing P to the reservoir the amount of P entering the system from internal loading is far greater inside the bund. Inside the bund also contains

high ferric sediment from management of P inflow through ferric dosing. Iron-bound P analysis showed higher concentrations inside and outside the bund compared to negligible concentrations in the mid reservoir and main basin. This tells us P is successfully being bound at the inlet however, sediment saturation has caused newly bound P to flow out of the bund instead of joining the sediment-P pool.

4.3.3 Research Question 3. Can water chemistry help explain trends in metal-bound P fractions?

Dissolved oxygen, pH, and redox potential are the major contributing factors for the release of bound P from the sediment into the water column and supporting phytoplankton. pH was found to be nearly uniform throughout the reservoir at a neutral concentration with a small pull towards alkaline. Based on the ratios of Fe-P to Ca-P it can be said at the time of this study (autumn) pH was not driving internal loading into the system.

Dissolved oxygen was also found in a healthy range (6.8 – 11.2 mg/L) throughout the reservoir providing aerobic conditions to the sediment. Only the main basin had a borderline healthy concentration (6.28 mg/L), which may be caused by an increase in biological activity (i.e. fish) due to its much larger surface area and depth compared to the upper reservoir. Anaerobic conditions increase the release of P from the sediment, and while the main basin is well above anaerobic concentrations (<1 mg/L), the lower dissolved oxygen may be increasing internal loading to a greater degree than in the rest of the reservoir.

Analysis of water chemistry and nutrients on P fractions found only an effect on Ca-P and on no other bound fraction. This effect also did not change between sites. This may tell us that overall, Alton's biogeochemistry is influencing Ca-P, the largest bound fraction in the reservoir, which may be evidence for future internal loading.

4.3.4 Research Question 4. How effective is the bund wall in holding locked-P in the reservoir inlet?

At the surface, orthophosphate, organic, and total phosphorus (P) increase down the reservoir to form a gradient from the inlet to the main basin. The only exception was organic P, which decreased slightly from the mid reservoir to the main basin. Conversely, P fractions at the sediment-water interface were more variable, fluctuating from site to site. Both organic and total P increased from inside to outside the bund, the decreased going down the reservoir before increasing again in the main basin. Total P concentrations from site to site however were similar where inside the bund and the mid reservoir were similar and outside the bund and the main basin were similar. When averaged by upper and lower reservoir, the lower reservoir was higher only by 0.01 µg/L than the upper reservoir whereas the upper and lower reservoir averages for organic P where higher in the upper reservoir. Orthophosphate showed an opposite trend at each site and decreased from inside to outside the bund, increased in the mid reservoir then decreased in the main basin. The decrease (0.01 µg/L) however was small enough to be negligible and thus both sites could be considered the same. Orthophosphate concentrations in the mid reservoir and the main basin were also comparable

to each and higher than the upper reservoir. Based on this, orthophosphate at the sediment is higher in the lower reservoir compared to the top of the reservoir.

Overall, at both the water's surface and the sediment, orthophosphate and total P were higher in the lower reservoir (mid reservoir to the main basin) than in the upper inlet (inside and outside the bund). Organic P at the water's surface was also higher in the lower reservoir compared to the upper whereas organic P at the sediment was lower in the lower reservoir than the upper.

The decrease in organic P in the main basin may be explained by a process known as alkaline phosphatase activity (APA) where phytoplankton convert unusable organic P fractions into useable orthophosphate when orthophosphate in low. However, orthophosphate was highest in the main basin compared to the rest of the reservoir. This would then lead us to expect organic P to also be high in the basin if orthophosphate is readily available to support phytoplankton populations. Yet, this study was completed during the autumn bloom when biomass was increasing. Therefore, while orthophosphate was highest in the main basin, it may not have been high enough to support growth. Especially as the main basin is the largest and deepest part of the reservoir with a much larger community to support. Therefore, it is still feasible to conclude phytoplankton may be utilizing organic P to support growth through APA.

CHAPTER 5

TESTING THE STABILITY OF A MANAGED PHOSPHATE REDUCTION GRADIENT IN ALTON WATER

5.0 INTRODUCTION

The response of phytoplankton to *in situ* nutrient enrichment assays is one of the most utilized methods for detecting nutrient limitation in freshwater ecology (Elser and Kimmel, 1986). Yet, it has sometimes fallen to criticism due to confounding and potential unmeasured limiting factors such as community composition and micronutrient concentrations (Elser et al., 1990; Healey, 1979; Kalff, 1971). Nonetheless, enrichment bioassays offer important insight into what controls algal biomass under current and future nutrient scenarios.

Two main approaches to nutrient bioassays are frequently used to identify limitation. The first, Liebig limitation, looks at the maximum yield of phytoplankton. Liebig limitation will not identify which nutrient is limiting if any, but instead, that a certain nutrient will become the limiting factor with continued growth (Beardall et al., 2001). The second approach considers sudden growth, where the addition of one or more nutrients encourages growth and in turn identifies that nutrient(s) as limiting (Beardall et al., 2001).

The latter approach and the one used in this study, relies on natural a community assemblage where samples from various sites throughout the waterbody were spiked with phosphorus, nitrogen and a combination of the two. Based on phytoplankton response to the enrichment, we were able to identify spatial limitation as well as response under eutrophic conditions. Most importantly for phosphorus concentrations, which is not only the most abundant nutrient to enter freshwater systems but also the most managed.

Agricultural runoff (i.e. soil and manure) (Reid et al., 2018; Sharpley et al., 1994), catchment source waters (i.e. wastewater and storm water) (Brudler et al., 2019; WHO, 2007), and internal loading (i.e. labile-Phosphorus) (Lee et al., 2019; Sondergaard et al., 2001) all serve as sources of phosphorus input to freshwater bodies. In these nutrient rich waters, phytoplankton mop-up the bioavailable phosphorus which quickly increases biomass, especially during warm summer months. As biomass increases, more phosphorus is removed from the system and the reservoir enters a state of nutrient limitation. Despite this, many phytoplankton thrive and biomass can continue to increase. This is due in part to some phytoplankton's ability to convert the unusable, yet plentiful dissolved organic phosphorus to useable inorganic fractions utilizing an enzyme known as Alkaline Phosphatase (AP) (Kang et al., 2019). During times of inorganic phosphorus limitation, AP enzymes will sever the monophosphate esters of organic phosphorus molecules freeing them for uptake by the plankton (Young et al., 2010). This process is known as Alkaline Phosphatase Activity or APA. During periods of nutrient limitation, when bioavailable phosphorus becomes deficient (<0.2µM), the APA of

phytoplankton cells will increase (Nausch, 1998). This makes APA measurements an important tool to explain increasing algal biomass despite apparent low phosphorus concentrations.

In Alton Water, phytoplankton blooms are a serious concern due to the reservoir's usage as a drinking water system and year-round recreation. Both long (i.e. catchment reductions and waste water treatment for river discharge) and short term efforts (i.e. ferric dosing) have been in place to reduce phosphorus input to the system however, high cell counts (>70,000 cells/mL) and cyanobacteria blooms have occurred consistently during recent years during the spring, summer, and autumn seasons. To understand the current state of phosphorus in Alton Water and potential activation of APA from nutrient limitation, this study performed sudden-growth nutrient bioassay experiments and APA measurements along a known reservoir productivity gradient in July 2019 and proposed the following hypotheses:

H1. Site 1 (inside a management bund) is phosphorus limited due to ferric dosing which binds phosphorus at the top of the reservoir, preventing it from travelling downstream to the main basin.

H2. The rate of nutrient limitation decreases down the reservoir gradient as less phosphorus is being locked through ferric binding allowing it to move freely downstream.

H3. Alkaline Phosphatase Activity will be highest inside the bund where inorganic phosphorus is actively bound. In turn, phytoplankton will work to convert organic phosphorus to a usable inorganic form allowing it to support growth.

5.1 MATERIALS AND METHODS

5.1.1 Study Sites

A description of the study site (Alton Water) is presented in Chapter 4, Sections 4.1.1

5.1.2 Nutrient Bioassay: An *in situ* microcosm experiment

Surface water samples were collected from inside the bund (site 1), outside the bund (site 2), Lemon Hill bridge (site 3), and the main basin (site 4) in July 2019. Samples were placed in 2-litre polyethylene terephthalate (PET) plastic bottles with screw-top lids. For each site, three bottles were enriched with 1 mg/L of monopotassium phosphate (H_2KPO_4), a second set of three bottles enriched with 2 mg/L of ammonium chloride (NH_4Cl), a third set of three containing both nitrogen and phosphorus additions at 2 mg/L and 1 mg/L respectively and a fourth set of bottles acted as untreated controls. Concentrations for both nitrogen and phosphorus additions were calculated according to (Perkins and Underwood, 2000).

Within each bottle, a 500 mL headspace was allocated for gas exchange. The bottle top was then tied with string to orange marker buoys and anchored to the reservoir bottom with 440 x 215 x 215 mm concreate blocks. Approximately 1/4 of the bottle floated above the water's surface allowing for light penetration.

All 48 bottles were anchored in 4 m of water approximately 50 m from shore in the main basin of Alton Water. Initial chlorophyll-*a* concentrations were captured on day zero followed by sub-sampling (100 mL) from each bottle on day two and a final measurement of 500 mL from all bottles on day six. A six-day incubation cycle was chosen based on the pilot study which found die-off after seven-days across all treatments.

5.1.3 Algal Biomass as Chlorophyll-*a*

To quantify algal biomass (as chlorophyll-*a*), 500 mL of reservoir surface water was filtered on day zero followed by 100 mL on day two and 500 mL on day six onto 47mm glass microfiber filters. Both day two and day six subsamples were taken from the bottles. Filters were analysed according to methods described in Chapter 2 section 2.2.2.

5.1.4 Alkaline Phosphatase Activity (APA)

Surface samples were collected in triplicate at sites 1, 2, 3, and 4 in July 2019 for the determination of Alkaline Phosphatase Activity (APA) (Perkins and Underwood, 2000). Samples were transported to the laboratory where analysis was performed immediately upon return. 0.44 mL of 107.78 µM pNPP solution was added to 20 mL of unfiltered sample and standards. After gentle mixing, 0.89 mL of 50mM HEPES buffer solution was added followed by the addition of 0.5 mL of glycine solution. Samples and standards were then sealed, mixed in a 25°C water bath and incubated for 1 hour. After incubation, 1 mL of sample/standard was placed in a 1.5 mL cuvette and read on a Shimadzu UV-1800 spectrophotometer at 405nm.

To obtain the final APA concentration from the absorbance and standard curve the following equation was used:

$$\frac{\left(\frac{(Abs - c)}{m}\right) X \frac{V}{1000}}{\text{Chlorophyll-a (ug)} \times V\text{ (ml)} \times T\text{(hr)}}$$

Where:

Abs = Spec reading at 405nm

C = c in the standard Curve Equation

V = Sample/standards volume

Chlorophyll-a = Chlorophyll-a concentration obtained alongside APA measurements

T(hr) = Incubation time in hours

5.1.5 Statistical Analysis

To test the effect of time (days) on chlorophyll-*a* concentrations under varying treatments and across sites, quasipoisson generalized linear models were used (GLMs). For APA analysis, GLMs with quasipoisson distribution were also used to test the change in APA concentrations across sites. Lastly, chlorophyll-*a* concentrations between sites was assessed using GLMs of the Gaussian distribution. All analyses were conducted in the R statistical language (R Core Team, 2019), using the following packages: 'dplyr' (Hadley et al., 2020), 'ggplot2' (Wickham, 2016), 'viridislight' (Garnier, 2018).

5.2 RESULTS

5.2.1 Nutrient Bioassay

Site 1 experienced a significant increase in biomass under P treatments between days (GLM; $F_{1, 7} = 9.653$, $P = 0.01$) while biomass under N treatments significantly declined (GLM; $F_{1, 7} = 11.448$, $P = 0.01$). Biomass under N+P treatments increased initially from day zero to day 2 but then declined from day two through day six. Overall, this was an increase however it was not significant (GLM; $F_{1, 7} = 3.310$, $P = 0.111$). Conversely, the control for site 1 experienced a significant decline in biomass between days (GLM; $F_{1, 7} = 28.026$, $P = 0.001$) (Fig. 5.1).

Site 2 experienced a significant increase in biomass under P (GLM; $F_{1, 7} = 7.663$, $P = 0.02$) and N+P (GLM; $F_{1, 7} = 170.55$, $P < 0.000$) treatments with the larger increase in the N+P bioassay. For N (GLM; $F_{1, 7} = 0.276$, $P = 0.615$) treatments and the control (GLM; $F_{1, 7} = 0.013$, $P = 0.910$), no significant change in biomass was observed (Fig. 5.1).

Biomass in site 3 responded similarly to site 2 with a significant increase in P (GLM; $F_{1, 7} = 57.955$, $P < 0.000$) and N+P (GLM; $F_{1, 7} = 22.76$, $P = 0.002$) treatments however, the larger increase at site 3 was in the P bioassay. For N (GLM; $F_{1, 7} = 0.159$, $P = 0.701$) treatments and the control (GLM; $F_{1, 7} = 0.192$, $P = 0.672$), no significant change was observed between days (Fig. 5.1).

Site 4 experienced no significant changes in biomass between days despite an increase in the control (GLM; $F_{1, 7} = 0.053$, $P < 0.823$), a decrease in N (GLM; $F_{1, 7} = 2.967$, $P < 0.128$), decrease in P (GLM; $F_{1, 7} = 0.000$, $P = 0.992$) and an increase in N+P (GLM; $F_{1, 7} = 2.550$, $P = 0.154$) (Fig. 5.1).

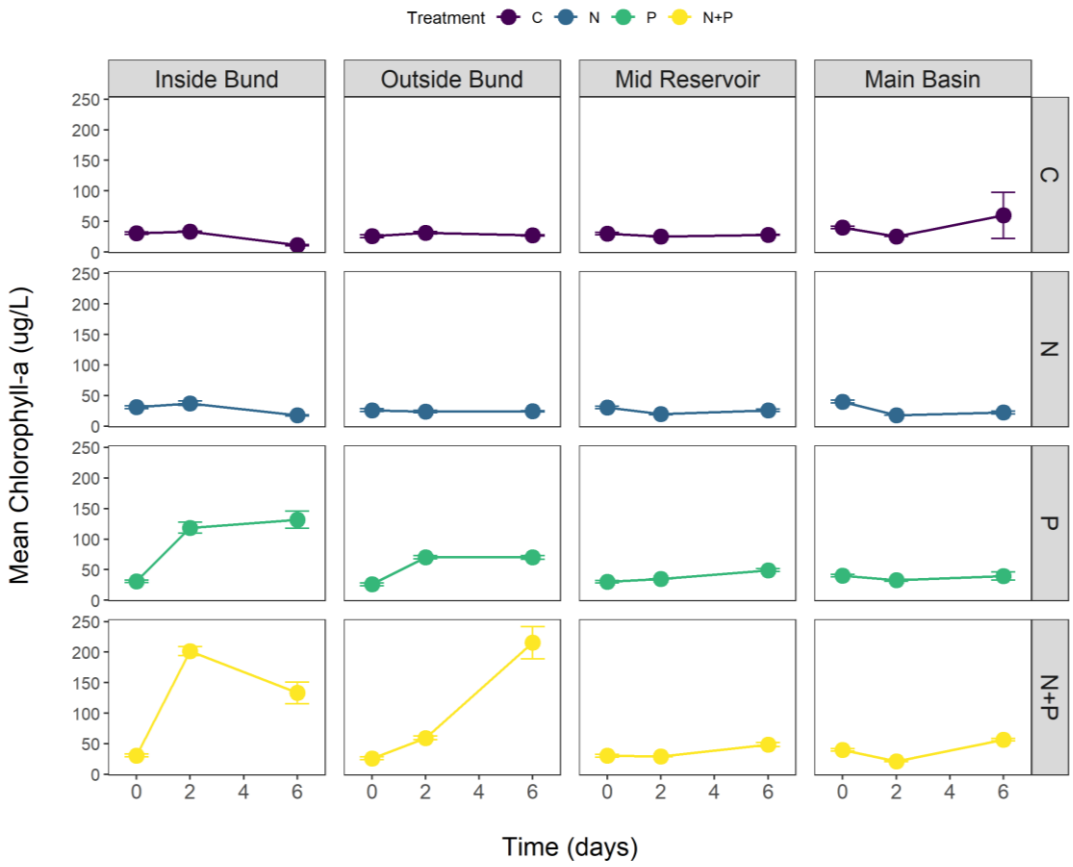

Figure 5.1 Mean chlorophyll-*a* concentrations (µg/L) (n=3) over six days at sites 1 (inside the bund), 2 (outside the bund), 3 (mid-reservoir) and 4 (main basin) in July 2019 after varying nutrient additions (P = 1 mg $P\text{-}PO_4$ l^{-1}, N = 2 mg $N\text{-}NH_4$ l^{-1}, N+P = 1 mg $P\text{-}PO_4$ l^{-1} + 2 mg $N\text{-}NH_4$ l^{-1}, and C = Control). Error bars indicate SE.

5.2.2 Phosphatase Activity (APA): laboratory-based experimentation

Alkaline Phosphatase Activity (APA) ranged from 0.006 (µmoles/µg of Chl-a/hr) (site 2) to 0.003 (µmoles/µg of Chl-a/hr) (site 4). The mean concentration between sites was also highest at site 2 (0.005 µmoles/µg of Chl-a/hr) and lowest at site 4 (0.003 µmoles/µg of Chl-a/hr). Generalized linear models using quasipoisson distribution found overall, APA concentrations differed significantly between sites (GLM; $F_{3, 8} = 8.384$, $P = 0.007$). More specifically, that difference was greatest between sites 2 and 4 (GLM; $F_{1, 4} = 21.924$, $P = 0.009$), followed by sites 2 and 3 (GLM; $F_{1, 4} = 11.939$, $P = 0.025$). Between sites 1 and 4, a borderline significance was observed (GLM; $F_{1, 4} = 7.289$, $P = 0.054$). For all other site interactions, no significant difference in APA concentrations was found (Fig. 5.2).

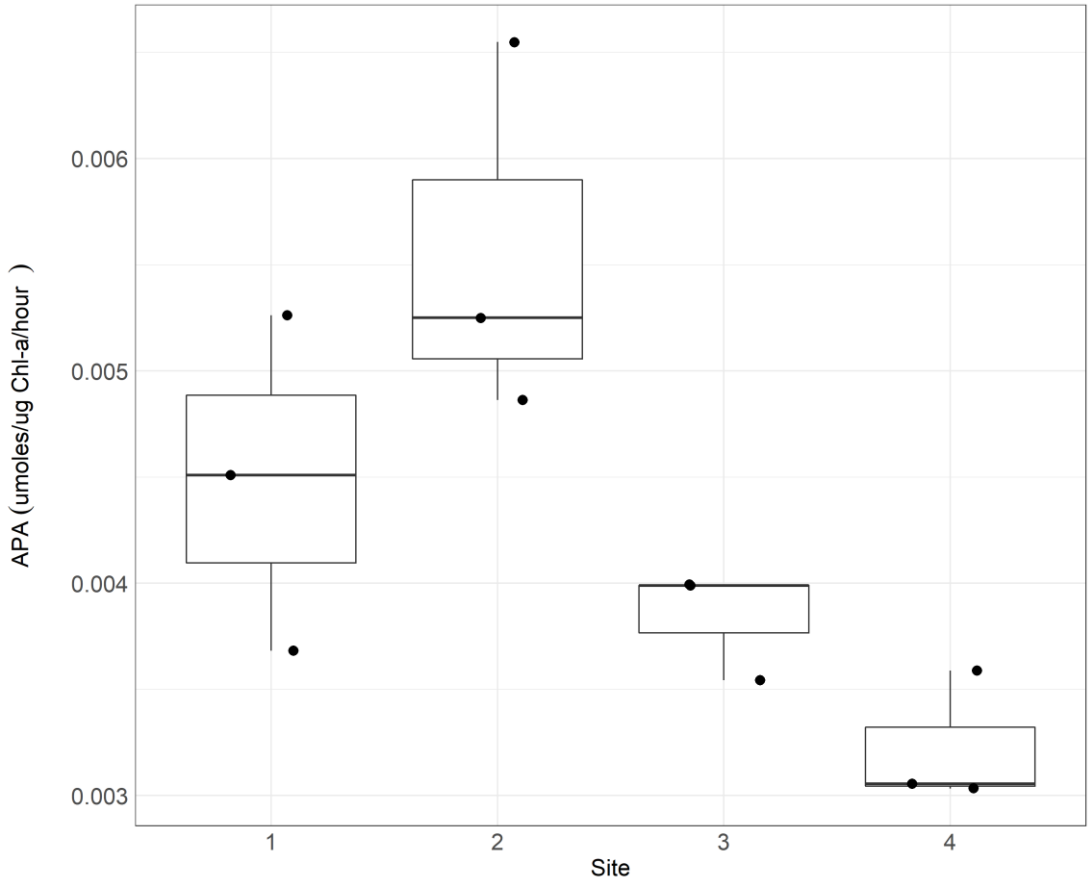

Figure 5.2 APA concentrations (µmoles/µg of Chl-a/hr) (n=3) at Sites 1 (inside the bund), 2 (outside the bund), 3 (mid-reservoir) and 4 (main basin) in July 2019. For each boxplot, the boundary of the box closest to zero indicates the 25th percentile, the black line within the box indicates the median, and the boundary of the box farthest from zero indicates the 75th percentile. Whiskers above and below the box mark the 10th and 90th percentiles while the points above and below the whiskers indicate outliers outside the 10th and 90th percentiles.

Chlorophyll-*a* concentrations collected in conjunction with APA ranged from 42.40 (µg/L) (site 4) to 21.38 (µg/L) (site 2). The mean concentration between sites was also highest at site 4 (40.11 µg/L) and lowest at site 2 (25.97 µg/L). Generalized linear models using Gaussian distribution found overall, APA concentrations differed significantly between sites (GLM; $F_{3, 8} = 8.177$, $P = 0.008$). More specifically, that difference was greatest between sites 1 and 4 (GLM; $F_{1, 4} = 9.428$, $P = 0.03$), followed by sites 2 and 3 (GLM; $F_{1, 4} = 8.963$, $P = 0.04$). For all other site interactions, no significant difference in APA concentrations was found (Fig. 5.3).

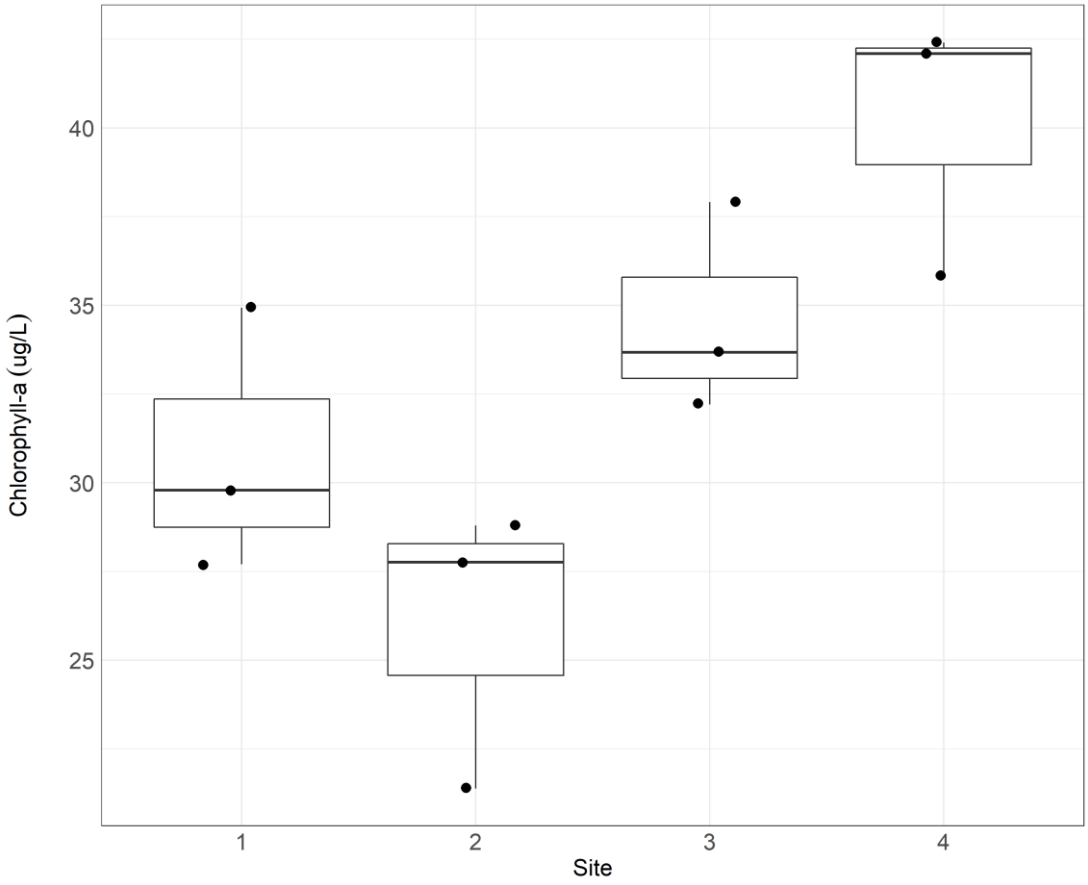

Figure 5.3 Chlorophyll-*a* concentrations (µg/L) associated with APA measurements (n=3) at sites 1 (inside the bund), 2 (outside the bund), 3 (mid-reservoir) and 4 (main basin) in July 2019. For each boxplot, the boundary of the box closest to zero indicates the 25th percentile, the black line within the box indicates the median, and the boundary of the box farthest from zero indicates the 75th percentile. Whiskers above and below the box mark the 10th and 90th percentiles while the points above and below the whiskers indicate outliers outside the 10th and 90th percentiles.

5.3 DISCUSSION

5.3.1 H1. Site 1 (inside a management bund) is phosphorus limited due to ferric dosing which binds phosphorus at the top of the reservoir, preventing it from travelling downstream to the main basin.

Inside the bund, biomass within the control treatment declined between day zero and day six. This decline was significant which is expected as the communities inside the bottle use up the baseline reservoir nutrients. With the addition of nitrogen, biomass also decreased and this decrease was significant. With the addition of nitrogen and phosphorus, biomass increased as well as with the addition of phosphorus alone. Based on this, we can accept the hypothesis and say during summer months, phytoplankton at the reservoir inlet and inside the bund wall are phosphorus limited. This conclusion agrees with earlier *in situ* enrichment studies that found Alton water to be phosphorus limited inside the bund (Perkins and Underwood, 2000). Similarly, phosphorus limitation in other UK reservoirs has been identified including three in the North-west midlands (Maberly et al., 2020). Phosphorus limitation inside the bund may be explained by ferric dosing which binds phosphorus at the top of the reservoir, preventing it from travelling downstream to the main basin. With the addition of the bund wall, phosphorus is trapped, allowing more time for binding before it sinks to the sediment or is flushed over the bund from water level increases or potential storm events.

5.3.2 H2. The rate of nutrient limitation decreases down the reservoir gradient as less phosphorus is being locked through ferric binding allowing it to move freely downstream.

In the upper reservoir, the response to nutrient enrichment experiments was higher than in the lower reservoir (mid reservoir-main basin). In addition, bioassays with P additions experienced a far great increase in biomass than bioassays in the lower reservoir. P growth response decreased down the reservoir to form a P limitation gradient whereas N+P bioassay response fluctuated between sites. However, it should be noted a growth response was found in the main basin control bottle for N+P treatments. Therefore, we cannot say if the growth response seen in the main basin is truly a response to nutrient additions. Nevertheless, we can accept the hypothesis and conclude P limitation decreases down the reservoir where the inlet is the most P limited and the main basin is the least P limited. This may be explained by ferric binding of P inside the bund resulting in less bioavailability to phytoplankton.

5.3.3 H3. Alkaline Phosphatase Activity will be highest inside the bund where inorganic phosphorus is actively bound. In turn, phytoplankton will work to convert organic phosphorus to a usable inorganic form allowing it to support growth.

Based on this study we can reject the hypothesis, as APA was highest outside the bund but overall greater in the upper reservoir compared to the lower reservoir. This correlates to our results of P limitation, which was also highest in the upper reservoir. As P limitation decreases down the reservoir so does

alkaline phosphatase activity. This is to be expected, as phytoplankton are less in need of P and therefore there is less need to exert energy to convert unusable P fractions. Conversely, as APA decreased down the reservoir gradient, biomass increases. This also aligns with our results, as biomass are able to support growth when P is non-limiting.

CHAPTER 6

GENERAL DISCUSSION

Climate change projections for the UK and to a greater extent the southeast and the East of England, have identified multiple stressors that will impact freshwater systems (Hering et al., 2010; Kendon et al., 2019). Drinking water reservoirs are even more vulnerable due to their role in providing clean water to millions of people as well as the many ecosystem services they provide to the community. Therefore, the aim of this thesis is to highlight how climate change may already be affecting these reservoirs and the problems they may face in the future with a special focus on risk. This was achieved by repeating studies conducted in the 1980s and 1990s through whole-reservoir assessments of priority climate stressors and correlating the findings to key management problems and questions.

6.1 Summary of Thesis Findings

6.1.1 Chapter 2 Summary

Chapter two investigated the following research questions, (1) What is the community composition of Alton and Ardleigh and how does it compare to the 1980s and 1990s? (2) Is there a relationship between biomass, abundance, and functional diversity within habitats? (3) Community composition is currently assessed from one sample in the pelagic habitat (draw-off tower), is this sample representative of the reservoir as a whole? (4) In this study, both

microscopy and in situ spectrofluorometery were used to assess community composition, how do these methods compare at the phylum level? To answer these questions, phytoplankton community composition and abundance were studied between shallow and deep-water habitats across a spatial and temporal scale to identify if a single, pelagic sample was representative of the reservoir and thus an appropriate management strategy for whole-system management as well as assessing reservoir changes since they were last studied 30 years ago.

The findings were as follows: In Alton, biomass did not differ between habitats during any month except Aug where the littoral had slightly more biomass than the pelagic. Ardleigh was spatially and temporally more variable where the littoral had greater biomass in summer and autumn. Total abundance presented similarly to biomass where no significant difference between habitats was observed in any month or in either reservoir. Species richness also did not differ between habitats in either reservoir. However, Alton contained a month where the lowest species richness in the pelagic also saw the highest in the littoral. Among diversity, both the littoral and pelagic of Alton were temporally the same but not spatially. In Ardleigh, diversity was variable both spatially and temporally.

Among community composition, cyanobacteria dominated Ardleigh reservoir in both the littoral and pelagic throughout the year. The exception was Apr, which was dominated by diatoms in the littoral. In addition, the draw-off tower had additional species that were not found in other pelagic sites. In Alton,

cyanobacteria also dominated in almost every month and in both habitats. Overall, in both reservoirs, phytoplankton community composition was not significantly different spatially but it was different temporally. However, when investigating the difference between community composition methods, microscopy and spectrofluorometery were significantly different. Microscopy found over 50% more cyanobacteria than the fluoroprobe but 92% less green algae.

For species richness, a decrease was observed with an increase in total cell counts. In the case of both habitats and both reservoirs, the relationship between total abundance and diversity was negative where diversity within the community decreased with an increase in cell count. Among biomass and diversity, no correlation was found in Alton littoral or pelagic. However, in Ardleigh, as biomass increased, diversity decreased.

In summary, both Ardleigh and Alton are different reservoirs than they were three decades ago. Eutrophication has increased, biodiversity has decreased, and they are both dominated by nuisance cyanobacteria. In addition, no relationship was found between abundance, biomass, and functional diversity between habitats. As such, a single sample collected at the draw-off tower is not representative of the reservoir and should be discarded as a monitoring strategy. Multiple samples collected in shallow and deep water, in the upper reservoir and main basins are more appropriate. Lastly, microscopy and spectrofluorometery were dissimilar enough that they should not be used for

phytoplankton taxonomy until they are validated against more sophisticated methods such as eDNA.

6.1.2 Chapter 3 Summary

Chapter three investigated the following research questions, (1) How toxic are the summer blooms in the East of England? (2) What is the Microcystin community composition within each bloom and which variants dominate throughout the year? (3) Is there a relationship between reservoir biogeochemistry and bloom toxicity? This was achieved by quantifying bloom composition and toxicity, strain dominance, and the biogeochemical parameters that may be driving these profiles. The findings were as follows: Reservoir A was dominated by toxin producers pre-bloom and non-producers post-bloom while at the height of the summer bloom, toxin producers dominated. In Reservoir B, non-producers dominated pre-bloom and during its peak while toxin producers dominated post-bloom. In Reservoir B, non-producers outcompeted toxin-producing strains in every month except directly after the summer bloom and in the middle of winter. In Reservoir A, toxin and non-toxin producing strains fluctuated between months however; toxin-producing cells outcompeted non-produces in most cases. Among toxin producers, Microcystin was found in both reservoirs and in every month except the winter in Reservoir B. In both reservoirs, Microcystin in the early spring was less variable than the summer. In addition, biogeochemistry analysis found nitrogen was significantly higher than phosphorus in both Reservoirs A and B. Nitrogen (as nitrate) was also found to correlate to abundance in Reservoir A toxin-producers where nitrogen increased as

abundance increased. Among all other anions and environmental variables, no significant correlations were found in either toxin producers or non-producers in either reservoir.

In summary, high concentrations of cyanobacteria toxins were found in two reservoirs in the East of England where the blooms contained all 12 toxin variants measured. Among explanatory variables, nitrogen was found to increase as toxins increased in Reservoir A.

6.1.3 Chapter 4 Summary

Chapter four investigated the following research questions, (1) What is the role of legacy P in supporting reservoir wide phytoplankton blooms? (2) Is Alton Water sediment a source or sink for bound phosphorus? (3) Can water chemistry help explain trends in metal-bound P fractions? (4) How effective is the bund wall in holding locked-P in the reservoir inlet? This was achieved by quantifying phosphorus concentrations from the sediment to the surface, calculating sediment's ability to act as a source or sink for phosphorus, and identifying the potential for internal loading to support phytoplankton growth in a changing climate. The findings were as follows: Analysis of Alton Water sediment found Labile P in a near uniform distribution throughout the reservoir. Ca-P was also found throughout the reservoir but in much higher concentrations inside the bund. Fe-P was highest in the upper reservoir compared to negligible concentrations in lower. Inside the bund, the ratio of Fe-P to Ca-P was 0.25 while the ratio of Fe-P to Ca-P in the lower reservoir was 0.01. Finally, Al-P was found is very low concentrations from the inlet

through to the main reservoir before it was undetectable in the main basin. Adsorption capacity experiments and isotherm modelling of the sediment found both inside the bund and the mid reservoir to be sources of phosphorus loading to the water column. While both areas are contributing P to the reservoir the amount of P entering the system from internal loading is far greater inside the bund. Water chemistry analysis found dissolved oxygen was in a healthy range of 6.8 – 11.2 mg/L throughout the reservoir with only the main basin slightly lower (6.28 mg/L). pH was found to be nearly uniform throughout the reservoir at a neutral concentration with a small pull towards alkaline. Among nutrient concentrations at both the surface and the sediment, orthophosphate and total P were higher in the lower reservoir than in the upper inlet. Organic P at the surface was also higher in the lower reservoir compared to the upper whereas organic P at the sediment was lower in the lower reservoir. Overall, water chemistry and nutrients were found to only effect Ca-P and no other bound fraction. This effect also did not change between sites.

In summary, of the four legacy P fractions investigated, Ca-P was found in the greatest concentration identifying potential long-term threats to the reservoir. Ca-P was also found to be the only metal-P fraction effected by water chemistry. In addition, this study identified Alton Water sediment to be a source of P to the water column, which is likely feeding year-round phytoplankton blooms. Lastly, phosphorus was found outside the bund wall and down the reservoir gradient identifying a strong need for management attention to the bund wall.

6.1.4 Chapter 5 Summary

Chapter five investigated the following hypotheses H1. Site 1 (inside a management bund) is phosphorus limited due to ferric dosing which binds phosphorus at the top of the reservoir, preventing it from travelling downstream to the main basin. H2. The rate of nutrient limitation decreases down the reservoir gradient as less phosphorus is being locked through ferric binding allowing it to move freely downstream. H3. Alkaline Phosphatase Activity will be highest inside the bund where inorganic phosphorus is actively bound. In turn, phytoplankton will work to convert organic phosphorus to a usable inorganic form allowing it to support growth. This was achieved by assessing the effectiveness of a management bund wall to trap nutrient inputs from source waters, document the status of nutrient limitation along a reservoir gradient and investigate phytoplankton's ability to support growth across that gradient under nutrient limitation. The findings were as follows: Nutrient enrichment experiments identified a decrease in phytoplankton biomass under nitrogen treatments, an increase in biomass with the addition of both nitrogen and phosphorus as well as an increase with the addition of phosphorus alone. In the upper reservoir, enrichment response was higher than in the lower reservoir especially for phosphorus where this response decreased down the reservoir to form a P limitation gradient. APA was found to be highest outside the bund and overall greater in the upper reservoir compared to the lower reservoir. As P limitation decreases down the reservoir so did alkaline phosphatase activity. Conversely, as APA decreased down the reservoir gradient, biomass increased.

In summary, P is the limiting nutrient in Alton Water however, despite the success of ferric binding; P is travelling outside the bund and down the reservoir where concentrations of P down the reservoir decrease. Lastly, APA was found to be highest outside the bund, not inside as hypothesised.

6.2 Multiple Stressors

Based on the results in this study, multiple climate stressors are already affecting drinking water reservoirs in the East of England through eutrophication, low biodiversity, and toxic cyanobacteria blooms. Water temperatures were found be high enough in the summer to support nuisance species and created a well-mixed system where nutrients support growth.

The true impact of multiple climate stressors on freshwater is still not fully understood and researches continue to see differing effects depending on waterbody type. For example, in a cyanobacteria study of 494 lakes encompassing eight different lake types across Europe, temperature was found to impact high latitude lakes the most whereas cyanobacteria in humic polymictic lakes were impacted by retention time and the relationship between total phosphorus and temperature. Clear polymictic lakes were instead only influenced by retention time (Richardson et al., 2018). This shows the true complexity of multiple stressors on freshwater and highlights the uniqueness of each system's explanatory variables.

Managing and mitigating these stressors is equally complex where science, technology, and management must all work together. An example of this

concept in Europe is Project MARS (Managing Aquatic ecosystems and water Resources under multiple Stress). Project MARS works in three stages to create tools and understanding of multiple stressors on aquatic systems using modelling, empirical approaches, and knowledge frameworks. MARS has been studying 16 European river basins on a large-spatial scale to help inform management and policy makes (Hering et al., 2015). Initiatives such as this may be beneficial to the water industry and is a viable tool to help predict and manage future climate scenarios.

6.3 Conclusions

This study identified variation in phytoplankton dynamics in space and time across both reservoirs. Specifically, internal loading is feeding algal blooms in Alton Water and is more severe inside the bund wall. This will continue well into the future as long-term phosphorus binding elements (i.e. Ca-P) were found is high concentrations throughout the reservoir. Specifically, Alton's biogeochemistry is affecting Ca-P, the most abundant bound fraction in the reservoir, which is further evidence for future internal loading. Nevertheless, during summer months, phytoplankton inside the bund wall are phosphorus limited, which agrees with historical findings. This limitation then decreases down the reservoir where the inlet is the most P limited and the main basin is the least P limited. Phosphorus limitation inside the bund may be explained by ferric dosing which binds phosphorus at the top of the reservoir, preventing it from travelling downstream to the main basin. While P is being bound at the inlet with some success, sediment saturation has caused newly bound P to flow out of the bund instead of joining the sediment-P pool. This is also

evidence of the bund wall not effectively or efficiently containing bound P at the inlet as was intended.

With regard to toxins and subsequent risk, shallow, well-mixed reservoirs in the East of England were found to contain serious neuro and hepatotoxins. Toxicity within the reservoirs however did fluctuate throughout the year presenting toxins even in months without a visible bloom. This was also correlated with lower algal biodiversity, which agrees with the literature. Therefore, water managers should caution against making risk-based decisions solely on cell counts or community composition alone because no matter which species are present, in what concentrations or abundance, there is no way of assessing risk without knowing the toxicity. As such, the current management practice of collecting water samples from a single location at the draw-off tower, which is located in pelagic waters, is not advisable as it overestimates some species and underestimates others throughout the year. In addition, the methods used to assess community composition and toxic species in the East of England need to be revaluated as they apply to toxic species. Microscopy may cause unnecessary management decisions by overestimating cyanobacteria while the fluoroprobe could increase risk by underestimating communities. However, it is not possible to know which method is the most accurate without individual assessment against more advanced methodologies. Quantitative real-time PCR is one such method and has been found to detect species microscopy could not while reducing analysis time and the limitations of human error and bias. Furthermore,

methods for assessing these impacts should be evaluated and new risk-based actions plans should be developed for cyanotoxins specifically.

Lastly, this study brought to light the significant difference in ecology between reservoirs that are relatively close together and managed in similar ways. Therefore, when thinking about climate change mitigation and adaptation, water managers need to create site-specific profiles for individual reservoirs that includes whole-system sampling throughout the year.

REFERENCES

Abdul-Hussein, M.M., Mason, C.F., 1988. The phytoplankton community of a eutrophic reservoir. Hydrobiologia 169, 265–277.

Allen-Gil, S.M., Gilroy, D.J., Curtis, L.R., 1995. An Ecoregion Approach to Mercury Bioaccumulation by Fish in Reservoirs. Arch. Environ. Contain. Toxico 28, 61–68.

Apel, K., Hirt, H., 2004. Reactive Oxygen Species: Metabolism, Oxidative Stress, and Signal Transduction. Annu. Rev. Plant Biol. 55, 373–399.

APHA, 2017. Standard Methods for the Examination of Water and Wastewater, 23rd ed. American Public Health Association, American Water Works Association, Water Environment Federation, United States.

Arvola, L., 1986. Spring phytoplankton of 54 small lakes in southern Finland. Hydrobiologia 137, 125–134.

Badr, G., 2019. Impact of heat stress on the immune response of fishes. J. Surv. Fish. Sci. 5, 149–159.

Barik, S.K., Bramha, S.N., Mohanty, A.K., Bastia, T.K., Behera, D., Rath, P., 2016. Sequential extraction of different forms of phosphorus in the surface sediments of Chilika Lake. Arab. J. Geosci. 9, 1–12.

Beardall, J., Young, E., Roberts, S., 2001. Approaches for determining phytoplankton nutrient limitation. Aquat. Sci. 63, 44–69.

Belokda, W., Khalil, K., Loudiki, M., Aziz, F., Elkalay, K., 2019. First assessment of phytoplankton diversity in a Marrocan shallow reservoir

(Sidi Abderrahmane). Saudi J. Biol. Sci. 26, 431–438.

Berry, J.P., Lind, O., 2010. Toxicon First evidence of ‘“ paralytic shellfish toxins ”’ and cylindrospermopsin in a Mexican freshwater system , Lago Catemaco , and apparent bioaccumulation of the toxins in ‘“ tegogolo ”’ snails (Pomacea patula catemacensis). Toxicon 55, 930–938.

Bleiker, W., Schanz, F., 1997. Light climate as the key factor controlling the spring dynamics of phytoplankton in Lake Zürich. Aquat. Sci. 59, 135–157.

Bol, R., Gruau, G., Mellander, P., Dupas, R., Bechmann, M., Skarbøvik, E., Bieroza, M., Djodjic, F., Glendell, M., Jordan, P., 2018. Challenges of Reducing Phosphorus Based Water Eutrophication in the Agricultural Landscapes of Northwest Europe 5, 1–16.

Bolster, C.H., Hornberger, G.M., 2007. On the Use of Linearized Langmuir Equations. Soil Sci. Soc. Am. J. 71, 1796–1806.

Briand, E., Escoffier, N., Straub, C., Sabart, M., Quiblier, C., Humbert, J.-F., 2009. Spatiotemporal changes in the genetic diversity of a bloom-forming *Microcystis aeruginosa* (cyanobacteria) population. ISME J. 3, 419–429.

Briand, E., Yéprémian, C., Humbert, J.F., Quiblier, C., 2008. Competition between microcystin- and non-microcystin-producing *Planktothrix agardhii* (cyanobacteria) strains under different environmental conditions. Environ. Microbiol. 10, 3337–3348.

Brudler, S., Rygaard, M., Arnbjerg-Nielsen, K., Hauschild, M.Z., Ammitsøe,

C., Vezzaro, L., 2019. Pollution levels of stormwater discharges and resulting environmental impacts. Sci. Total Environ. 663, 754–763.

Brutemark, A., Engstrom-Ost, J., Vehmaa, A., Gorokhova, E., 2015. Growth, toxicity and oxidative stress of a cultured cyanobacterium (*Dolichospermum sp.*) under different CO_2/pH and temperature conditions. Phycol. Res. 63, 56–63.

Cardoso, L. de S., Faria, D.M. de, Crossetti, L.O., da Motta Marques, D., 2019. Phytoplankton, periphyton, and zooplankton patterns in the pelagic and littoral regions of a large subtropical shallow lake. Hydrobiologia 831, 119–132.

Carmichael, W.W., Boyer, G.L., 2016. Health impacts from cyanobacteria harmful algae blooms : Implications for the North American Great Lakes. Harmful Algae 54, 194–212.

Carpenter, S.R., Kitchell, J.F., Hodgson, J.R., 1985. Cascading Trophic Interactions and Lake Productivity. Bioscience 35, 634–639.

Carvalho, L., Miller, C.A., Scott, E.M., Codd, G.A., Davies, P.S., Tyler, A.N., 2011. Cyanobacterial blooms: Statistical models describing risk factors for national-scale lake assessment and lake management. Sci. Total Environ. 409, 5353–5358.

Cattaneo, A., de Sève, M., Morabito, G., Mosello, R., Tartari, G., 2011. Periphyton changes over 20 years of chemical recovery of Lake Orta, Italy: Differential response to perturbation of littoral and pelagic communities. J. Limnol. 70, 177–185.

Chellappa, N., Borba, J., Rocha, O., 2008. Phytoplankton community and physical-chemical characteristics of water in the public reservoir of Cruzeta, RN, Brazil. Brazilian J. Biol. 68, 477–494.

Chorus, I., Falconer, I.R., Salas, H.J., Bartram, J., 2000. Health risks caused by freshwater cyanobacteria in recreational waters. J. Toxicol. Environ. Heal. - Part B Crit. Rev. 3, 323–347.

Clarke, S.J., 2009. Adapting to Climate Change: Implications for Freshwater Biodiversity and Management in the UK. Freshw. Rev. 2, 51–64.

Corbel, S., Mougin, C., Bouaïcha, N., 2014. Cyanobacterial toxins: Modes of actions, fate in aquatic and soil ecosystems, phytotoxicity and bioaccumulation in agricultural crops. Chemosphere 96, 1–15.

Crossetti, L.O., Bicudo, D.C., Bicudo, C.E.M., Bini, L.M., 2008. Phytoplankton biodiversity changes in a shallow tropical reservoir during the hypertrophication process. Brazilian J. Biol. 68, 1061–1067.

Daniel, T.C., Sharpley, A.N., Lemunyon, J.L., 1998. Agricultural Phosphorus and Eutrophication: A Symposium Overview 257, 251–257.

Dari, B., Nair, V.D., Colee, J., Harris, W.G., Mylavarapu, R., 2015. Estimation of phosphorus isotherm parameters: A simple and cost-effective procedure. Front. Environ. Sci. 3, 1–9.

Davis, T.W., Berry, D.L., Boyer, G.L., Gobler, C.J., 2009. The effects of temperature and nutrients on the growth and dynamics of toxic and non-toxic strains of *Microcystis* during cyanobacteria blooms. Harmful Algae 8, 715–725.

De Figueiredo, D.R., Azeiteiro, U.M., Esteves, S.M., Goncalves, F.J.M., Pereira, M.J., 2004. *Microcystin*-producing blooms—a serious global public health issue. Ecotoxicol. Environ. Saf. 59, 151–163.

Ding, W.X., Ong, C.N., 2003. Role of oxidative stress and mitochondrial changes in cyanobacteria-induced apoptosis and hepatotoxicity. FEMS Microbiol. Lett. 220, 1–7.

Dolman, A.M., Rücker, J., Pick, F.R., Fastner, J., Rohrlack, T., Mischke, U., Wiedner, C., 2012. Cyanobacteria and Cyanotoxins: The Influence of Nitrogen versus Phosphorus. PLoS One 7, 38-57.

Edwards, C., Beattie, K.A., Scrimgeour, C.M., Codd, G.A., 1992. Identification of anatoxin-A in benthic cyanobacteria (blue-green algae) and in associated dog poisonings at Loch Insh, Scotland. Toxicon 30, 1165–1175.

Elliott, J.A., 2020. Modelling lake phytoplankton communities: recentapplications of the PROTECH model. Hydrobiologia 848, 209–217.

Elliott, J.A., Jones, I.D., Thackeray, S.J., 2006. Testing the Sensitivity of Phytoplankton Communities to Changes in Water Temperature and Nutrient Load, in a Temperate Lake. Hydrobiologia 559, 401–411.

Elser, J.J., Kimmel, B.L., 1986. Alteration of phytoplankton phosphorus status during enrichment experiments: implications for interpreting nutrient enrichment bioassay results. Hydrobiologia 133, 217–222.

Elser, J.J., Marzolf, E.R., Goldman, C.R., 1990. Phosphorus and Nitrogen

Limitation of Phytoplankton Growth in the Freshwaters of North America: A Review and Critique of Experimental Enrichments. Can. J. Fish. Aquat. Sci. 47, 1468–1477.

Environment Agency, 2017. Ardleigh Reservoir Catchment Data Portal [WWW Document].

European Environment Agency, 2020. Climate Change Mitigation [WWW Document].

Farrer, D., Counter, M., Hillwig, R., Cude, C., 2015. Health-based cyanotoxin guideline values allow for cyanotoxin-based monitoring and efficient public health response to cyanobacterial blooms. Toxins (Basel). 7, 457–477.

Florczyk, M., Łakomiak, A., Wozny, M., Brzuzan, P., 2014. Neurotoxicity of cyanobacterial toxins. Environ. Biotechnol. 10, 26–43.

Garnier, S., 2018. viridisLite: Default Color Maps from ‘matplotlib’ (Lite Version).

Garrido, M., Cecchi, P., Malet, N., Bec, B., Torre, F., Pasqualini, V., 2019. Evaluation of FluoroProbe® performance for the phytoplankton-based assessment of the ecological status of Mediterranean coastal lagoons. Environ. Monit. Assess. 191.

Gonsiorczyk, T., Casper, P., Koschel, R., 1998. Phosphorus-binding forms in the sediment of an oligotrophic and an eutrophic hardwater lake of the Baltic Lake District (Germany). Water Sci. Technol. 37, 51–58.

Gupta, R.S., Mukhtar, T., Singh, B., 1999. Evolutionary relationships among

photosynthetic prokaryotes *(Heliobacterium chlorum, Chloroflexus aurantiacus*, cyanobacteria, *Chlorobium tepidum* and proteobacteria): implications regarding the origin of photosynthesis. Mol. Microbiol. 32, 893–906.

Hadley, W., François, R., Henry, L., Müller, K., 2020. dplyr: A Grammar of Data Manipulation: R Package.

Hansson, L.A., Ekvall, M.K., He, L., Li, Z., Svensson, M., Urrutia-Cordero, P., Zhang, H., 2020. Different climate scenarios alter dominance patterns among aquatic primary producers in temperate systems. Limnol. Oceanogr. 1–9.

Hardy, F.J., Johnson, A., Hamel, K., Preece, E., 2015. Cyanotoxin bioaccumulation in freshwater fish, Washington State, USA. Environ. Monit. Assess. 187.

Harke, M.J., Gobler, C.J., 2013. Global Transcriptional Responses of the Toxic Cyanobacterium, *Microcystis aeruginosa*, to Nitrogen Stress, Phosphorus Stress, and Growth on Organic Matter. PLoS One 8, 1–15.

Hartikainen, H., Rasa, K., Withers, P.J.A., 2010. Phosphorus exchange properties of European soils and sediments derived from them. Eur. J. Soil Sci. 61, 1033–1042.

Hayes, C.R., Greene, L.A., 1984. The evaluation of eutrophication impact in public water supply reservoirs in East Anglia. Water Pollut. Control 83, 42–51.

Healey, F.P., 1979. Short-Term Responses of Nutrient-Deficient Algae to

Nutrient-Addition. J. Phycol. 15, 289–299.

Hering, D., Carvalho, L., Argillier, C., Beklioglu, M., Borja, A., Cardoso, A.C., Duel, H., Ferreira, T., Globevnik, L., Hanganu, J., Hellsten, S., Jeppesen, E., Kodeš, V., Solheim, A.L., Nõges, T., Ormerod, S., Panagopoulos, Y., Schmutz, S., Venohr, M., Birk, S., 2015. Managing aquatic ecosystems and water resources under multiple stress - An introduction to the MARS project. Sci. Total Environ. 503–504, 10–21.

Hering, D., Haidekker, A., Schmidt-Kloiber, A., Barker, T., Buisson, L., Graf, W., Grenouillet, G., Lorenz, A., Sandin, L., Stendera, S., 2010. Monitoring the Responses of Freshwater Ecosystems to Climate Change, in: Climate Change Impacts on Freshwater Ecosystems. pp. 84–118.

Hillebrand, H., Steinert, G., Boersma, M., Malzahn, A., Meunier, C.L., Plum, C., Ptacnik, R., 2013. Goldman revisited: Faster-growing phytoplankton has lower N : P and lower stoichiometric flexibility. Limnol. Oceanogr. 58, 2076–2088.

Hilt, S., Brothers, S., Jeppesen, E., Veraart, A.J., Kosten, S., 2017. Translating Regime Shifts in Shallow Lakes into Changes in Ecosystem Functions and Services. Bioscience 67, 928–936.

House, W.A., Denison, F.H., 2000. Factors influencing the measurement of equilibrium phosphate concentrations in river sediments. Water Res. 34, 1187–1200.

House, W.A., Denison, F.H., Smith, J.T., Armitage, P.D., 1995. An investigation of the effects of water velocity on inorganic phosphorus

influx to a sediment. Environ. Pollut. 89, 263–271.

Huang, Q., Wang, Z., Wang, C., Wang, S., Jin, X., 2005. Phosphorus release in response to pH variation in the lake sediments with different ratios of iron-bound P to calcium-bound P. Chem. Speciat. Bioavailab. 17, 55–61.

Huber, V., Adrian, R., Gerten, D., 2008. Phytoplankton response to climate warming modified by trophic state. Limnol. Oceanogr. 53, 1–13.

Hutchinson, G.E., 1961. The Paradox of the Plankton XCV, 137–145.

Hwang, C.P., Lackie, T.H., Huang, P.M., 1976. Adsorption of inorganic phosphorus by lake sediments. J. Water Pollut. Control Fed. 48, 2754–2760.

Iacarella, J.C., Barrow, J.L., Giani, A., Beisner, B.E., Gregory-Eaves, I., 2018. Shifts in algal dominance in freshwater experimental ponds across differing levels of macrophytes and nutrients. Ecosphere 9, 1–15.

Jakhar, P., 2013. Role of Phytoplankton and Zooplankton as Health Indicators of Aquatic Ecosystem : A Review. Int. J. Innov. Res. Stud. 2, 490–500.

Jensen, H.S., Andersen, F.O., 1992. Importance of temperature, nitrate, and pH for phosphate release from aerobic sediments of four shallow, eutrophic lakes. Limnol. Oceanogr. 37, 577–589.

Jesus, T.F., Rosa, I.C., Repolho, T., Lopes, A.R., Pimentel, M.S., Almeida-Val, V.M.F., Coelho, M.M., Rosa, R., 2018. Different ecophysiological

responses of freshwater fish to warming and acidification. Comp. Biochem. Physiol. -Part A Mol. Integr. Physiol. 216, 34–41.

Jindal, R., Thakur, R.K., Singh, U.B., Ahluwalia, A.S., 2014. Phytoplankton dynamics and water quality of Prashar Lake, Himachal Pradesh, India. Sustain. Water Qual. Ecol. 3, 101–113.

Johansson, E., Legrand, C., Björnerås, C., Godhe, A., Mazur-Marzec, H., Säll, T., Rengefors, K., 2019. High diversity of microcystin chemotypes within a summer bloom of the cyanobacterium microcystis botrys. Toxins (Basel). 11, 1–16.

John C. Rodda, 2006. Sustaining water resources in South East England. Atmos. Sci. Lett. 7, 75–77.

John, R. V., Saroyda, R., Cruz, Y.S., Antonio, R., Carl, J.C., Flestado, L.P., Ryan, J., Magalong, K., Zagala, Z.P., Barbacena, C.L., Bumatay, J.M., Bautista, L.F., Deocaris, C.C., 2020. PUPAIM: A Collection of Physical and Chemical Adsorption Isotherm Models.

Johnk, K.D., Huisman, J., Sharples, J., Sommeijer, B., Visser, P.M., Stroom, J.M., 2008. Summer heatwaves promote blooms of harmful cyanobacteria. Glob. Chang. Biol. 14, 495–512.

Jorda-Capdevila, D., Gampe, D., Huber García, V., Ludwig, R., Sabater, S., Vergoñós, L., Acuña, V., 2019. Impact and mitigation of global change on freshwater-related ecosystem services in Southern Europe. Sci. Total Environ. 651, 895–908.

Jüttner, F., Watson, S.B., 2007. Biochemical and ecological control of

geosmin and 2-methylisoborneol in source waters. Appl. Environ. Microbiol. 73, 4395–4406.

Kalff, J., 1971. Nutrient Limiting Factors in an Arctic Tundra Pond. Ecology 52, 655–659.

Kang, W., Wang, Z.H., Liu, L., Guo, X., 2019. Alkaline phosphatase activity in the phosphorus-limited southern Chinese coastal waters. J. Environ. Sci. (China) 86, 38–49.

Kendon, E.J., Fosser, G., Murphy, J., Chan, S., Clark, R., Harris, G., Lock, A., Lowe, J., Martin, G., Pirret, J., others, 2019. UKCP Convection-permitting model projections: Science report 1–153.

Kernan, M., 2015. Climate change and the impact of invasive species on aquatic ecosystems. Aquat. Ecosyst. Heal. Manag. 18, 321–333.

Klausmeier, C.A., Litchman, E., 2012. Successional dynamics in the seasonally forced diamond food web. Am. Nat. 180, 1–16.

Korhonen, J., 2006. Long-term changes in lake ice cover in Finland. Nord. Hydrol. 37, 347–363.

Kundzewicz, Z.W., 2008. Climate change impacts on the hydrological cycle. Ecohydrol. Hydrobiol. 8, 195–203.

Latifi, A., Ruiz, M., Zhang, C.-C., 2009. Oxidative stress in cyanobacteria. FEMS Microbiol. Rev. 33, 258–278.

Leduc, A.O.H.C., Munday, P.L., Brown, G.E., Ferrari, M.C.O., 2013. Effects of acidification on olfactorymediated behaviour in freshwater and marine ecosystems: A synthesis. Philos. Trans. R. Soc. B Biol. Sci. 368.

Lee, H.W., Lee, Y.S., Kim, J., Lim, K.J., Choi, J.H., 2019. Contribution of internal nutrients loading on the water quality of a reservoir. Water (Switzerland) 11, 1–17.

Li, M., Hou, Y.L., Zhu, B., 2007. Phosphorus sorption-desorption by purple soils of China in relation to their properties. Aust. J. Soil Res. 45, 182–189.

Lloyd, J.W., Harker, D., Baxendale, R.A., 1981. Recharge mechanisms and groundwater flow in the chalk and drift deposits of southern East Anglia. Q. J. Eng. Geol. 14, 87–96.

Lodge, D.M., Barko, J.W., Strayer, D., Melack, J.M., Mittelbach, G.G., Howarth, R.W., Menge, B., Titus, J.E., 1988. Spatial Heterogeneity and Habitat Interactions in Lake Communities, in: Complex Interactions in Lake Communities. Springer-Verlag New York Inc. 1988, pp. 181–208.

Logez, M., Roy, R., Tissot, L., Argillier, C., 2016. Effects of water-level fluctuations on the environmental characteristics and fish-environment relationships in the littoral zone of a reservoir. Fundam. Appl. Limnol. 189, 37–49.

Lowe, J.A., Bernie, D., Bett, P., Bricheno, L., Brown, S., Calvert, D., Clark, R., Eagle, K., Edwards, T., Fosser, G., others, 2018. UKCP18 science overview report. Met Off. Hadley Cent. Exet. UK 2018, 1–73.

Maberly, S.C., Pitt, J.A., Davies, P.S., Carvalho, L., 2020. Nitrogen and phosphorus limitation and the management of small productive lakes. Inl. Waters 10, 159–172.

Malmqvist, B., Rundle, S., 2002. Threats to the running water ecosystems of the world. Environ. Conserv. 29, 134–153.

Mantyka-Pringle, C.S., Martin, T.G., Moffatt, D.B., Linke, S., Rhodes, J.R., 2014. Understanding and predicting the combined effects of climate change and land-use change on freshwater macroinvertebrates and fish. J. Appl. Ecol. 51, 572–581.

Medsker, L.L., Jenkins, D., Thomas, J.F., 1968. Odorous Compounds in Natural Waters: An Earthy-Smelling Compound Associated with Blue-Green Algae and Actinomycetes. Environ. Sci. Technol. 2, 461–464.

Mei-Lin, W., You-Shao, W., Yu-Tu, W., Fu-Lin, S., Cui-Ci, S., Zhao-Yu, J., Hao, C., 2014. Influence of environmental changes on phytoplankton pattern in Daya Bay, South China Sea. Rev. Biol. Mar. y Oceanogr. 49, 323–337.

Morabito, G., Rogora, M., Austoni, M., Ciampittiello, M., 2018. Could the extreme meteorological events in Lake Maggiore watershed determine a climate-driven eutrophication process? Hydrobiologia 824, 163–175.

Mukhortova, O. V., Bykova, S. V., Tarasova, N.G., Unkovskaya, E.N., Bolotov, S.E., 2015. Plankton Community in the Pelagic and Littoral Zones of the Overgrown Lake Beloe (Volzhsko-Kamskiy Biosphere Natural State Reserve, Republic of Tatarstan, Russian Federation). J. Sib. Fed. Univ. Biol. 8, 66–84.

Munoz, M., Nieto-Sandoval, J., Cirés, S., de Pedro, Z.M., Quesada, A., Casas, J.A., 2019. Degradation of widespread cyanotoxins with high impact in drinking water (microcystins, cylindrospermopsin, anatoxin-a

and saxitoxin) by CWPO. Water Res. 163, 1–10.

Nausch, M., 1998. Alkaline phosphatase activities and the relationship to inorganic phosphate in the Pomeranian Bight (southern Baltic Sea). Aquat. Microb. Ecol. 16, 87–94.

Navarrete, I.A., Dicen, G.P., Perez, T.R., Mendoza, S.M., Rallos, R. V., Labides, J.L.R., Rivera, C.T., Hallare, A. V., Claveria, R.J.R., 2019. Towards integrated management of a shallow tropical lake: assessment of water quality, sediment geochemistry, and phytoplankton diversity in Lake Palakpakin, Philippines. Environ. Monit. Assess. 191, 1–16.

Nürnberg, G.K., LaZerrte, B.D., 2016. More than 20 years of estimated internal phosphorus loading in polymictic, eutrophic Lake Winnipeg, Manitoba. Freshw. Res. 42, 18–27.

Orihel, D.M., Baulch, H.M., Casson, N.J., North, R.L., Parsons, C.T., Seckar, D.C.M., Venkiteswaran, J.J., 2017. Internal phosphorus loading in Canadian fresh waters: A critical review and data analysis. Can. J. Fish. Aquat. Sci. 74, 2005–2029.

Oyama, Y., Fukushima, T., Matsushita, B., Matsuzaki, H., Kamiya, K., Kobinata, H., 2015. Monitoring levels of cyanobacterial blooms using the visual cyanobacteria index (VCI) and floating algae index (FAI). Int. J. Appl. Earth Obs. Geoinf. 38, 335–348.

Paerl, H., Fulton, R., Moisander, P., Dyble, J., 2001. Harmful freshwater algal blooms, with an emphasis on cyanobacteria. TheS Cient. World J. 1, 76–113.

Paerl, H., Huisman, J., 2008. Climate-Blooms Like It Hot. Science. 320, 57–58.

Paerl, H., Otten, T., 2013a. Blooms Bite the Hand That Feeds Them. Science. 342, 433–434.

Paerl, H., Otten, T., 2013b. Harmful Cyanobacterial Blooms: Causes, Consequences, and Controls. Microb. Ecol. 65, 995–1010.

Paerl, H.W., Huisman, J., 2009. Climate change: a catalyst for global expansion of harmful cyanobacterial blooms. Environ. Microbiol. Rep. 1, 27–37.

Palmer-Felgate, E.J., Jarvie, H.P., Withers, P.J.A., Mortimer, R.J.G., Krom, M.D., 2009. Stream-bed phosphorus in paired catchments with different agricultural land use intensity. Agric. Ecosyst. Environ. 134, 53–66.

Paraskevopoulou, S., Tiedemann, R., Weithoff, G., 2018. Differential response to heat stress among evolutionary lineages of an aquatic invertebrate species complex. Biol. Lett. 14, 1–5.

Parris, A.L., 2017. Professional Internships for NERC-facing Early Career Scientists (PINES) Programme: Environmental Data Science and Analysis for Drinking Water Solutions. Colchester.

Pasztaleniec, A., 2016. An advanced phytoplankton trophic index: Test and validation with a nationwide lake survey in Poland. Int. Rev. Hydrobiol. 101, 20–35.

Perkins, D.M., McKie, B.G., Malmqvist, B., Gilmour, S.G., Reiss, J., Woodward, G., 2010a. Environmental warming and biodiversity-

ecosystem functioning in freshwater microcosms. Partitioning the effects of species identity, richness and metabolism. Adv. Ecol. Res. 43, 177–209.

Perkins, D.M., Reiss, J., Yvon-Durocher, G., Woodward, G., 2010b. Global change and food webs in running waters. Hydrobiologia 657, 181–198.

Perkins, R.G., Underwood, G.J.C., 2002. Partial recovery of a eutrophic reservoir through managed phosphorus limitation and unmanaged macrophyte growth. Hydrobiologia 481, 75–87.

Perkins, R.G., Underwood, G.J.C., 2001. The Potential for Phosphorus Release Across the Sediment-Water Interface in an Eutrophic Reservoir Dosed with Ferric Sulphate. Water Res. 35, 1399–1406.

Perkins, R.G., Underwood, G.J.C., 2000. Gradients of chlorophyll a and water chemistry along an eutrophic reservoir with determination of the limiting nutrient by in situ nutrient addition. Water Res. 34, 713–724.

Pierzynski, G.M., Sharpley, A.N., 2009. Bioavailable phosphorus in soil. Methods phosphorus Anal. soils, sediments, residuals, waters, 2nd edn. South. Coop Ser. Bull 38–43.

Postel, S., Carpenter, S.R., 1997. Freshwater Ecosystem Services, in: Daily, G. (Ed.), Nature’s Services: Societal Dependence On Natural Ecosystems. Island Press, Washington D.C., pp. 195–214.

Psenner, R., Bostrom, B., Dinka, M., Pettersson, K., Pucsko, R., Sager, M., 1988. Fractionation of phosphorus in suspended matter and sediment. Ergebnisse der Limnol. 30, 98–103.

Qiao, Y., Wang, W., Lu, X., 2020. High Light Induced Alka(e)ne Biodegradation for Lipid and Redox Homeostasis in Cyanobacteria. Front. Microbiol. 11, 1–12.

R Core Team, 2019. R: A language and environment for statistical computing.

Rabalais, N.N., Díaz, R.J., Levin, L.A., Turner, R.E., Gilbert, D., Zhang, J., 2010. Dynamics and distribution of natural and human-caused hypoxia. Biogeosciences 7, 585–619.

Redfield, A.C., 1958. The biological control of chemical factors in the environment. Am. Sci.

Reichwaldt, E.S., Ghadouani, A., 2011. Effects of rainfall patterns on toxic cyanobacterial blooms in a changing climate : Between simplistic scenarios and complex dynamics. Water Res. 46, 1372–1393.

Reid, K., Schneider, K., McConkey, B., 2018. Components of Phosphorus Loss From Agricultural Landscapes, and How to Incorporate Them Into Risk Assessment Tools. Front. Earth Sci. 6, 1–15.

Reynolds, C.S., 1984. The ecology of freshwater phytoplankton. Cambridge University Press.

Richardson, J., Miller, C., Maberly, S.C., Taylor, P., Globevnik, L., Hunter, P., Jeppesen, E., Mischke, U., Moe, S.J., Pasztaleniec, A., Søndergaard, M., Carvalho, L., 2018. Effects of multiple stressors on cyanobacteria abundance vary with lake type. Glob. Chang. Biol. 24, 5044–5055.

Roberts, E.J., Cooper, R.J., 2018. Riverbed sediments buffer phosphorus concentrations downstream of sewage treatment works across the River Wensum catchment, UK. J. Soils Sediments 18, 2107–2116.

Sanchez, J., Otero, P., Alfonso, A., Ramos, V., Vasconcelos, V., Aráoz, R., Molgó, J., Vieytes, M., Botana, L., 2014. Detection of Anatoxin-a and Three Analogs in *Anabaena spp*. Cultures: New Fluorescence Polarization Assay and Toxin Profile by LC-MS/MS. Toxins (Basel). 6, 402–415.

Sartory, D.P., 1982. TR 115: Spectrophotometric analysis of chlorophyll a in freshwater phytoplankton. Republic of South Africa.

Scheffer, M., Rinaldi, S., Kuznetsov, Y.A., Nes, E.H. Van, Nes, V., Seasonal, E.H., 1997. Seasonal dynamics of *Daphnia* and algae explained as a periodically forced predator-prey system. Oikos 80, 519–532.

Schweizer, A., 1997. From littoral to pelagial: Comparing the distribution of phytoplankton and ciliated protozoa along a transect. J. Plankton Res. 19, 829–848.

Sharma, P., Jha, A.B., Dubey, R.S., Pessarakli, M., 2012. Reactive Oxygen Species, Oxidative Damage, and Antioxidative Defense Mechanism in Plants under Stressful Conditions. J. Bot. 2012, 1–26.

Sharpley, A.N., Chapra, S.C., Wedepohl, R., Sims, I.T., Daniel, T.C., Reddy, K.R., 1994. Managing Agricultural Phosphorus for Protection of Surface Waters: Issues and Options. J. Environ. Qual. 23, 437–451.

Singh, S.P., Häder, D.P., Sinha, R.P., 2010. Cyanobacteria and ultraviolet radiation (UVR) stress: Mitigation strategies. Ageing Res. Rev. 9, 79–90.

Skopp, J., 2009. Derivation of the Freundlich adsorption isotherm from kinetics. J. Chem. Educ. 86, 1341–1343.

Smith, V.H., 2003. Eutrophication of freshwater and coastal marine ecosystems: A global problem. Environ. Sci. Pollut. Res. 10, 126–139.

Smolders, E., Baetens, E., Verbeeck, M., Nawara, S., Diels, J., Verdievel, M., Peeters, B., De Cooman, W., Baken, S., 2017. Internal Loading and Redox Cycling of Sediment Iron Explain Reactive Phosphorus Concentrations in Lowland Rivers. Environ. Sci. Technol. 51, 2584–2592.

Sommer, U., Lengfellner, K., 2008. Climate change and the timing, magnitude, and composition of the phytoplankton spring bloom. Glob. Chang. Biol. 14, 1199–1208.

Søndergaard, M., Jensen, J.P., Jeppesen, E., 2003. Role of sediment and internal loading of phosphorus in shallow lakes. Hydrobiologia 135–145.

Sondergaard, M., Jensen, P.J., Jeppesen, E., 2001. Retention and internal loading of phosphorus in shallow, eutrophic lakes. Sci. World J. 1, 427–442.

Spears, B.., Carvalho, L., Paterson, D.., 2007. Phosphorus partitioning in a shallow lake: implications for water quality management. Water Environ. J. 47–53.

Steinman, Alan D, Spears, B.M., 2020. Internal Phosphorus Loading in Lakes. Causes, Case Studies, and Management. J. Ross Publishing.

Sun, Y., Zheng, Q., Sun, Y.-T., Huang, P., Guo, Z.-L., Xu, L.-H., 2014. Microcystin-LR induces protein phosphatase 2A alteration in a human liver cell line. Environ. Toxicol. 29, 1236–44.

Tang, X., Wu, M., Dai, X., Chai, P., 2014. Phosphorus storage dynamics and adsorption characteristics for sediment from a drinking water source reservoir and its relation with sediment compositions. Ecol. Eng. 64, 276–284.

Taranu, Z., Zurawell, R.W., Pick, F., I, G., 2012. Predicting cyanobacterial dynamics in the face of global change : the importance of scale and environmental context. Glob. Chang. Biol. 18, 3477–3490.

Taylor, A.W., Kunishi, H.M., 1971. Phosphate Equilibria on Stream Sediment and Soil in a Watershed Draining an Agricultural Region. J. Agric. Food Chem. 19, 827–831.

Tessier, C., Cattaneo, A., Pinel-Alloul, B., Hudon, C., Borcard, D., 2008. Invertebrate communities and epiphytic biomass associated with metaphyton and emergent and submerged macrophytes in a large river. Aquat. Sci. 70, 10–20.

Todd, B., Macdonald, N., Chiverrell, R.C., Caminade, C., Hooke, J.M., 2013. Severity, duration and frequency of drought in SE England from 1697 to 2011. Clim. Change 121, 673–687.

Turner, A.D., Dhanji-Rapkova, M., O'Neill, A., Coates, L., Lewis, A., Lewis,

K., 2018. Analysis of microcystins in cyanobacterial blooms from freshwater bodies in England. Toxins (Basel). 10, 1–29.

Tye, A.M., Rawlins, B.G., Rushton, J.C., Price, R., 2016. Understanding the controls on sediment-P interactions and dynamics along a non-tidal river system in a rural-urban catchment: The River Nene. Appl. Geochemistry 66, 219–233.

U.S. Environmental Protection Agency, 1993. EPA Method 300.1, Revision 1.0: Determination of Inorganic Anions in Drinking Water by Ion Chromatography 0–39.

United Nations, 2018. Sustainable Development Goal 6 Synthesis Report 2018 on Water and Sanitation, United Nations.

United Nations, World Meteorological Organization, Global Carbon Project (GCP), UNESCO Intergovernmental Oceanographic Commission (UNESCO-IOC), Intergovernmental Panel on Climate Change (IPCC), UN Environment Programme (UNEP), Met Office, 2020. United In Science.

Westrick, J.A., Szlag, D.C., Southwell, B.J., Sinclair, J., 2010. A review of cyanobacteria and cyanotoxins removal/inactivation in drinking water treatment. Anal. Bioanal. Chem. 397, 1705–1714.

WHO, 2007. Protecting Surface Water for Health. Identifying, Assessing and Managing Drinking-water Quality Risks in Surface-Water Catchments, In Our Backyard. Geneva, Switzerland.

Wickham, H., 2016. ggplot2: Elegant Graphics for Data Analysis.

Wickham, H., Henry, L., 2020. tidyr: Tidy Messy Data.

Wilson, D., 2012. Abberton Reservoir Enhancement.

Winfield, I.J., 2004. Fish in the littoral zone: Ecology, threats and management. Limnologica 34, 124–131.

Wonnacott, S., Gallagher, T., 2006. The Chemistry and Pharmacology of Anatoxin-a and Related Homotropanes with respect to Nicotinic Acetylcholine Receptors. Mar. Drugs 4, 228–254.

World Wildlife Fund International, Zoological Society of London, Global Footprint Network, Water Footprint Network, 2014. Living Planet Report 2014, 2014th ed. WWF International, Switzerland.

Wright, C., Nyberg, D., 2017. An inconvenient truth: How organizations translate climate change into business as usual. Acad. Manag. J. 60, 1633–1661.

Xie, L., Xie, P., Guo, L., Li, L., Miyabara, Y., Park, H.-D., 2005. Organ Distribution and Bioaccumulation of Microcystins in Freshwater Fish at Different Trophic Levels from the Eutrophic Lake Chaohu, China. Environ. Toxicol. 20, 293–300.

Xu, H., Paerl, H.W., Qin, B., Zhu, G., Gao, G., 2010. Nitrogen and phosphorus inputs control phytoplankton growth in eutrophic Lake Taihu, China. Limnol. Oceanogr. 55, 420–432.

Yin, H., Han, M., Tang, W., 2016. Phosphorus sorption and supply from eutrophic lake sediment amended with thermally-treated calcium-rich attapulgite and a safety evaluation. Chem. Eng. J. 285, 671–678.

Young, E.B., Tucker, R.C., Pansch, L.A., 2010. Alkaline phosphatase in freshwater cladophora-epiphyte assemblages: Regulation in response to phosphorus supply and localization. J. Phycol. 46, 93–101.

Zamor, R.M., Glenn, K.L., Hambright, K.D., 2012. Incorporating molecular tools into routine HAB monitoring programs: Using qPCR to track invasive *Prymnesium*. Harmful Algae 15, 1–7.

Zilliges, Y., Kehr, J.-C., Meissner, S., Ishida, K., Mikkat, S., Hagemann, M., Kaplan, A., Börner, T., Dittmann, E., 2011. The Cyanobacterial Hepatotoxin Microcystin Binds to Proteins and Increases the Fitness of *Microcystis* under Oxidative Stress Conditions. PLoS One 6, e17615.

Zohary, T., Ostrovsky, I., 2011. Ecological impacts of excessive water level fluctuations in stratified freshwater lakes. Inl. Waters 1, 47–59.

APPENDICES

Appendix 1

Table S2.1 Cumulative list of dominant genus/species and their respective relative abundance to the community in Ardleigh Reservoir from 2017-2018. Note: The draw-off tower has been added as a separate line within the Habitat column due to its community composition differing from that of the pelagic.

Month	Year	Habitat	Waterbody	Genus spp.	Phylum	Relative Abundance
Jan	2018	Littoral	Ardleigh	*Microcystis spp.*	Cyanobacteria	0.82
Jan	2018	Pelagic	Ardleigh	*Microcystis spp.*	Cyanobacteria	0.80
Mar	2018	Littoral	Ardleigh	*Microcystis spp.*	Cyanobacteria	0.50
Mar	2018	Pelagic	Ardleigh	*Fragilaria spp.*	Diatom	0.43
Mar	2018	Tower	Ardleigh	*Fragilaria spp.*	Diatom	0.58
Apr	2018	Littoral	Ardleigh	*Dinobryon spp.*	Golden Algae	0.53
Apr	2018	Pelagic	Ardleigh	*Coelastrum spp.*	Green Algae	0.60
Apr	2018	Tower	Ardleigh	*Oscillatoria spp.*	Cyanobacteria	0.36
May	2017	Littoral	Ardleigh	*Microcystis spp.*	Cyanobacteria	0.99
May	2017	Pelagic	Ardleigh	*Microcystis spp.*	Cyanobacteria	0.83
May	2017	Tower	Ardleigh	*species (Cyanophyceae)*	Cyanobacteria	0.76
Jun	2017	Littoral	Ardleigh	*Microcystis spp.*	Cyanobacteria	1.00
Jun	2017	Pelagic	Ardleigh	*Microcystis spp.*	Cyanobacteria	0.92
Jun	2017	Tower	Ardleigh	*Pediastrum spp.*	Green Algae	0.41
Jun	2017	Tower	Ardleigh	*Microcystis spp.*	Cyanobacteria	0.41
Jul	2017	Littoral	Ardleigh	*Microcystis spp.*	Cyanobacteria	0.95
Jul	2017	Pelagic	Ardleigh	*Microcystis spp.*	Cyanobacteria	0.89
Jul	2017	Tower	Ardleigh	*species (Cyanophyceae)*	Cyanobacteria	0.53
Aug	2017	Littoral	Ardleigh	*Microcystis spp.*	Cyanobacteria	0.74
Aug	2017	Pelagic	Ardleigh	*Microcystis spp.*	Cyanobacteria	0.92
Aug	2017	Tower	Ardleigh	*Microcystis spp.*	Cyanobacteria	0.96
Sep	2017	Littoral	Ardleigh	*Microcystis spp.*	Cyanobacteria	0.98
Sep	2017	Pelagic	Ardleigh	*Microcystis spp.*	Cyanobacteria	0.97
Sep	2017	Tower	Ardleigh	*Microcystis spp.*	Cyanobacteria	0.76
Oct	2017	Littoral	Ardleigh	*Microcystis spp.*	Cyanobacteria	0.83
Oct	2017	Pelagic	Ardleigh	*Microcystis spp.*	Cyanobacteria	0.83

Table S2.1 Continued

Month	Year	Habitat	Waterbody	Genus spp.	Phylum	Relative Abundance
Nov	2017	Littoral	Ardleigh	*Microcystis spp.*	Cyanobacteria	0.69
Nov	2017	Pelagic	Ardleigh	*Melosira spp.*	Diatom	0.65
Nov	2017	Tower	Ardleigh	*Microcystis spp.*	Cyanobacteria	0.89
Dec	2017	Littoral	Ardleigh	*Microcystis spp.*	Cyanobacteria	0.91
Dec	2017	Pelagic	Ardleigh	*Microcystis spp.*	Cyanobacteria	0.48
Dec	2017	Tower	Ardleigh	*Microcystis spp.*	Cyanobacteria	0.98

Appendix 2

Table S2.2 Cumulative list of least common genus/species in Ardleigh Reservoir from 2017-2018. Note: The draw-off tower has been added as a separate line within the Habitat column due to its community composition differing from that of the pelagic.

Month	Year	Habitat	Waterbody	Genus spp.	Phylum
Jan	2018	Littoral	Ardleigh	*Scenedesmus spp.*	Green Algae
Jan	2018	Pelagic	Ardleigh	*Scenedesmus spp.*	Green Algae
Mar	2018	Littoral	Ardleigh	*Peridinium spp.*	Dinoflagellate
Mar	2018	Littoral	Ardleigh	*Chlamydomonas spp.*	Green Algae
Mar	2018	Pelagic	Ardleigh	*Peridinium spp.*	Dinoflagellate
Mar	2018	Tower	Ardleigh	*Rhodomonas spp.*	Cryptophyta
Apr	2018	Littoral	Ardleigh	*Chlamydomonas spp.*	Green Algae
Apr	2018	Littoral	Ardleigh	*Ankyra spp.*	Green Algae
Apr	2018	Littoral	Ardleigh	*Mallomonas spp.*	Ochrophyta
Apr	2018	Pelagic	Ardleigh	*Euglena spp.*	Euglenozoa
Apr	2018	Pelagic	Ardleigh	*species (Bacillariophyceae)*	Diatom
Apr	2018	Pelagic	Ardleigh	*species (green)*	Green Algae
Apr	2018	Tower	Ardleigh	*Cryptomonas spp.*	Cryptophyta
May	2017	Littoral	Ardleigh	*Closteriopsis spp.*	Green Algae
May	2017	Pelagic	Ardleigh	*Melosira spp.*	Diatom
May	2017	Tower	Ardleigh	*species (green)*	Green Algae
Jun	2017	Littoral	Ardleigh	*species (Bacillariophyceae)*	Diatom
Jun	2017	Pelagic	Ardleigh	*Chlamydomonas spp.*	Green Algae
Jun	2017	Tower	Ardleigh	*species (Bacillariophyceae)*	Diatom
Jul	2017	Littoral	Ardleigh	*species (flagellated green)*	Green Algae
Jul	2017	Littoral	Ardleigh	*species (green)*	Green Algae
Jul	2017	Pelagic	Ardleigh	*Peridinium spp.*	Dinoflagellate
Jul	2017	Tower	Ardleigh	*species (flagellated green)*	Green Algae
Aug	2017	Littoral	Ardleigh	*Mallomonas spp.*	Ochrophyta
Aug	2017	Littoral	Ardleigh	*Peridinium spp.*	Dinoflagellate
Aug	2017	Littoral	Ardleigh	*species (Bacillariophyceae)*	Diatom
Aug	2017	Littoral	Ardleigh	*Staurastrum spp.*	Green Algae

Table S2.2 Continued

Month	Year	Habitat	Waterbody	Genus spp.	Phylum
Aug	2017	Pelagic	Ardleigh	*species (green)*	Green Algae
Aug	2017	Pelagic	Ardleigh	*species (Bacillariophyceae)*	Diatom
Aug	2017	Tower	Ardleigh	*species (green)*	Green Algae
Sep	2017	Littoral	Ardleigh	*species (Bacillariophyceae)*	Diatom
Sep	2017	Pelagic	Ardleigh	*Oscillatoria spp.*	Cyanobacteria
Sep	2017	Tower	Ardleigh	*Stephanodiscus spp.*	Diatom
Oct	2017	Littoral	Ardleigh	*species (flagellated green)*	Green Algae
Oct	2017	Littoral	Ardleigh	*Euglena spp.*	Euglenozoa
Oct	2017	Pelagic	Ardleigh	*species (Bacillariophyceae)*	Diatom
Oct	2017	Pelagic	Ardleigh	*species (flagellated green)*	Green Algae
Oct	2017	Pelagic	Ardleigh	*species (green)*	Green Algae
Oct	2017	Tower	Ardleigh	*species (Bacillariophyceae)*	Diatom
Nov	2017	Littoral	Ardleigh	*species (flagellated green)*	Green Algae
Nov	2017	Pelagic	Ardleigh	*species (Cyanophyceae)*	Cyanobacteria
Nov	2017	Pelagic	Ardleigh	*Chlamydomonas spp.*	Green Algae
Nov	2017	Tower	Ardleigh	*Scenedesmus spp.*	Green Algae
Dec	2017	Littoral	Ardleigh	*Peridinium spp.*	Dinoflagellate
Dec	2017	Littoral	Ardleigh	*species (green)*	Green Algae
Dec	2017	Pelagic	Ardleigh	*species (flagellated green)*	Green Algae
Dec	2017	Pelagic	Ardleigh	*Asterionella spp.*	Diatom
Dec	2017	Tower	Ardleigh	*Asterionella spp.*	Diatom

Appendix 3

Table S2.3 Cumulative list of dominant species and their respective relative abundance to the community in Alton Water from 2017-2018.

Month	Year	Habitat	Waterbody	Genus spp.	Phylum	Relative Abundance
Jan	2017	Littoral	Alton	*Aphanizomenon spp.*	Cyanobacteria	0.98
Jan	2017	Pelagic	Alton	*Aphanizomenon spp.*	Cyanobacteria	0.96
Feb	2017	Littoral	Alton	*Aphanizomenon spp.*	Cyanobacteria	0.96
Feb	2017	Pelagic	Alton	*Aphanizomenon spp.*	Cyanobacteria	0.93
Mar	2017	Littoral	Alton	*Aphanizomenon spp.*	Cyanobacteria	0.97
Mar	2017	Pelagic	Alton	*Aphanizomenon spp.*	Cyanobacteria	0.93
Apr	2017	Littoral	Alton	*Oscillatoria spp.*	Cyanobacteria	0.79
Apr	2017	Pelagic	Alton	*Aphanizomenon spp.*	Cyanobacteria	0.61
May	2018	Littoral	Alton	*Gomphosphaeria spp.*	Cyanobacteria	0.46
May	2018	Pelagic	Alton	*Coelastrum spp.*	Green Algae	0.60
Jun	2018	Littoral	Alton	*Aphanizomenon spp.*	Cyanobacteria	0.76
Jun	2018	Pelagic	Alton	*Aphanizomenon spp.*	Cyanobacteria	0.87
Jul	2018	Littoral	Alton	*Aphanizomenon spp.*	Cyanobacteria	0.42
Jul	2018	Pelagic	Alton	*Aphanizomenon spp.*	Cyanobacteria	0.68
Aug	2018	Littoral	Alton	*Aphanizomenon spp.*	Cyanobacteria	0.81
Aug	2018	Pelagic	Alton	*Aphanizomenon spp.*	Cyanobacteria	0.70
Sep	2018	Littoral	Alton	*Aphanizomenon spp.*	Cyanobacteria	0.92
Sep	2018	Pelagic	Alton	*Aphanizomenon spp.*	Cyanobacteria	0.96
Oct	2018	Littoral	Alton	*Aphanizomenon spp.*	Cyanobacteria	0.98
Oct	2018	Pelagic	Alton	*Aphanizomenon spp.*	Cyanobacteria	0.98
Nov	2018	Littoral	Alton	*Aphanizomenon spp.*	Cyanobacteria	0.98
Nov	2018	Pelagic	Alton	*Aphanizomenon spp.*	Cyanobacteria	0.97
Dec	2018	Littoral	Alton	*Aphanizomenon spp.*	Cyanobacteria	0.99
Dec	2018	Pelagic	Alton	*Aphanizomenon spp.*	Cyanobacteria	0.83

Appendix 4

Table S2.4 Cumulative list of rare or least common genus/species in Alton Water from 2017-2018. Note: The draw-off tower has been added as a separate line within the Habitat column due to its community composition differing from that of the pelagic.

Month	Year	Habitat	Waterbody	Genus spp.	Group
Jan	2017	Littoral	Alton	*Rhodomonas spp.*	Cryptophyta
Jan	2017	Littoral	Alton	*species (Bacillariophyceae)*	Diatom
Jan	2017	Pelagic	Alton	*species (Bacillariophyceae)*	Diatom
Jan	2017	Tower	Alton	*Ankistrodesmus spp.*	Green Algae
Feb	2017	Littoral	Alton	*Stephanodiscus spp.*	Diatom
Feb	2017	Pelagic	Alton	*Asterionella spp.*	Diatom
Feb	2017	Tower	Alton	*species (Bacillariophyceae)*	Diatom
Mar	2017	Littoral	Alton	*Closterium spp.*	Green Algae
Mar	2017	Littoral	Alton	*Gymnodinium spp.*	Dinoflagellate
Mar	2017	Pelagic	Alton	*species (Bacillariophyceae)*	Diatom
Mar	2017	Tower	Alton	*Gymnodinium spp.*	Dinoflagellate
Apr	2018	Littoral	Alton	*Closterium spp.*	Green Algae
Apr	2018	Pelagic	Alton	*Mallomonas spp.*	Ochrophyta
Apr	2018	Pelagic	Alton	*Rhodomonas spp.*	Cryptophyta
Apr	2018	Pelagic	Alton	*Closterium spp.*	Green Algae
Apr	2018	Tower	Alton	*species (Bacillariophyceae)*	Diatom
May	2018	Littoral	Alton	*Trachelomonas spp.*	Euglenozoa
May	2018	Pelagic	Alton	*Oocystis spp.*	Green Algae
Jun	2018	Littoral	Alton	*Ceratium spp.*	Dinoflagellate
Jun	2018	Pelagic	Alton	*Ceratium spp.*	Dinoflagellate
Jun	2018	Tower	Alton	*species (Bacillariophyceae)*	Diatom
Jul	2018	Littoral	Alton	*Ceratium spp.*	Dinoflagellate
Jul	2018	Littoral	Alton	*Chlamydomonas spp.*	Green Algae
Jul	2018	Littoral	Alton	*Closteriopsis spp.*	Green Algae
Jul	2018	Littoral	Alton	*Euglena spp.*	Euglenozoa
Jul	2018	Pelagic	Alton	*species (Bacillariophyceae)*	Diatom
Jul	2018	Tower	Alton	*Mallomonas spp.*	Ochrophyta
Aug	2018	Littoral	Alton	*Cosmarium spp.*	Green Algae
Aug	2018	Pelagic	Alton	*Euglena spp.*	Euglenozoa
Aug	2018	Pelagic	Alton	*Staurastrum spp.*	Green Algae
Aug	2018	Tower	Alton	*Cosmarium spp.*	Green Algae

Table S2.4 Continued

Month	Year	Habitat	Waterbody	Genus spp.	Group
Sep	2018	Littoral	Alton	*Peridinium spp.*	Dinoflagellate
Sep	2018	Littoral	Alton	*Staurastrum spp.*	Green Algae
Sep	2018	Littoral	Alton	*Mallomonas spp.*	Ochrophyta
Sep	2018	Littoral	Alton	*species (Bacillariophyceae)*	Diatom
Sep	2018	Pelagic	Alton	*Mallomonas spp.*	Ochrophyta
Sep	2018	Tower	Alton	*Staurastrum spp.*	Green Algae
Oct	2018	Littoral	Alton	*Staurastrum spp.*	Green Algae
Oct	2018	Littoral	Alton	*species (Bacillariophyceae)*	Diatom
Oct	2018	Littoral	Alton	*Staurastrum spp.*	Green Algae
Oct	2018	Pelagic	Alton	*Staurastrum spp.*	Green Algae
Oct	2018	Tower	Alton	*Cosmarium spp.*	Green Algae
Oct	2018	Tower	Alton	*Stephanodiscus spp.*	Diatom
Nov	2018	Littoral	Alton	*species (Bacillariophyceae)*	Diatom
Nov	2018	Pelagic	Alton	*Oocystis spp.*	Green Algae
Dec	2018	Littoral	Alton	*Rhodomonas spp.*	Cryptophyta
Dec	2018	Littoral	Alton	*Euglena spp.*	Euglenozoa
Dec	2018	Pelagic	Alton	*Closterium spp.*	Green Algae
Dec	2018	Tower	Alton	*Scenedesmus spp.*	Green Algae

Appendix 5

Figure S4.0 Corer

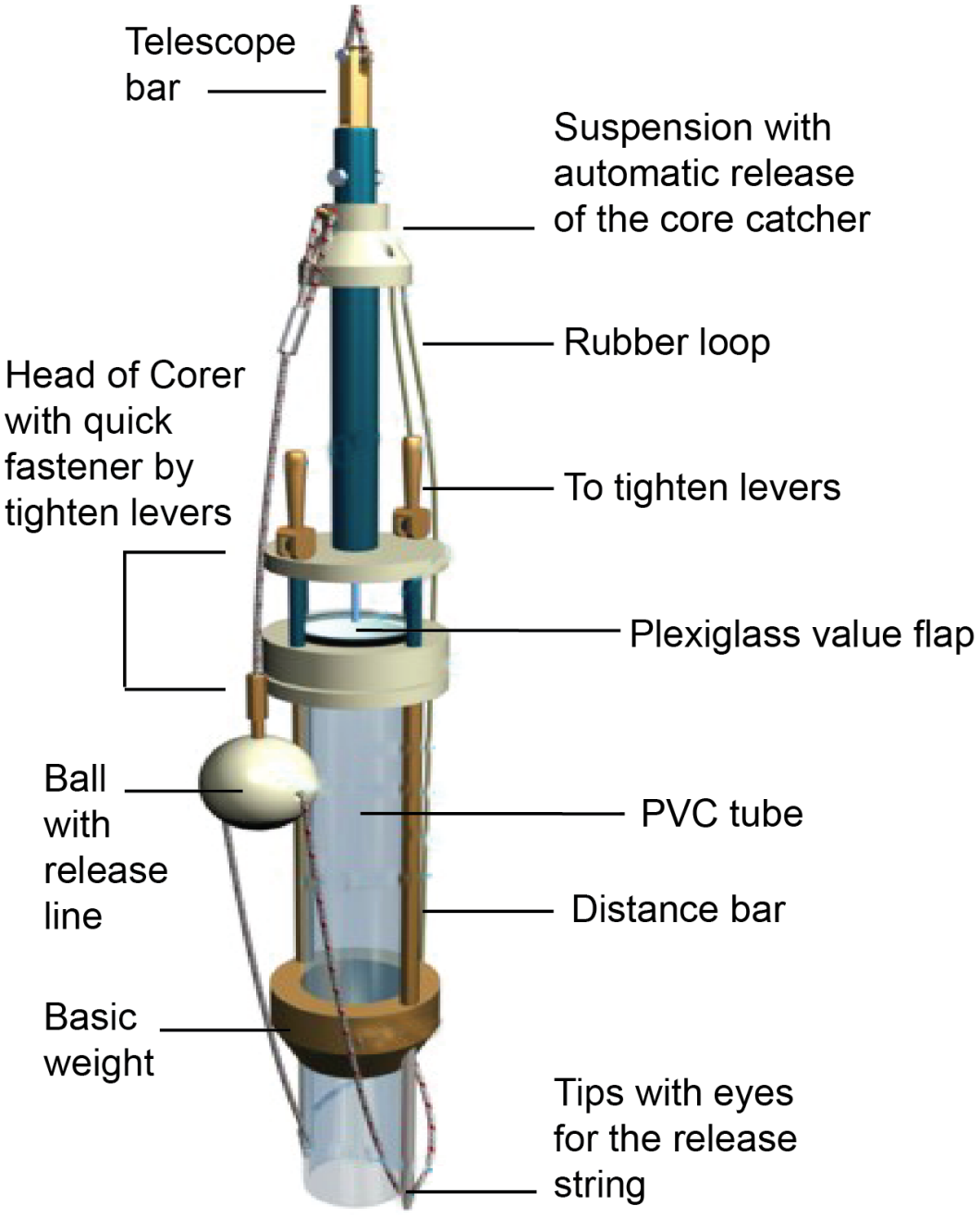

Appendix 6

Figure 4.S.1 Core cutter